Alma Mater Studiorum · Università di Bologna

FACOLTÀ DI SCIENZE MATEMATICHE, FISICHE E NATURALI
Corso di Laurea Magistrale in Matematica, Curriculum applicativo

Noisy Oncology: applications of bounded noise induced transitions to modelling tumor growth

Tesi di Laurea in Biomatematica

Relatore:
Chiar.mo Prof.
Mirko Degli Esposti

Correlatore:
Chiar.mo Dr.
Alberto D'Onofrio

Presentata da:
Sara Gattoni

Seconda Sessione
Anno Accademico 2010-2011

Contents

List of Figures

Introduction

In former times, mathematics was considered as an intellectual, even spiritual discipline, that had little to do with the real word. Nowadays, mathematics finds application in the physical, biological, and social sciences, and in some of the humanities as well. There appears to be no branch of organized knowledge that cannot benefit -at least to some extent- from the use of mathematical reasoning. Cancer research belongs to one of the various field of biology that may benefit from mathematical treatment.
Macroscopic and microscopic tumors are, quite soon after their first phases of growth, composed by a large to huge number of cells. Thus, in absence of external perturbations, their growth and, in some cases ,as we shall see in this thesis,only up to some extent, equilibrium may be described by differential equations. These can also be used to model perturbations due to human intervention to cure the disease. However, tumor strongly interact on its macroenvironment and as a result a totally deterministic description may be sometime highly inappropriate. In this case the interplay with the statistical fluctuation due to external disturbances ("extrinsic noises") can be take into account by using Ito-Langevin stochastic differential equations (SDE) fields. This is specially true when modelling highly immunogenic tumors interplaying with the immune system, since the complexity of this interaction results in multistability. Thus, the noise may induce noise-induced state transitions (NITs). We point of that a NIT in the tumor size has deep implication on the life of a patient, since a transition from a small equilibrium state of the tumor size to a macroscopic equilibrium in most cases means, unfortunately, a transition from life to death. Note also that, from the point of view of the tumor, this is a clear illustration of the emerging concept that in many cases "noise is not a nuisance".

Apart oncology, SDE-based models and NITs were extensively used in all fields of biomathematics in last 35 years, since seminal works by Horstemke, Lefever and the late Nobel laureate Ilya Prigogine. The standard approach is to model stochastic fluctuations of parameters by means of white or colored Gaussian noise. Very recently, it has pointed out that in some important cases this procedure is highly inappropriate, due to the intrinsic unboundedness of Gaussian noises, which can lead to serious biological inconsistencies: bounded noises must be used, which, however, are far less studied than gaussian noises. Moreover, the onset of NITs depends on the kind of chosen noise, which reveals a novel level of complexity in biology.

The aim of this thesis is to study the applications of bounded-noise induced transitions in two important cases: Tumor Immune-System interplay, and chemotherapy of tumors. In the former case, we also introduce a novel mathematical model of the therapy, which in a new way extends the well-known Norton-Simon biological hypothesis and model.

The thesis is organized as follows:

The first chapter gives an introduction to cancer. I will explain causes, symptoms,diagnosis, stages and treatments of the disease giving also a classification of tumor different types.

In the second chapter I will show some Mathematical models in cancer research divided in carcinogenesis models and models of tumor growth giving also an introduction to chemotherapy models.

In the third chapter I will explain a family of models modeling tumor-immune system competition, and also some numerical simulations regarding the interplay lymphoma-Immune System in chimeric mice.

The forth chapter gives an introduction to noise explaining the meaning of white noise and how to introduce it in some deterministic equations leading to stochastic differential equations.

In chapter five I introduce bounded noises, with particular regard to the creation of bounded "Sine Wiener noise" and bounded "Cai noise".

In chapter six I illustrate the effect of bounded stochastic fluctuations in some key parameters of the above mentioned model of tumor-immune system interaction, by means of the use of Sine-Wiener and Cai noises.

In chapter seven I will study a realistic biophysical model of tumor growth in

presence of the delivering of a constant continuous chemotherapy introducing some stochastic bounded fluctuations that affect both carrying capacity of the tumor and drug level in the blood and showing that they might cause the transition from a low equilibrium to a larger value, not compatible with the life of the host.

Chapter 1

Understanding Cancer

In most people's minds there is no scarier diagnosis than that of cancer. Cancer is often thought of as an untreatable, unbearably painful disease with no cure. **Although in last 40 years treatment of some kind of tumors has luckily had remarkable success, cancer is undoubtedly a very serious and potentially life-threatening illness.** Millions of people die from cancer every year and worldwide trends indicate that millions more will die from this disease in the future. For example, it is the leading cause of death in Americans under the age of 85, and the second leading cause of death in older Americans [Eve10]. However popular this view of cancer may be, it is over-generalized. It is a misconception to think that all forms of cancer are untreatable and deadly. The truth of the matter is that there are multiple types of cancer, many of which can today be effectively treated so as to eliminate, reduce or slow the impact of the disease on patients' lives. Great progress has been achieved in fields of cancer prevention and surgery and many novel drugs are available for medical therapies. While a diagnosis of cancer may still leave patients feeling helpless and out of control, in many cases today there is cause for hope rather than hopelessness.

1.0.1 What is Cancer?

Human's body is composed of many millions of tiny cells, each a self-contained living unit. Normally, each cell coordinates with the others that compose tissues and organs of the body. One way that this coordination occurs is

reflected in how cells reproduce themselves. Normal cells in the body grow and divide for a period of time and then stop growing and dividing. Thereafter, they only reproduce themselves as necessary to replace defective or dying cells. Cancer occurs when this cellular reproduction process goes out of control. In other words, cancer is a disease characterized by uncontrolled, uncoordinated and undesirable cell division. Unlike normal cells, cancer cells continue to grow and divide for their whole lives, replicating into more and more harmful cells. The abnormal growth and division observed in cancer cells is caused by damage in these cells' DNA (genetic material inside cells that determines cellular characteristics and functioning). There are a variety of ways that cellular DNA can become damaged and defective. For example, environmental factors (such as exposure to tobacco smoke) can initiate a chain of events that results in cellular DNA defects that lead to cancer. Alternatively, defective DNA can be inherited from parents. As cancer cells divide and replicate themselves, they often form into a clump of cancer cells known as a tumor. Tumors cause many of the symptoms of cancer by pressuring, crushing and destroying surrounding non-cancerous cells and tissues.

1.0.2 Tumor classification

We may classify tumors in two different ways:

- **Behavioral classification**:
  The greatest distinction of tumor types is between Benign and Malignant:

  Benign Tumors: are not cancerous, thus they do not grow and spread to the extent of cancerous tumors. They are generally slow growing expensive masses , often with "pushing margins" and enclosed within a fibrous capsula.

  Malignant Tumors: They are usually rapidly growing, invading local tissue and spreading to distant sites. The process whereby cancer cells travel from the initial tumor site to other parts of the body is known as metastasis.

It must be noticed that there are some benign tumors that predispose to malignancy and some in situ carcinomas that progress so slowly that they may never achieve malignancy. Anyway the ability to metastasize is evidence of malignancy.

- **Histogenetic classification:**
  The most efficient way to classify tumors is according to the tissue of origin and the cell type involved. Problems in this kind of classification arise because some tumor cells grow in such a way that they bear no resemblance to any structure or cell type. Such anaplastic tumors require more detailed investigation to discover their histogenesis [1]. A further problem is that sometimes a tumor resembles tissue which is not normally present at the site of origin.

1.0.3 The causes of cancer

Cancer is basically a genetic disease even if there are some viral cancer types. There are two differences between it and other genetic diseases:

1. Cancer is generally caused by somatic mutations whereas other genetic disease arise as result of germ line mutations, although a sizable minority.

2. Each individual cancer appears to arise from several sequential mutations (Multi-Hit or Multi-Stage theory of carcinogenesis)

A common general feature of carcinogenesis in both humans and experimental studies is that a relatively long time period elapses between the application of a carcinogenic stimulus and the emergence of clinically recognizable cancer. This is known as the *latent period* and can be from few months to many years. The most likely reason for the latent period is that carcinogenic agent does not cause cancer in one step ,but rather genetically alters normal cell(s) so that it enjoys a proliferative advantage over its normal neighbors. This altered cell(s) then undergos clonal expansion driven by mutation, and the resultant cell could be more susceptible to further changes. Accordingly,

[1] **Histogenesis**: the cellular origin of a tissue or a tumor.

one of these cells later acquires a further mutation allowing its progeny to overgrow its neighbors and perhaps form a small benign tumor. Further phases of clonal expansion and mutation will eventually give rise to a cell with a a sufficient number of mutations ('hits') to bestow the malignant phenotype upon cells arising from it, so that they invade surrounding tissue and metastasize to other organs- thus multi-stage carcinogenesis.
Most carcinomas are rare under 30 years old but then the incidence rate increases dramatically with age. The explanation is that 3 to 7 'hits' are required for a cancer to form.

Initiators and promoters

There are two types of chemical involved in causing cancer:

1. Initiating agents: are "genotoxic agents", binding to DNA and causing mutations. Their effects are irreversible.

2. Promoting agents: circumstances which "promote" the expansion of altered cells. They are ineffective in producing cancer on their own or when given before the initiator.

Thus the process of chemical and irradiation-induced carcinogenesis are thought to initially involve genotoxic events which irreversibly damage DNA (initiators) followed by circumstances which promote the expansion of altered cells. Such progeny could than be 'at risk' of further mutation, leading to cycles of initiation and promotion before emergence of the malignant phenotype.

The environment

The common fatal cancers occurs as a result of lifestyle and other environmental factors and can be preventable. It is not surprising that the environment is implicated in carcinogenesis, as the vast majority of tumors are carcinomas arising from epithelium in direct contact with the environment. Environmental risk factors fall into 3 categories:

1. Physical agents (X-ray,UV-light..)

2. Chemical agents

3. Infectious agents (bacteria,fungi,virus)

Identifying the causes

Through a combination of epidemiological and experimental studies it has been possible, with a reasonable degree of certainty, to identify certain agents which have something to do with the carcinogenic process. Doll and Peto (1981) suggested that there are three determinants for cancer development:

1. Nature: a person's genetic make-up at conception.

2. Nurture: relates to what people do during their lives.

3. Luck.

We must observe that some occupations , medical and social hazards may contribute to the developing of cancer. Years of research have brought to light risk factors that increase people's chances of getting particular types of cancer. Some of these risk factors are inevitable, while others can be avoided by choosing to live a healthy lifestyle. For example, smoking cigarettes is an avoidable risk factor. Changing your lifestyle to get rid of unhealthy choices such as smoking can be difficult to accomplish (tobacco is an addictive drug and stopping smoking means beating that addiction), but the rewards are real. Stopping smoking and similar healthy lifestyle changes will not insure that you never get cancer, but they will reduce your cancer risk. This is true whether you have never had cancer before, or if you have previously beaten cancer and are wondering what you can do to reduce your chances of relapse. It is important to note that cancer is not a uniform illness, but rather has many forms. Each specific type of cancer is different and consequently has a different set of associated risk factors.

Cancer caused by viruses

As we said at the beginning of this chapter, Cancer can be a genetic disease or a viral one.
The relationship between virus and cancer is becoming of profound importance as virus lifestyle inherently affect host cell DNA. Cancer causing viruses

are called oncogenic viruses. Only 17-20 percent of human cancer is thought to be associated with viruses. Oncogenic viruses are classified according to wether they contain DNA or RNA in their genome. DNA viruses are the major cause of human virally-induced cancers.

- DNA oncogenic viruses:
  Such viruses encode proteins which interact with critical cellular growth regulatory molecules sabotaging their function. (EBV,HBV,HPV..)

- RNA oncogenic viruses:
  Only a family of RNA viruses called retrovirus [2] cause tumors. How these retrovirus induce neoplasia [3] is not entirely clear but it may be a combination of an impairment of the immune system to kill tumor cells together with a stimulation of cell proliferation in uninfected or infected immune competent or other cells.

Genetic basis of cancers

Proto-oncogenes are normal cellular genes encoding cytoplasmic and nuclear proteins, responsible for the cell's normal proliferation and differentiation programmes. These genes encode a variety of proteins involved in mitogenesis [4] and differentiation which are organized into a cascade of reactions. For example, the oncogenic activity of the *v-onc* genes seems to be due to either quantitative changes in the levels of expression or differences between the viral and cellular homologues leading to the production of a protein with oncogenic activity. More important probably, in the case of human tumors, proto-oncogenes can be involved in tumorogenesis through point mutation [5], gene amplification [6] or chromosomal translocation [7]. It is now gener-

[2]**Retrovirus:** is a virus whose genome is on the form of single-strained RNA and requires the activity of reversal transcriptase to produce the appropriate DNA because it can complete its intracellular life cycle by becoming incorporated into the DNA of the infected host cell for replication.

[3]**Neoplasia:** the process of tumor formation.

[4]**Mitogenesis:** activity of initiating cell division.

[5]**Point Mutation:** mutation at one single base in a gene, resulting in coding for a different amino acid at this location, thus producing a different protein.

[6]**Gene Amplification:** increase in gene copy number.

[7]**Chromosomal Translocation:** change of location of a gene either on the same chromosome or to different chromosome; when aberrant can cause proximity of genes that

ally believed that most human neoplasia results from abnormalities in the proto-oncogene expression, genes whose normal function is to control cell proliferation and/or differentiation; thus these genes become oncogenes (cancer-causing). They may function as oncogenes because their protein product is abnormal or there is a quantitative defect (too much or too little) in transcription of the gene. Two fundamentally different genetic mechanisms appear to be operative during tumor development:

- Enhanced or aberrant expression of proto-oncogenes.
- Loss or inactivation of tumor suppressor genes.

Oncogenes can be regarded as a foot on the accelerator in the drive toward cell proliferation. Anti-oncogenes, better known as tumor suppressor genes are, on the other hand, a foot on the brake, in that their protein products appear to inhibit cell proliferation. So, the behavior of normal cells seems to be regarded by growth promoting proto-oncogenes , counterbalanced by the growth-constraining tumor suppressor genes. Alterations (point mutations,gene amplification,insertional mutagenesis [8] ,translocation) that potentiate the activities of proto-oncogenes create the oncogenes that promote growth and the establishment of the malignant phenotype. Conversely, genetic alterations in tumor suppressor genes result in a loss of growth restraint normally imposed by the protein products of these genes. The end product of these two events would seem to be the same- deregulated cell behavior (proliferation and differentiation). However , accumulating evidence suggests that the development of many malignant tumors requires both types of change in the tumor genome.

1.0.4 Cancer Symptoms

Every type of cancer is different, and has a unique set of symptoms associated with it. Some cancer symptoms are manifest outwardly, and are relatively

influence each other with overall deleterious effect.

[8] **Insertional Mutagenesis:** retroviral mechanism of cellular transformation. Virus RNA is the template for provirus double-strained DNA and this, in its entirely, is inserted into the host genome, causing mutation.

easy to notice and identify (such as a lump in the breast for breast cancer, or blood in the stool corresponding to colorectal cancer). Other symptoms are observable, but harder to decipher. For instance, two of the major symptoms for lung cancer are a bronchitis-like deep cough and excessive shortness of breath. Few people would assume these symptoms were serious and fewer would associate them with cancer. Still other forms of cancer produce no observable symptoms until they are at a very advanced (and therefore hard to treat) stage.

1.0.5 Cancer Diagnosis

A physician who suspects a patient may have a specific form of cancer will perform a series of tests and procedures to diagnose (or rule-out) a cancer. Commonly, doctors will collect a sample of tissue or fluid from the area believed to contain a cancerous tumor so that it may be analyzed in the laboratory under a microscope. This collection and observation procedure is known as a biopsy. Often, performing a biopsy and analyzing the resulting samples is the only way that doctors can accurately determine a diagnosis of cancer.

1.0.6 Stages of cancer

Following a positive identification of cancer, doctors will try to establish the stage of the cancer. Cancers are ranked into stages depending on the specific characteristics that they possess; stages correspond with severity. Determining the stage of a given cancer helps doctors to make treatment recommendations, to form a likely outcome scenario for what will happen to the patient (prognosis), and to communicate effectively with other doctors. There are multiple staging scales in use. One of the most common ranks cancers into five progressively more severe stages: 0, I, II, III, and IV.

- Stage 0 cancer is cancer that is just beginning, involving just a few cells.
- Stages I, II, III, and IV represent progressively more advanced cancers, characterized by larger tumor sizes, more tumors, the aggressiveness

with which the cancer grows and spreads, and the extent to which the cancer has spread to infect adjacent tissues and body organs.

Another popular staging system is known as the TNM system, a three dimensional rating of cancer extensiveness. Using the TNM system, doctors rate the cancers they find on each of three scales:

- T stands for tumor size.
- N stands for lymph node involvement.
- M stands for metastasis (the degree to which cancer has spread beyond its original locations).

Larger scores on each of the three scales indicate more advanced cancer. For example, a large tumor that has not spread to other body parts might be rated T3, N0, M0, while a smaller but more aggressive cancer might be rated T2, N2, M1 suggesting a medium sized tumor that has spread to local lymph nodes and has just gotten started in a new organ location.
Still another staging system, called summary staging, is in use by the National Cancer Institute for its SEER program. Summary stages include:

- "In situ" or early cancer (stage 0 cancer).
- "localized" cancer which has not yet begun to spread.
- "regional" cancer which has spread to local lymph nodes but not yet to distant organs.
- "distant" cancer which has spread to distant organs.
- "unknown" cancer to describe.

1.0.7 Cancer treatments

Doctors prescribe cancer treatment regimens based on a variety of factors specific to patients' individual circumstance. These factors often include the cancer's stage (type, location, and size of the cancer being treated), as well as patients' age, medical history, and overall health. The doctor may also

ask patients to specify their treatment preferences before determining an optimal treatment plan as far as their condition does not require emergency intervention. In general, it is not a good idea to rush into a treatment plan merely as a way to reduce the understandable anxiety of having a cancer diagnosis.
Each form of cancer is different and calls for a different set of treatment approaches. The main stay of treatment is usually surgical resection combined with systemic chemotherapy or localized irradiation. The use of multiple treatment modalities is known as *Adjuvant Therapy* and the simultaneous use of a number of anticancer drugs is referred to *Combination Therapy*.
Clearly, successful treatments of neoplastic disease largely depends on inflicting the maximum damage on the tumor stem cells and the minimum damage on normal tissue stem cells.
As we said before, there are two types of treatment:

- **Chemotherapy**: is one of the most commonly used methods to treat cancer patients. It is commonly prescribed for patients whose cancer is not localized but instead has possibly metastasized, or spread, to various locations in the body. Chemotherapy can be used to reduce the symptoms and pain associated with cancer as well as to slow the growth of cancerous tumors. In some circumstances chemotherapy may even kill spreading cancerous cells.

  Chemotherapy utilizes a powerful combination of drugs that are either taken by mouth or injected directly into the bloodstream. Drug doses are commonly given in a repeating pattern over a set amount of time. Treatment frequency and duration depend on the type of cancer each patient has, and the manner in which the patient tolerates and responds to the drugs. Chemotherapy drugs target cells in the body that divide and grow quickly and are usually able to destroy these cells. Unfortunately cancer cells are not the only cells in the body which divide and replicate quickly. In addition to cancerous cells, chemotherapy drugs also kill some regular healthy cells, causing side effects such as the fatigue, nausea, and hair loss. To some extent, side effects can be controlled or alleviated with other medications or by altering the

schedule of chemotherapy treatments. Unfortunately, one of the major obstacles to the ultimate success of cancer chemotherapy is the ability of malignant cells to develop resistance to cytotoxic drugs. This may be resistance to a single agent or multi-drug resistance to cytotoxic drugs (MDR) which confers upon cells the ability to withstand to lethal doses of many structurally unrelated agents.

- **Radiation Therapy**: is a method of treating cancer that utilizes radiation energy. Radiation is most commonly used to treat localized cancers as opposed to cancer that has spread throughout the body. The goal of radiation therapy is to kill cancer cells or at least limit their ability to grow and divide by damaging their genetic material. Like chemotherapy, radiation therapy is not perfectly precise in its targeting of cancer cells, and some normal, healthy cells can also become damaged. Patients should not become too concerned about damage to healthy cells, however. Doctors generally do a good job shielding and protecting healthy cells surrounding cancer areas from radiation damage. Also, healthy cells that do sustain damage during radiation treatment are usually able to repair their genetic material when treatment ends.

  There are two main ways in which radiation therapy can be administered: externally and internally. When delivered externally, special machines are used to project a focused beam of radiation into targeted areas of tissue within the body. Internal radiation therapy involves surgical placement of radioactive materials near cancerous tumors or afflicted body areas. When placed internally, the source of radiation is often sealed in a small compartment such as a catheter or capsule prior to implantation.

Chapter 2

Mathematical Models in cancer research

There appears to be no branch of organized knowledge that cannot benefit - at least to some extent - from the use of mathematical reasoning. Biology, the science basic to cancer research, is intermediate between physics and literature in the use which it makes of mathematics. Hence, mathematics can be useful in at least some areas of cancer research and the application of mathematical models to a series of contemporary topics related to the understanding and treatment of cancer is possible.

2.1 Carcinogenesis models

Theoretical carcinogenesis deals with the ways in which malignant disease comes into being. Its scope ranges from detailed molecular theories of the nature of cancer to phenomenological descriptions of the probability of tumor occurrence under specific conditions. The phenomenological end of the spectrum provides the less ambitious goals and also lends itself more readily to the application of mathematical models.

2.1.1 The age incidence pattern of cancer

A natural starting point for many descriptive mathematical models has been the observed age-incidence pattern of human cancer. It is found that most

adult cancers increase rapidly in incidence with increasing age. Each tumor type has is own pattern of occurrence as a function of age which can be modulate by lots of factors. In spite of this , some broad generalizations are possible. For a wide class of human tumors the age incidence pattern is found to conform to an equation of the form:

$$I(t) = Ct^k \tag{2.1}$$

where I(t) is the incidence rate at time t since birth, C,k are constants.

2.1.2 Initiation and promotion

Another very important finding that has influenced carcinogenesis modeling is the observation of a distinction between initiation and promotion in the causation of cancer by chemical carcinogens. It has been found that different chemical substances may play different roles in bringing about a recognizable tumor. Some theories have been proposed that incorporate this feature in their quantitative description of carcinogenesis.

2.1.3 A single cell origin of cancer

A third general idea which is important for some of the models considered here is the single-cell origin (monoclonality) of many human tumors. This implies that all the cells of the tumor are direct descendants from a single cell which has experienced malignant transformation and undertaken unlimited proliferation.

2.1.4 The single-stage theory of cancer

The simplest approach to quantitative carcinogenesis models was developed by Iverson and Arley in 1950. This has been reviewed by Whittemore (1978). Suppose the carcinogenic transformation of a clonogenic cell required only a single irreversible event to occur (events are envisaged as occurring spontaneously as well as being direct consequence of exposure to some carcinogens). The rate $l(t)$ at which normal cell are transformed into malignant cells is:

$$l(t) = s + pC(t) \tag{2.2}$$

where: s is the probability of spontaneous transformation, $C(t)$ is the concentration of carcinogen, p is a constant expressing the dose response relationship for the carcinogen.
If N cells are at risk and carcinogenic transformation occur in depletion of number, the rate $r(t)$ of generation of malignant cells per unit time is:

$$r(t) = (s + pC(t))N \tag{2.3}$$

For anyone of the transformed cells to give rise to a detectable tumor it is presumed that it must proliferate until a detectable cell number N_d has been produced. Iverson and Arley supposed that a transformed cell has a probability β per unit time of dividing and that is independent on unit time and concentration of carcinogen. They calculated on this basis $G(t)$, the proportion of transformed cells whose time of detectability is less than t.

2.1.5 The multi-cell transformation theory

Suppose now that malignant transformation is not a single cell event but requires the cooperation of several cells. If k cooperating cells are needed, the rate at which the kth alteration occurs in the tissue is approximately proportional to $(NpC)^k t^{k-1}$ where $C = const$ is the concentration of the carcinogen.
Whit some other simplifying assumptions it is found that the incidence rate should be proportional to the kth power of carcinogen and $(k-1)$power of time. The observed age incidence curve could be interpreted to mean that seven cooperating cells are necessary for the genesis of a tumor. The evidence on monoclonality of tumors implies that it is unlikely to be true in general. As a result interest has shifted to multistage theories which incorporate the hypothesis of monoclonality.

2.1.6 The multistage theory of cancer

The multistage theory owes its conceptual origins to Muller (1951) and Nordling (1954) and its mathematical formulation to Stocks (1953). The central assumption of the multistage theory is that a single clonogenic cell is transformed to a malignant state as a result of experiencing a sequence of k

events, no one of which can bring about transformation on its own. These may be thought of as being a sequence of k somatic mutations affecting DNA, although this interpretation is not a necessary one. Consider k stages or steps through which a cell must pass sequentially in order to reach the end state or full blown malignant transformation. Let $\lambda_1, \lambda_2, ..., \lambda_k$ be the probabilistic rate constants for entering to a state from the immediately preceding state. The probability that the first event has not occurred by time t is $e^{-\lambda_1 t}$. The probability that the second event is not occurred given that the first is occurred is $e^{-\lambda_2 t}(1 - e^{-\lambda_1 t})$ and so on k terms. The probability of malignant transformation of any cell by time t or less is given by:

$$P(t) = \prod_{j=1}^{k} [1 - e^{-\lambda_j t}] \tag{2.4}$$

provided that successive stages of transformation are mutually independent. Now, since malignancy transformation is rare, λ_i will be very small and we may write:

$$e^{-\lambda_j t} \approxeq (1 - \lambda_j t) \tag{2.5}$$

hence

$$P(t) = A\lambda_1\lambda_2...\lambda_k t^k \tag{2.6}$$

where A is a compound constant (a function of the λ terms).
If there are N cells at risk in the tissue, the age specific incidence rate may be equated to the product of the cell number and the rate of change $P(t)$.

$$I(t) = N\frac{dP(t)}{dt} = NA\lambda_1...\lambda_k k t^{k-1} = B\lambda_1\lambda_2...\lambda_k t^{k-1} \tag{2.7}$$

The general form of multistage theory is consistent with monoclonality , the dorm of age-incidence curves and the initiation-promotion phenomenon.

2.1.7 Epigenetic formulation of the multistage theory

It is not necessary to visualize the k states of the multistage theory as corresponding to a sequence of DNA mutations. An epigenetic version of the theory was developed in 1977 by Watson, involving gene-switching networks

rather than point mutations and was invoked to make the math model consistent with the biological idea that malignant change might involve a derangement of the cellular differentiated state rather than a series of conventional mutations.

2.2 Models of tumor growth

The capacity for progressive growth is one of the most conspicuous property of a malignant tumor once established. Many tissues are in a long-term steady state of cell renewal in which proliferation and cell loss are in equilibrium. Many are also capable of sustained periods of regrowth or regeneration following injury during which the rate of proliferation greatly exceeds the cell loss rate. All normal tissues, however, cease net growth when cell numbers have been restored to the original level or close to it. This behavior suggest a feedback mechanism of some kind. Tumor differs in that the equilibrium level is unattainable or is set so high as to be incompatible with the survival of the host. The regulation of growth control is a very mysterious process. It has been known for a long time that the rate of tumor growth differs between tumors and varies with time for a single tumor. So, it is generally misleading to derive any 'general pattern' of tumor growth; but it is evident that some models of growth occur more commonly than others. It is perhaps not unreasonable to think of typical growth patterns rather than universal or general ones, keeping in mind that some tumors may follow individualistic growth patterns that are quite untypical. With these reservations in mind consider now the simplest possible picture of how a tumor grows. Suppose a tumor at time zero is composed of N_0 cells which divide regularly with a time interval T_c between successive doublings. Assuming the cells are not synchronized , there will be an ongoing increase in cell number given by

$$N(t) = N_0 2^{\frac{t}{T_c}} \tag{2.8}$$

$$log_2(\frac{N(t)}{N_0}) = \frac{t}{T_c} \tag{2.9}$$

This exponential growth pattern is the simplest which it is reasonable to consider. In more complex cases, the doubling time, usually denoted T_D ,

will not be identical with the interdivision time T_c though there will usually be a close relation between them.

2.2.1 The Gompertz growth model

For tumor following decelerating growth curves, a variety of empirical mathematical descriptions have been used to describe the growth mode. Gompertz equation dates back to B.Gompertz who, in 1825, first used it in the context of actual statistics. However, the Gompertz model owes its present popularity to Laird (1964) who developed its use as a growth model.
The algebraic form of the Gompertz equation, applied to a growing cell population, states that:

$$N(t) = N_0 exp(\frac{\alpha N_0}{\beta}[1 - exp(-\beta t)]) \tag{2.10}$$

where $N(t)$ is the cell population at time t, N_0 the population at time t_0 and αN_0 and β are kinetic parameters characteristic of the tumor concerned.
The parameter αN_0 corresponds to the instantaneous specific growth rate of N_0 cells at time zero, if N_0 is the starting size of the tumor at time origin.
The parameter β provides a measure of how rapidly the curve departs from a simple exponential and curves over to assume its characteristic shape.
The model implies a limiting cell number N_∞ which the tumor cell population will approach asymptotically:

$$N_\infty = lim_{t\to\infty} N(t) = N_0 exp\frac{\alpha N_0}{\beta} \tag{2.11}$$

In most cases N_∞ is so large that the tumors burden result in death of the host long before it is reached. It is best regarded as a match abstraction not physically achievable.
The Gompertz equation may be written in a variety of ways. One is the equation represented an exponentially growing cell population whose specific growth rate parameters itself declined with time:

$$\frac{dN(t)}{dt} = \alpha(t)N(t) \tag{2.12}$$

with

$$N(0) = N_0 \tag{2.13}$$

and

$$\frac{d\alpha(t)}{dt} = -\beta\alpha(t) \tag{2.14}$$

with

$$\alpha(0) = \alpha_0 \tag{2.15}$$

However, it is intuitively unreasonable that the specific growth rate parameter $\alpha(t)$ should be a function of clock time. More likely, $\alpha(t)$ depends on some other set of biological variables, and the time dependence arise indirectly.
The Gompertz model is best formulated as differential equation representing the instantaneous rate of change of tumor cell number with time. A differential equation formulation is in fact the most natural and general representation of a growth model. It has the advantage that perturbations of growth can be incorporated by addition of appropriate terms to differential equation.
The equation

$$\frac{dN(t)}{dt} = \beta N(t) ln(\frac{K}{N(t)}) \tag{2.16}$$

is a non-linear differential equation which can be shown to yield the Gompertz algebraic equation on integration.

2.2.2 Tumor growth during latency

All the actual data considered were for the observable phase of growth. The question of how tumors really grow during "latency" is an important one. Some indirect evidence suggesting that Gompertz curves do not provide an accurate representation over the whole growth range. Evidence that is so comes from studies of the relationship between the number of tumor cells implanted in an experimental animal and the time for the resultant tumor to become detectable (the latent period). Suppose growth following implantation of N_0 cells is exponential with constant specific growth parameter α_0. If N is the cell number at which the tumor fist becomes detectable and τ the latent period we have:

$$N' = N_0 exp(\alpha_0 \tau) \tag{2.17}$$

or

$$\tau = \frac{1}{\alpha_0}[ln(N') - ln(N_0)] \tag{2.18}$$

Now suppose the growth follows Gompertz kinetics with parameters αN_0 and β then:

$$N' = N_0 exp(\frac{\alpha N_0}{\beta}[1 - exp(-\beta\tau)]) \tag{2.19}$$

which gives, on rearrangement,

$$\tau = -\frac{1}{\beta} ln(1 - \frac{\beta}{\alpha N_0} ln(N')) - \frac{1}{\beta} ln(\frac{\beta}{\alpha N_0} ln(N_0)) \tag{2.20}$$

In almost all cases studied, the experimental data support the exponential model of growth delay during latency. The implications of these findings is that tumor growth from one cell upwards must be considered in at least two phases: exponential growth during latency and Gompertz kinetics during the observable phase.

2.2.3 The 'Gomp-Ex' growth model

Studies suggested that tumors initially follow an exponential growth pattern which gives rise to a Gompertz pattern after some critical cell number N_C has been reached. This suggest a composite " Gompertz- exponential " growth model described by a piecewise-continuous differential equation:

$$\frac{1}{N(t)} \frac{dN(t)}{dt} = \begin{cases} \lambda & if N \leqslant N_c \\ \lambda - \beta ln(N(t)/N_c) & if N \geqslant N_c \end{cases} \tag{2.21}$$

where N_c is tumor cell number at which transition between growth model occurs.
The integrated form of 'Gomp-ex' equation is

$$N(t) = \begin{cases} N_0 exp(\lambda t) & if N \leqslant N_c \\ N_c exp(\frac{\lambda}{\beta}(1 - exp[-\beta(t - t_c)])) & if N \geqslant N_c \end{cases} \tag{2.22}$$

where

$$t_c = \frac{1}{\lambda} ln(\frac{N_c}{N_0}) \tag{2.23}$$

represents the time to reach N_c from the initial starting size.

2.2.4 A stochastic version of the Gompertz growth model

As a modification of the Gompertz model, Speer et al (1984) introduced a stochastic component. They suggested that the theoretical population limit N_∞ was pre-set as a mutational property of the cells concerned and could be changed by further mutations which were envisaged as taking place randomly over time. An important aspect of these stochastic growth models is that active growth takes place in a series of spurts with intermediate periods during which the tumor is close to the asymptotic limit.

2.2.5 Alternative models for growth retardation

All these models incorporates the feature that tumor growth occurs more slowly as some limit is approached. The cause of this is that growth of a tumor cell population reflect the net balance of tumor cell production and tumor cell loss. Retardation of growth with increasing size might than be attributed to lesser cell production , increased losses or both. Other models have been created but we will not discuss them here.

2.2.6 Compartmental model based on cellular differentiated state

The existence of differentiated cells warrants attention in the construction of growth models. The simplest kinetic picture of a differentiating tumor assigns tumor cells to one of the three compartments:

1. True tumor cells with full clonogenic potential (immortal stem cells in proliferative normal tissues).

2. Cells which have begun differentiation.

3. Differentiated cells, no longer capable of cell division.

As a first simple model we may assume there is constant probability per unit time of a clonogenic cell being induced to differentiate (proportional to the size of the clonogenic compartment). Once induced, differentiated cells

move through the intermediate developmental stage in programmed fashion in fixed time. Loss may be either random or result from programmed ageing (we assume random losses).
These conditions give rise to a compartmental model:

$$\frac{dN_1(t)}{dt} = H[t, N_1, N_2, N_3]N_1(t) - \omega_1 N_1(t) - F(t) \tag{2.24}$$

$$\frac{dN_2(t)}{dt} = F(t) + (\alpha - \omega_2)N_2(t) - exp[(\alpha - \omega_2)\tau]F(t - \tau) \tag{2.25}$$

$$\frac{dN_3(t)}{dt} = exp[(\alpha - \omega_2)\tau]F(t - \tau) - \omega_3 N_3(t) \tag{2.26}$$

where $N_1(t)$ represents the number of clonogenic cells with proliferative rate α_0 and loss rate ω_1, $N_2(t)$ represents the number of developing cells with proliferative rate α and loss rate ω_2, $N_3(t)$ represents the number of differentiated cells with loss rate ω_3, H is a mathematical function. We have supposed the rate of loss of clonogenic cells due to induction of differentiation is directly proportional to clonogenic cells number:

$$F(t) = \mu N_1(t) \tag{2.27}$$

Thus we have:

$$\frac{dN_1(t)}{dt} = H[t, N_1, N_2, N_3]N_1(t) - (\omega_1 + \mu)N_1(t) \tag{2.28}$$

$$\frac{dN_2(t)}{dt} = \mu N_1(t) + (\alpha - \omega_2)N_2(t) - exp[(\alpha - \omega_2)\tau] \tag{2.29}$$

$$\frac{dN_3(t)}{dt} = \mu exp[(\alpha - \omega_2)\tau]N_1(t - \tau) - \omega_3 N_3(t) \tag{2.30}$$

Clearly, solutions depend on H, specific proliferative rate of clonogenic cells.

2.3 Models for tumor response to chemotherapy

Cancer chemotherapy is a very much more complex treatment modality to consider than radiotherapy. This is because chemotherapy is not a single modality at all but a collective name for as many modalities as there are anti-cancer drugs. Commonly, several drugs, often with different modes of action, are used together in combination regimes and are more effective than treatment using single agents. These features do not make cancer chemotherapy a very promising subject for mathematical modeling. Quantitative modeling has the potential to be useful but is likely to require knowledge of the numerical values of large numbers of parameters necessary to characterize combination chemotherapy regimes. This information is very seldom available, consequently , though a considerable literature has grown up on mathematical modeling in cancer chemotherapy, this had a significant impact on clinical treatment in only a few cases.

2.3.1 Drug Action

The spectrum of drugs now available in cancer chemotherapy sterilize cells by a variety of mechanisms. An important class of drugs, *alkylating agents* achieve their major effects by cross-linking DNA [DH09]. Another important group of drugs are the *metabolic inhibitors* which selectively interfere with particular enzymes. The *antibiotic actinomycin D* has found some application in cancer chemotherapy, it is thought it achieves its cytotoxic effect by inhibiting the transcription of RNA to DNA. These examples show a few of the different mechanisms by which anti-cancer drugs kill cells. It is generally not known why some drugs are more effective than others in treating cancer. In practice, the most important criterion for drug classification is in terms of their cycle specificity. Most anti-cancer drugs are more toxic to rapidly proliferating cells than resting G_0 cells [DH09]. However, this cell kinetic differential varies greatly in magnitude between drugs. For alkylating agents and similar drugs, cycle specificity of action is not very pronounced; we can call such drugs **cycle-non-specific**. For other drugs, the difference between

the sensitivities of cycling and non cycling cells is much greater. These drugs are often called **cycle-specific**. In terms of tumor response to chemotherapy is important this distinction.
A great consideration in cancer chemotherapy concerns the drug dose to tumor and to critical normal tissues. A natural fist step in determine the "right dose" would be to find drug concentration as a function of time for each relevant tissue as well as tumor. This is the subject of pharmacokinetics in which mathematical models often play a useful role, usually representing important tissues or body regions as a series of compartments and formulating differential equations to describe the movement of drug from one compartment to another.
I will now consider mainly the general principles of how cancer chemotherapy works assuming that drug concentrations are usually known.

2.3.2 Exposed cells and effects of chemotherapy

- Normal Tissues:
  Usually cancer chemotherapy is given systemically; all normal tissues and organs will be exposed to the drug and any of them may be injured. It's fundamental to consider normal tissue damage as a constraint that must be built into any model used to predict optimum schedules. The effectiveness of chemotherapy over normal tissues depends on the intensity with which therapy can be given. Some chemotherapy drugs are very diverse and tissues may be dose-limiting for different drugs or drug combinations. At the present to little is known about mathematical dose-response relationships for normal tissue toxicity so it is difficult to apply general models; some empirical rules have been found in practice but they do not usually take analytical form which leads to prediction of tolerance doses when the schedule is changed.

- Tumoral cells:
  Rapidly growing tumors are usually the most responsive to cancer chemotherapy. This is probably due to the cycle-specific mode of action of many chemotherapeutic drugs.

2.3.3 Cycle non-specific chemotherapy of a tumor cell population conforming to Gompertz kinetics

Recall:
Gompertzian growth of an untreated tumor cell population may be described by the non-linear differential equation:

$$\frac{1}{N(t)}\frac{dN(t)}{dt} = \alpha_{N_0} - \beta ln(\frac{N(t)}{N_0}) \tag{2.31}$$

where α_{N_0}, β are kinetic parameters. In equivalent form:

$$\frac{1}{N(t)}\frac{dN(t)}{dt} = -\beta ln(\frac{N(t)}{N_\infty}) \tag{2.32}$$

where $N_\infty = N_0 exp(\frac{\alpha_{N_0}}{\beta})$ and represents the theoretical maximum size to which the growth curve is asymptotic.

Consider now the effect of exposing the tumor cell population to a cycle-non-specific drug at concentration $C(t)$. For the case of an exponential dose-response relationship between drug concentration and rate of cell killing, we may write

$$\frac{1}{N(t)}\frac{dN(t)}{dt} = -\beta ln(\frac{N(t)}{N_\infty}) - \lambda C(t) \tag{2.33}$$

provided the cells sterilized by the drug disappear quickly from the population. The solution depends on the functional form of the drug concentration $C(t)$. In many real situations $C(t)$ would be obtained by interpolation from measurement of drug concentration in blood or by solution of pharmacokinetic model (by numerical integration).
Considering the idealized case where drug concentration remains constant throughout the time of interest $C(t) = C(0)$ we have

$$\frac{1}{N(t)}\frac{dN(t)}{dt} = -\beta ln(\frac{N(t)}{N_\infty}) - \lambda C(0) \tag{2.34}$$

which can be solved by change of variable leading to

$$log(\frac{N(t)}{N(0)}) = (\frac{\alpha_{N_0}}{\beta} - \frac{\lambda C_0}{\beta})[1 - exp(-\beta t)] \tag{2.35}$$

It is useful to compare this equation with the algebraic expression for Gompertzian growth of an untreated cell population

$$log(\frac{N(t)}{N(0)}) = \frac{\alpha_{N_0}}{\beta}[1 - exp(-\beta t)] \tag{2.36}$$

Equations (2.35) (2.36), have the same form.
For low drug concentrations the term $(\frac{\alpha_{N_0}}{\beta} - \frac{\lambda C_0}{\beta})$ is positive and the tumor continues to grow, more slowly than in the untreated case. A new asymptotic limit, depending on drug concentration, $N_\infty(C_0)$ can be defined. Equation (2.35) can be rewritten

$$N(t) = N(0)exp[(\frac{\alpha_{N_0}}{\beta} - \frac{\lambda C_0}{\beta})[1 - exp(-\beta t)]] \tag{2.37}$$

therefore

$$N_\infty(C_0) = lim_{t\to\infty}(N(t)) = N_\infty exp(\frac{-\lambda C_0}{\beta}) \tag{2.38}$$

For higher drug concentrations the term $(\frac{\alpha_{N_0}}{\beta} - \frac{\lambda C_0}{\beta})$ is negative, the asymptotic limit $N_\infty(C_0)$ will be less than the initial cell number N_0 and the tumor does not grow but regress.

2.3.4 Cycle-specific therapy

Changing loss factor

In the case of cycle-specific therapy the analysis differs. First consider the case where the growth fraction remains constant and retardation is entirely due to changing loss factor.
The most important factor is the proportion of cycling cells. Assume the growth fraction f to be constant. Then, in the presence of cycle-specific drug we have

$$\frac{1}{N(t)}\frac{dN(t)}{dt} = -\beta ln(\frac{N(t)}{N_\infty}) - f\mu C(t) \tag{2.39}$$

where μ is the appropriate drug sensitivity parameter. In this case only proliferation cells are vulnerable to cycle-specific therapy in fact the parameter λ is replaced by $f\mu$. The decline of tumor cells number follow the same pattern as for cycle-non-specific drug.

Changing growth fraction

Now consider the case where Gompertz retardation is entirely due to a changing growth fraction. In this case the growth fraction $f(t)$ is not constant but varies with cell population size. If C(t) is the concentration and K(t) the rate of cell kill due to a cycle-specific drug, we have

$$K(t) = \mu f(t) N(t) C(t) \tag{2.40}$$

where μ is the sensitivity parameter for the effect of the drug on cycling cells. Thus we have

$$\frac{1}{N(t)} \frac{dN(t)}{dt} = -\beta ln(\frac{N(t)}{N_\infty}) \tag{2.41}$$

$$\frac{1}{N(t)} \frac{dN(t)}{dt} = \lambda f(t) \tag{2.42}$$

where λ is the specific growth rate for constantly cycling cells.
Equating last two we obtain the following expression for instantaneous growth fraction f(t):

$$f(t) = \frac{\beta}{\lambda} ln(\frac{N(t)}{N_\infty}) \tag{2.43}$$

which allows to represent the effects of cycle- specific killing agent

$$\frac{1}{N(t)} \frac{dN(t)}{dt} = -\beta ln(\frac{N(t)}{N_\infty}) - \mu f(t) C(t) \tag{2.44}$$

$$= -\beta ln(\frac{N(t)}{N_\infty}) - \mu[-\frac{\beta}{\lambda} ln(\frac{N(t)}{N_\infty})] C(t) \tag{2.45}$$

$$= -\beta ln(\frac{N(t)}{N_\infty})(1 - \frac{\mu}{\lambda} C(t)) \tag{2.46}$$

and to find the critical drug concentration to initiate depopulation. This requires

$$\frac{1}{N(t)} \frac{dN(t)}{dt} < 0 \tag{2.47}$$

Therefore

$$1 - \frac{\mu}{\lambda} C(t) < 0 \tag{2.48}$$

or

$$C(t) > \frac{\lambda}{\mu} \tag{2.49}$$

This condition is independent of cell population size. This means that a drug concentration sufficient to initiate depopulation should be sufficient to maintain it. The phenomenon of Kinetic resistance [1] cannot occur in this situation.
It is also informative to consider the case of constant drug concentration $C(t) = C(0)$. This gives for equation (2.46),

$$\frac{1}{N(t)}\frac{dN(t)}{dt} = -\beta ln(\frac{N(t)}{N_\infty})(1 - \frac{\mu C_0}{\lambda}) \tag{2.50}$$

This may be integrated to give

$$ln(\frac{N(t)}{N_0}) = (-ln(N_\infty))(1 - exp[\beta(\frac{\mu C_0}{\lambda} - 1)t]) \tag{2.51}$$

which is a function whose decline accelerates with time, provided the drug concentration C_0 conforms to inequality (2.49) and therefore is sufficient to initiate depopulation in the first place.
It must be noticed that this model incorporates the implicit assumption that the growth fraction of the tumor cell population responds instantaneously to cell killing by chemotherapy.

[1] **Kinetic resistance** means that a chemotherapy schedule which initiates depopulation may nevertheless fail to achieve tumor cure, however long treatment is continued. Consider the drug concentration level which produce a rate of cell kill just sufficient to balance cell repopulation. Let this critical concentration be $C_0^{(c)}$. Then if $C_0 < C_0^{(c)}$ a net depopulation would occur and the tumor will regress. For a tumor cell population whose growth conforms to Gompertz kinetics, treated by cycle-non-specific drug, the net rate of change is given by $\frac{1}{N(t)}\frac{dN(t)}{dt} = -\beta ln(\frac{N(t)}{N_\infty}) - \lambda C(0)$. If the drug concentration is just sufficient that the rate of cell kill balances rate of repopulation we have: $\frac{1}{N(t)}\frac{dN(t)}{dt}|_{C=C_0^{(c)}} = 0$ so that $-\beta ln(\frac{N(t)}{N_\infty}) = \lambda C_0^{(c)}$. Therefore, at any instant, the requirement for depopulation to proceed is that $C_0 > C_0^{(C)}$ that is $C_0 > -\frac{\beta}{\lambda} ln(\frac{N(t)}{N_\infty})$. This means that the condition to initiate tumor cell depopulation is itself a function of population size. The drug concentration to initiate depopulation is larger the smaller the population size. A corollary is that the drug concentration to maintain depopulation will become larger as the population shrinks. The possibility than arises that drug concentration which initiates depopulation will not be sufficient to maintain it which is the meaning of Kinetic resistance.

The general case

Last consider the case where Gompertz retardation is not exclusively due either to changing loss rate or changing growth fraction but a mixture of the two:

$$\frac{1}{N(t)}\frac{dN(t)}{dt} = \lambda f(t) - L(t) \tag{2.52}$$

$$\frac{1}{N(t)}\frac{dN(t)}{dt} = -\beta ln(\frac{N(t)}{N_\infty}) \tag{2.53}$$

Equating (2.52) and (2.53)

$$\lambda f(t) - L(t) = -\beta ln(\frac{N(t)}{N_\infty}) \tag{2.54}$$

Hence

$$f(t) = \frac{1}{\lambda}[L(t) - \beta ln(\frac{N(t)}{N_\infty})] \tag{2.55}$$

Evaluate this in explicit terms requires knowledge of loss function $L(t)$; no general solution is possible for this case. Intuitively, it seems reasonable that if the retardation is mainly due to loss-factor changes then kinetic resistance would occur, but if the retardation is mainly due to a changing growth fraction, the kinetics of depopulation would be accelerating in form. Intermediate situations are possible, it may not be possible to reach clear-cut conclusions.[2].

[2]It is not difficult to see how the results would be modified if we assume 'Gomp-ex' kinetics instead of Gompertz one. For more detailed explanation see [Whe98]

Chapter 3

Modeling tumor-immune system competition

The complex and non-linear interplay of the immune system (IS) with non-self entities offers and ideal area of research and has long been a source of great interest for physicists. In particular, the interaction of IS with tumors is a classical challenge in the world of biophysics.
Molecular biology has shown that tumor cells (TCs) are characterized by a vast number of genetic events leading to the appearance of specific antigens, which trigger action by the IS. These experimental observations have provided a theoretical basis to the old empirical hypothesis of immune surveillance i.e that the IS may act to control or eliminate tumors. Only in recent years, experimental and epidemiologic evidence has been accumulated in favor of the hypothesis and it has been demonstrated that the IS can suppress tumors. The competitive interaction between TCs and the IS, involves a considerable number of events and molecules, and as such is extremely complex and, as a consequence, the IS is not able to eliminate a neoplasm in all cases, which may escape from IS control. Of course, a dynamic equilibrium may also be established, such that the tumor may survive in a microscopic steady state (MISS), which is undetectable by diagnostic equipment. However, consider a tumor which is constrained by the IS in a MISS. Over a long period of time (a significant fraction of the mean life span in men), the neoplasm may develop multiple strategies to circumvent the action of the IS , which, in the

long term, may allow it to evade immune surveillance and to re-commence growing to its carrying capacity . The tumor has adapted itself to survive in a hostile environment, in which antitumor immune response is activated. In other words the immunogenic phenotype of the tumor is "sculpted" by the interaction with the host's IS. For this reason, the theory of IS-Tcs interaction has been called immunoediting theory by Dunn et al.

Finally, the study of the interaction tumor-immune system led to the proposal and implementation of an interesting therapeutic approach: the immunotherapy, consisting in stimulating the IS in order to better fight, and hopefully eradicate, a cancer. The basic idea of immunotherapy is simple and promising, but the results obtained in medical investigations are globally controversial, even if in recent years there has been evident progress.

Coming to the mathematical way to model the above interactions, the basic idea of the ecological modeling of TCs-IS interaction is simple: TCs and effector cells (ECs) of IS are seen as two competing populations. TCs are mainly the prey of the ECs, whose proliferation is stimulated, in turn, by the presence of TCs. However, TCs also induce a loss of ECs; and there is an influx of ECs, whose intensity may depend on the size of the tumor. Based on this simple scheme and on its generalizations, many works have appeared using a finite dimensional approach based on specific models with constant or tunable parameters (and references therein).

However an approach based on a specific model is in contrast with the polymorphic nature of cancer, and it does not allow easily to catch the general features of the TC-IS interaction.

We now propose and investigate a family of models, which admits as particular cases some well known mathematical models of tumor-immune system interaction, with the additional assumption that the influx of immune system cells may be a function of the number of cancer cells.

3.1 A general family of models and its properties

A very interesting Volterra-like model for the interaction between a population of tumor cells ,whose number is denoted by (X), and a population of lymphocyte cells,whose number is denoted by (Y) was proposed by Sotolongo-Costa et al.[OCCR03]:

$$X' = aX - bXY \tag{3.1}$$

$$Y' = dXY - fY - kX + u + P(t) \tag{3.2}$$

where the tumor cells are supposed to be in exponential growth (which is, however, a good approximation only for the initial phases of the growth) and the presence of tumor cells implies a decrease of the "input rate" of lymphocytes. In non-dimensional form [OCCR03]:

$$x' = \alpha x - xy \tag{3.3}$$

$$y' = xy - \frac{1}{\alpha}y - kx + \sigma + p(t) \tag{3.4}$$

(in short notation $(x', y') = C(x, y)$).
The function $p(t) \geq 0$ is assumed periodic with period T and it models the effect of immunotherapy.
The model shows two equilibria (one of which is tumor-free) and also unbounded growth. However, the systems allows negative solutions for non-small x, which is not physically acceptable. In fact:

$$C(x, 0) = \alpha x, \sigma + p(t) - kx \tag{3.5}$$

implies that for $x > \frac{(\sigma + p_{max})}{k}$ it is $C(x, 0) = (0, -1) > 0$, and $y(t)$ becomes negative in finite times. Furthermore, the second equilibrium point is a consequence of the negativity of $\sigma - kx$.

The model in [OCCR03], though it has this problem of lack of physical consistency, is, however, of great interest because the killing of lymphocytes is seen as function of the x variable. Alternatively, the influx of lymphocytes may be thought of as a function of the entity of the disease, which we

will denote as Q(x). Indeed, it has been observed that in some cases cancer progression may cause generalized immunosuppression [J.S01]. Thus in [OCCR03], $Q(x) = \sigma(1 - (k/\sigma)x)$, which may be read as a first order Taylor approximation of a more general non-increasing function.
However, a general influx function is only one of the possible modifications of models: there may be others, which are also biologically reasonable. One might take into the account many factors: different functional forms for the interaction term, saturation in the predation term and, mainly, non-exponential growth of the cancer: logistic, Gompertzian, generalized logistic, etc. All these modifications are reasonable and useful.
Thus, it might be useful to define and study the following general family of models:

$$x' = x(\alpha f(x) - \phi(x)y) \tag{3.6}$$

$$y' = \beta(x)y - \mu(x)y + \sigma q(x) + \theta(t) \tag{3.7}$$

where:

- x and y are the non-dimensionalized numbers of, respectively, tumor cells and effectors cell of immune system;

- $0 < f(0) \leq +\infty$, $f'(x) \leq 0$ and in some relevant cases we shall suppose that it exists an $0 < \bar{x} \leq \infty$ such that $f(\bar{x}) = 0$, $lim_{x\to 0^+} xf(x) = 0$. Thus, $f(x)$ summarizes many widely used models of tumor growth rates, such as the Exponential model: $f(x) = 1$ [Whe98], the Gompertz: $f(x) = log(\frac{A}{x})$ [Whe98] and its generalizations [Whe98].

- $\phi(x) > 0$, $\phi(0) = 1$, $\phi'(x) \leq 0$ and $x\phi(x) \to l \leq +\infty$;

- $q(x)$ is such that $q(0) = 1$ (as a consequence $\sigma = Q(0)$) and it may be non-increasing or also initially increasing and then decreasing, i.e. we may assume that either the growth of tumor decreases the influx of immune cells or that, on the contrary, it initially stimulates the influx;

- $\beta(x) \geq 0$, $\beta(0) = 0$ and $\beta'(x) \geq 0$;

- $\mu(x) > 0$ and $\mu'(x) > 0$.

For the sake of simplicity we define the following function $\Psi(x) = \mu(x) - \beta(x)$ and write:

$$x' = x(\alpha f(x) - \phi(x)y) \tag{3.8}$$

$$y' = -\Psi(x)y + \sigma q(x) + \theta(t). \tag{3.9}$$

$\Psi(x)$ is assumed to be positive, otherwise it may be positive in $[0, x1) \bigcup (x2, +\infty)$ with $\Psi(x1) = \Psi(x2) = 0$. We may assume that it has an absolute minimum in $[0, +\infty)$. We may use $\Psi(x)$ to classify the tumors depending on their degree of aggressiveness against the immune system:

- $\Psi(x) > 0$: in such a case the ability of destroying immune cells is never won by the stimulatory effect on the immune system, therefore the tumor may be indicated as "highly aggressive"/"lowly immunogenic";
- Variable sign of $\Psi(x)$: since in such a case the destruction of cells may be compensated by the stimulatory effect, we will refer to such a tumors as "lowly aggressive"/"highly immunogenic".

Note that Nani and Freedman proposed an interesting model of adoptive cellular immunotherapy in which generic functions are used [F.N00]. However, their approach differs from ours since in their model the proliferation of cells of the immune systems is not stimulated by cancer cells. In other words in the Nani and Freedman model the interaction tumor cells-immune system is only destructive for immune cells. Furthermore, in their model the 'loss rates' are proportional (in our notation we might write $\mu(x) = \mu(0) + const\phi(x)$).

In the absence of treatment, systems (3.8) and (3.9) admits the existence of a cancer free equilibrium $CF = (0, \frac{\sigma}{\Psi(0)})$.
If $f(0) < +\infty$, we have that if $\sigma > \sigma_{cr} = \frac{\alpha\Psi(0)f(0)}{\phi(0)}$ CF is locally asymptotically stable (LAS), unstable if $\sigma < \sigma_{cr}$. Biologically, $\sigma > \sigma_{cr}$ means that the immune system works very well and that it is able to destroy small tumors. On the contrary $\sigma \approx 0$ means that there is immunodepression.

Furthermore, when $\phi(x) = constant = \varphi$ and $\Psi(x) \leq \Psi^* < \infty$ if $\sigma > \sigma^* = \frac{\alpha f(0)\Psi^*}{(q_{min}\varphi)}$ it follows that CF is globally asymptotically stable (GAS). In fact, from $y' = -\Psi(x)y + \sigma q(x) \geq -\Psi^* y + \sigma q_{min}$ it follows that asymptotically $y(t) \geq \frac{\sigma q_{min}}{\Psi^*}$ As a consequence, asymptotically $x' \leq (\alpha f(0) - \varphi(\frac{\sigma q_{min}}{\Psi^*}))x$, i.e. if $\sigma > \sigma^*$ it is $x(t) \to 0 \Rightarrow y(t) \to \frac{\sigma}{\Psi(0)}$.
A relevant problem, up to now, is that the immunotherapeutic agents are characterized by strong toxicity, thus $\sigma > \sigma^*$ might be too biologically high,even in cases in which it is mathematically small.

If $f(0) = +\infty$, as in the Gompertzian case and in other tumor growth models, then CF is unstable anyway because in such a cases the derivative of $xf(x)$ at $x = 0$ is $+\infty$. In the light of our generalization, this implies that the immune system would never be able to totally suppress even the smallest tumor cell aggregates, which is a very strong inference. This instability result deserves some comments because it has deep medical implications: the impossibility to completely recover from any type of tumors whatsoever. On the contrary, it is commonly held that the immune system may be able, in some cases, to kill a relatively small aggregate of cancer cells. In the background of all cancer therapies (which are of finite duration) there is the implicit hypothesis that the drug will kill the vast majority of the malignant cells and that the relatively few residual cells may in some cases be killed by the immune system. Accepting this hypothesis, the equilibrium CF should have the possibility to be LAS and, as a consequence, for small x the function $f(x)$ should be bounded.
The modeling of cancer by means of the Gompertz law of growth was introduced in early sixties by Laird [Lai64], [Lai65]. She conducted pioneering data-fitting work using a vast amount of real data and justified the law in terms of increasing mean generation time. There is much research showing that the Gompertzian model fits data well from experimental and in vivo tumors [I.D94, JtA94, A.M94, IM03]. From a theoretical point of view, Gyllenberg and Webb [M.G89], Calderon and Kwembe [CC91], Calderon and Afenya [E.K00, E.K04] proposed physico-mathematical justification of the Gompertz model. Furthermore, some interesting physical properties of the Gompertz model have been elucidated by Konarski and Molski [M.M03] and

by Konarski and Waliszewski [P.W03]. However, the doubling time of a population of cells cannot be lower than the minimal time needed by a cell to divide, which is obviously non-null. This biological constraint is in contrast with the unboundedness of $f(x)$ in the Gompertz and other models, as stressed by Wheldon [Whe98]. More recently, inconsistency at low number of cells have been recognized by Castorina and Zappala' in their derivation of the Gompertzian model based on methods of statistical mechanics [P.C04b, P.C04a]. They showed that the validity of the Gompertz model starts above a minimum threshold for the number of cells, whereas under the threshold there is exponential growth. In other words, they derived biophysically the Gomp-Ex model proposed in the second chapter [Whe98]. Using data from multicellular tumor spheroids, Marusic et al. performed a systematic comparison of many models [JSP94], which showed that Gompertzs model fitted their data very well, but slightly less well than the Piantadosi model [S.P85], which has finite $f(0)$. Furthermore, in their fittings, it was not possible to discriminate between the pure Gompertz model and the Gomp-Ex model. Demicheli et al. used Gomp-Ex model on in vitro and in vivo data obtaining results strongly supporting this model [CM89]. Moreover, in general,van Leeuwen and Zonneveld [IL01] claims that it may be not possible to discriminate between exponential, logistic and Gompertzian models in the early phases of growth. Recent experimental studies conducted by Bru and coworkers support an initial phase of exponential growth [GAI03]. Summarizing, the results by de Vladar and Gonzalez are valuable, but they may be read in a dichotomic way:

- A tumor is permanent: the innate immune surveillance is never able to completely eradicate even the smallest tumor.

- Since there is relevant evidence that the immune system is able in some cases to eliminate small tumors [GR02, G.P04] (the ability of eradicate the disease or not depends on initial conditions), the properties of the de Vladar Gonzalez model may be seen as an evidence that Gompertzian and other models characterized by $f(0) = +\infty$ are not appropriate for very small tumors, (in coherence with [Whe98, P.C04b, P.C04a, GAI03]).

In case of the absence of influx of immune cells ($q(x) = 0$) and for laws of growth in which $\bar{x}$ exists,there is a different particular equilibrium point, which we shall call "immune free": IF =($\bar{x}$,0), which is LAS.

Other multiple non-null equilibria may be found by finding the positive intersection of the two nullclines:

$$y_c(x) = \alpha \frac{f(x)}{\phi(x)} \tag{3.10}$$

$$y_I(x) = \frac{\sigma q(x)}{\Psi(x)} \tag{3.11}$$

The functions $y_c(x)$ and $y_I(x)$ are useful in the determination of the LAS of the equilibria , since the characteristic polynomial of the Jacobian, calculated at a given equilibrium point (x_e, y_e), is:

$$\lambda^2 + (\Psi(x_e) - x_e\phi(xe)y_c'(x_e))\lambda + \Psi(xe)xe\phi(xe)(-y_c'(xe) + y_I'(xe)) = 0. \tag{3.12}$$

So the LAS condition is:

$$y_c'(xe) < \frac{\Psi(x_e)}{x_e\phi(x_e)}$$

AND

$$y_I'(xe) > y_c'(xe)$$

Note that the first part of the AND condition is automatically fulfilled when $y_c'(x) = 0$ (because x_e cannot lie in an interval where $\Psi(x) < 0$), whereas the second part has a straightforward geometrical interpretation.
Finally, it is interesting to note that the above family of model may admit limit cycles if $f(x) = 1$ (exponential growth) and $q(x)$ is identically null for $x > x_q$ with $x_q < x_1$. In fact, in such a case there is the equilibrium point (x_1, α) whose characteristic polynomial is:

$$\lambda^2 + h^2 = 0 \quad h^2 := -x_1\Psi'(x_1)\alpha > 0$$

In effect, some cases of sustained oscillations (or slow oscillations with very small damping) have been reported in the medical literature [B.J70,

H.T97]. Periodic solutions in absence of influx of immunocompetent cells are also predicted [D.K98].

On the contrary, if $y_c'(x) \leq 0$ (for example when $\Psi(x)$ is constant), by applying the Dulac - Bendixon theorem with multiplicative factor $\frac{1}{(xy\phi(x))}$ one obtains that the presence of limit cycles is not possible. In fact:

$$Div(\frac{1}{xy\phi(x)}(x'(x,y),y'(x,y))) = \frac{\alpha y_c'(x)}{y} - \sigma\frac{q(x)}{x\phi(x)y^2} < 0 \tag{3.13}$$

3.2 On immunotherapies

3.2.1 Therapy schedulings

A realistic anticancer therapy may be modeled with sufficient approximation as constant (e.g. via a constant intravenous infusion) or periodic (e.g. the agent is delivered each day as a bolus):

$$\theta(t) = \theta_m + \Omega(t) \geq 0,\ \theta(t+T) = \theta(t),\quad \theta_m = \frac{1}{T}\int_0^T \theta(t)dt \tag{3.14}$$

For humans, typical periods ranges between 8 hours to 7 days [VVJ97, Edi03]. A particular case of periodic therapy is pulsed therapy, i.e. a therapy which induces an instantaneous increase of the number of lymphocytes:

$$\theta(t) = \gamma\sum_{n=0}^{+\infty}\delta(t-nT) \tag{3.15}$$

In the case of constant infusion therapy (CIT) ($\theta(t) = \theta_m$) by defining:

$$\widehat{\sigma} := \sigma + \theta_m,\quad \widehat{q}(x) := \frac{\sigma+\theta_m}{\widehat{\sigma}} \tag{3.16}$$

3.2.2 Continuous infusion therapy

All the considerations we have done the absence of therapy hold also in case of CIT. In particular, for $f(0) < +\infty$, the condition for the LAS of the cancer-free equilibrium is:

$$\sigma + \theta_m > \sigma_{cr} \tag{3.17}$$

Because of the co-presence of other equilibria, the above criterion is not global, i.e. the immunotherapy is not able to guarantee the disease eradication from whatever initial values $(x(0), y(0))$. However, observing that in models in which $\Psi(x) > 0$:

$$y_I^{withtherapy}(x) = \frac{\sigma q(x) + \theta_m}{\Psi(x)} > y_I^{notherapy}(x) \tag{3.18}$$

(e.g. in Stepanova's model with low μ_1) it happens that, roughly speaking, the stable equilibrium size of the cancer becomes smaller and the unstable equilibria greater, so that the basin of attraction of the unbounded solution is reduced. When $f(0) = +\infty$ the total elimination cannot be achieved by immunotherapy alone. Furthermore, even the suboptimal target of reducing the cancer to a microscopic size in many relevant cases cannot be achieved for therapies of finite duration, however they may be long. In fact, let it be $\Psi(x) > 0$ (aggressive tumor) and let there be a unique GAS macroscopic equilibrium E_{MACRO}. By applying a CIT with θ sufficiently high there is a unique GAS microscopic equilibrium. However, when the therapy ceases θ falls to zero and the cancer restarts growing macroscopically, since E_{MACRO} is again GAS. We note in brief that if the original equilibrium is microscopic (e.g. micrometastasis) the effect of the therapy is simply to create another and temporary microscopic equilibrium.

Let us suppose that there are three co-existing equilibria: E^o_{micro} (LAS), E^o_U (Unstable and through which a separatrix Σ^o passes) and E^o_{MACRO} (LAS). Applying a CIT with $\theta > \tilde{\theta}$ there is an unique GAS microscopic equilibrium. Thus at the end of the therapy (at $t = t_f$) depending on the position of $P_f = (x(t_f), y(t_f))$ relatively to Σ^o, we have that either $(x(t), y(t)) \to E_{micro}$ or $(x(t), y(t)) \to E_{MACRO}$.

We note that θ acts a global bifurcation parameter, and we point out that these behavior may be observed in case of bounded $f(0)$ when therapy is applied for an insufficient time.

3.2.3 Periodic Scheduling

In the case of periodic drug schedulings, there is a periodically varying cancer-free solution $CF^* = (0, z(t))$, where $z(t)$ is the asymptotic periodic solution

of:

$$y' = -\Psi(0)y + \sigma + \theta_m + \Omega(t) \tag{3.19}$$

that, assuming $\Omega(t) = \sum_{n=1}^{+\infty} C_k Cos(k(2\pi/T)t - \zeta_n)$, can be rewritten as::

$$z(t) = \frac{\sigma + \theta_m}{\Psi(0)} + \sum_{n=1}^{+\infty} \frac{C_k}{\sqrt{\Psi^2(0) + k^2(\frac{2\pi}{T})^2}} Cos(k\frac{2\pi}{T}t - \zeta_n - Arg(\Psi(0) + ik\frac{2\pi}{T})). \tag{3.20}$$

Note that if $T << 1/\Psi(0)$ there is a filtering effect and $z(t) \approx (\sigma + \theta_m)/\Psi(0)$.

Two basic models of therapy may be:

- $$\theta_u(t) = A(1 + bcos(\omega t)) \tag{3.21}$$

  which is rather unrealistic, but whose functional form is commonly used to assess the effect of periodic forcing on nonlinear systems. The asymptotic solution of (3.19) corresponding to (3.21) is given by:

  $$z_u(t) = \frac{\sigma + A}{\Psi(0)} + \frac{Ab}{\sqrt{\Psi^2(0) + \omega^2}} Cos(\omega t - Arg(\Psi(0) + i\omega))$$

- the more realistic function:

  $$\theta_r(t) = \frac{G}{1 - Exp(-cT)} exp(-cMod(t, T)) \ , \quad \theta_m = \frac{G}{cT}, \tag{3.22}$$

  which represent a boli-based delivery. The "shape" of $\theta_r(t)$ depends on c and the corresponding asymptotic periodic solution of (3.19) is given by:

  $$z_r(t) = \frac{\sigma}{\Psi(0)} + \frac{G}{\Psi(0) - c} X(\frac{E^{-cMod(t,T)}}{1 - E^{-cT}} - \frac{E^{-\Psi(0)Mod(t,T)}}{1 - E^{-\Psi(0)T}}\Big)$$

In case of impulsive therapy, by solving the impulsive differential equation

$$y' = -\Psi(0)y + \sigma, \quad y(nT^+) = y(nT^-) + \gamma, \quad n = 0, 1, \ldots \tag{3.23}$$

one obtains that:

$$z(t) = \frac{\sigma}{\Psi(0)} + \frac{\gamma}{1 - exp(-\Psi(0)T)} Xexp\Big(- \Psi(0)Mod(t, T)\Big). \tag{3.24}$$

Furthermore, it is easy to show that the condition $\sigma + \theta_m > \sigma_{cr}$ guarantees the LAS of CF. In fact, since the variational equations around $(0, z(t))$ are: $U' = (\alpha f(0) - \phi(0)z(t))U, W' = (\sigma q'(0) - \Psi'(0)z(t))U - \Psi(0)W$, we obtain that $\alpha f(0) - \phi(0) < z(t) >< 0 \Rightarrow U(t) \to 0 \Rightarrow W(t) \to 0$, and since $< z(t) >= (\sigma + \theta_m)/\Psi(0)$ we recover the LAS condition $\sigma + \theta_m > \sigma_{cr}$. Similarly, one may demonstrate the GAS condition: $\sigma + \theta_m > \sigma^*$.

3.3 Numerical simulations

I performed a set of simulations of the model proposed by Kuznetsov et al. in (3.6), (3.7), choosing parameter values fitted from real data of chimeric mice.

- Considering a "low aggressive tumor" I used the following parameters: $f(x) = 1.636(1 - 0.002x)$,$\phi(x) = 1$, $\beta(x) = \frac{1.131x}{20.19+x}$ $\sigma q(x) = 0.1181$, $\mu(x) = 0.00311x$+0.3743 and $t^{true} = 9.9t^{adim}$ days,$(X, Y) = 106(x, y)cells$.

- Considering a "more aggressive tumor" I used those parameters: $f(x) = 1.636(1 - 0.002x)$,$\phi(x) = 1$, $\beta(x) = \frac{1.131x}{20.19+x}$ $\sigma q(x) = 0.1181$, $\mu(x) = 10(0.00311x) + 0.3743$ and $t^{true} = 9.9t^{adim}$ days,$(X, Y) = 106(x, y)cells$.

Note that the dynamic of tumors in mouse is faster than that of human tumors, and that for periods of about 1 day or less (i.e. $T < 0.101$) it results that $(\frac{1}{\mu(0)}) \geq T$.
For the non-aggressive tumor $\sigma_c r \approx 0.612$ and $\sigma^* \approx 1.44 \gg \sigma$.
It clearly important to notice that in other kinds of anticancer therapies the shape of the therapy may be critical in determining whether or not the cancer will be eradicated. I found that:
In the absence of therapy non-aggressive tumor has two stable equilibria, one slightly less than the carrying capacity and the other corresponding to a small tumor. For the highly aggressive tumor there is one GAS equilibrium slightly less than the carrying capacity (see phase portrait in Fig. 3.1).

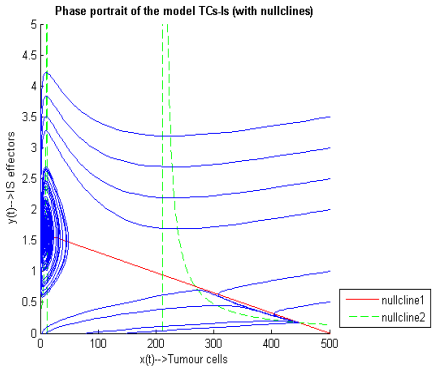

3.1.1 Non-Aggressive tumor

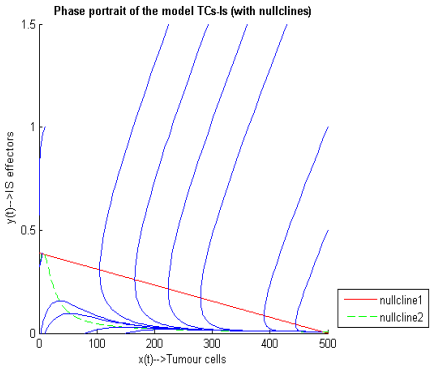

3.1.2 More-Aggressive tumor

Figure 3.1: On the left: Non-aggressive tumor, phase portrait of model ((3.6), (3.7)) in the absence of therapy. There are two LAS equilibria. The nullcline $y_C(x)$ is plotted in red, the nullcline $y_I(x)$ and its vertical asymptotes are plotted in green. On the right: More-aggressive tumor, phase portrait of model ((3.6),(3.7)) in the absence of therapy. There is one GAS equilibria slightly less than the carrying capacity. The nullcline $y_C(x)$ is plotted in red, the nullcline $y_I(x)$ is plotted in green.

Chapter 4

Noise and noise-induced transitions

One could say that in the course of its unfolding, life continuously chooses stochastically among many, perhaps infinitely many, possible scenarios. In one realization of the process, the scenario which will be followed cannot be predicted with certainty. So, we can say that macroscopic world is far less deterministic, i.e predictable in the classical sense, then we ever thought. In fact, completely new aspects of randomness have come to light which call for a profound reappraisal of the role and importance of random phenomena in nature. The investigation of self-organization in non equilibrium systems which are coupled to fluctuating environments has brought forth a great impetus to reappraise the role of randomness. In fact, in a large class of phenomena environmental randomness can, despite its apparently disorganizing influence, induce a much richer variety of behaviors than that possible under corresponding deterministic conditions. Astonishingly , an increase in environmental variability can lead to a structuring of non linear systems which has no deterministic analog. It is possible to extend the concept of phase transition to the new class of non equilibrium transition phenomena which are induced by environmental randomness. We can call them noise-induced non equilibrium phase transitions or noise induced transitions (This class is close to the classical equilibrium phase transition and the class of non equilibrium phase transition). It must be observed that for noise-induced

transitions the situation is not as neat as it is for classical equilibrium and non equilibrium phase transition, it is far from unpredictable and lawless. The notions an concepts, developed for classical transition phenomena and essentially rooted in a deterministic conception of nature , can be extended and adapted to deal with situations where noise plays an important role. A theoretical investigation is thus made possible and more important, the situation is accessible to experimental investigation.

4.1 Stochastic processes

Real environments vary randomly in the course of time. This can be modeled by using a random variable to describe the state of the environment at each instant of time. We thus obtain a family of random variables indexed by the parameter time t. The fluctuations of the environment induce in their turn random variations in the state of the system. Here again, we can describe the temporal evolution of the system by a family of random variables that at each instant of time represents the state of the system.

Definition: Random or stochastic process

A family of random variables indexed by the parameter time t is called a random (or stochastic) process. More precisely, a set $(X_t; t \in \theta)$ of real valued random variables, i.e $X_t : (\Omega, A, P) \to (R, B)$, is called a random process (or random function) with the index set θ and state space $\Re$. Ω represents the ensemble of elementary outcomes, A is the σ field (or σ algebra) of the events, P is the probability measure, B is the Borel σ field. As far as notation is concerned, stochastic processes will be denoted by X_t, whereas deterministic time-dependent functions will be written as $X(t)$.

4.1.1 Brownian motion

Brownian motion has played a central role in the theory of random phenomena in physics as well in mathematics. It is the rapid, perpetual, highly irregular motion of a small particle suspended in a fluid. The main features of Brownian motion, as established by experiments in the last century are:

- smaller particles move more rapidly.

- lowering the viscosity of the fluid also leads to more rapid motion.
- motion becomes more active when the fluid is heated.
- the motion is ceaseless and the trajectories are so irregular, their details are so fine, that they seem to have no tangent, i.e. the velocity of Brownian particle in undefined.

Quite a few explanations were proposed for this strange phenomenon before the true case of this perpetual motion was understood and the first theoretical treatment was given by Einstein. The chaotic motion of the suspended particle is maintained by the collisions with the molecules of the surrounding medium. There is a mathematical model of Brownian motion which is generally known as the Wiener process.

4.1.2 The Wiener Process

Definition: Brownian motion (or standard Wiener process)

A scalar standard Brownian motion, or standard Wiener process, over $[0, T]$ is a random variable W_t that depends continuously on $t \in [0, T]$ and satisfies the following three conditions:

1. $W_0 = 0$ (with probability 1).
2. For $0 \leq s < t \leq T$ the random variable given by the increment $W_t - W_s$ is normally distributed with mean zero and variance $t - s$; equivalently, $W_t - W_s \sim \sqrt{t-s}N(0, 1)$, where $N(0, 1)$ denotes a normally distributed random variable with zero mean and unit variance.
3. For $0 \leq s < t < u < v \leq T$ the increments $W_t - W_s$ and $W_v - W_u$ are independent.

The properties of the Wiener process, namely to be Gaussian distributed and to have independent increments, reflect closely the characteristic features of Brownian motion. The stochastic process W_t is thus a satisfactory mathematical model of the latter. Indeed, the displacement of a Brownian

particle is the sum of a very large number of independent infinitesimally small displacements due to the collisions. Invoking the central limit theorem we therefore expect the change in position of the Brownian particle to be Gaussian distributed. Furthermore, the displacements occurring over non overlapping time intervals should be stochastically independent, since they are due to collisions which are independent of each other. The stationarity of the displacements reflects the fact the fluid is in equilibrium.
The Wiener process itself is not a stationary process since probabilities $p(x, t+u) \neq p(x, t)$. The expectation value and the correlation function are easily calculated to be:

$$E[W_t] = 0 \tag{4.1}$$

$$E[(W_t)(W_s)] = min(t, s) \tag{4.2}$$

The mean square displacements of a Brownian particle

$$E[W_t^2] = t \tag{4.3}$$

increases only linearly in time. Thus the Wiener process is also not stationary in the wide sense. Though the sample paths of the Wiener process are with probability one continuous functions, the Wiener process is, as befits a model of Brownian motion, quite "irregular". With probability one, the sample functions are nowhere differentiable, i.e, the velocity of a Brownian particle is undefined, and they have infinite length on any finite time interval.

4.1.3 The Ornstein-Uhlenbeck Process

If the Wiener process is used to model Brownian motion, i.e is chosen as a stochastic process to represent the position of Brownian particle, then the instantaneous velocity is not defined in this model. It is infinite, since the sample paths of W_t are nowhere differentiable. This can be avoided by considering the velocity of the Brownian particle instead as the main random quantity as done by Uhlenbeck and Ornstein. This stochastic process is therefore known as the Ornstein-Uhlenbeck process.

4.2 Stochastic Models of Environmental Fluctuations

Three main elements characterize stochastic processes: the nature of the state variables, the index parameter set θ and the dependence relations among the random variables X_t.
The parameter set θ is trivially in all cases the time axis. As to the state space , we distinguish between continuously varying parameters and discrete parameters: the former can be modeled by a process with Gaussian probability law, the latter by a Poisson process. The motion of a Brownian particle we have just seen is a basic example for Gaussian stochastic process.
We now turn our attention to the dependence relation between the random variables making up the stochastic process used to model environmental fluctuations. It was observed that in a broad class of applications a clear cut separation of time scales exists, namely that the environmental state varies much faster than the macroscopic state of the system. This led to consider a stochastic process with extremely short memories and in a rather natural way the notion of white noise, a completely random process with independent values at every instant of time, arose. We shall now have a close look at the passage from a real noise with a short memory to the idealization of white noise with zero memory.

4.2.1 Correlation function and noise spectrum

As a first step towards a clear formulation of the way to model environmental fluctuations we have to quantify the notion of rapid external noise. We look for the characteristics defining the time scale of the system and that of the environment.
The systems we shall deal with here are governed by a phenomenological equation of the type:

$$\dot{X}(t) = h(X(t)) + \lambda g(X(t)) = f_\lambda(X(t)). \tag{4.4}$$

We denote by τ_{macro} the time that is typical for the macroscopic temporal evolution of the system (we shall usually identify τ_{macro} with the relaxation time of the system towards a reference steady state $\bar{X}$ found under the average environmental conditions). To be precise, $\bar{X}$ is defined by:

$$h(\bar{X}) + E[\lambda_t]g(\bar{X}) = 0, \tag{4.5}$$

and we determine τ_{macro} via the linear stability analysis. This yields to

$$\omega(\bar{X}) = \partial_X f_\lambda(X)|_{X=\bar{X}} \tag{4.6}$$

and hence the characteristic macroscopic time is the relaxation time of the system

$$\tau_{macro} = |\frac{1}{\omega(\bar{X})}| \tag{4.7}$$

A measure of the rapidity of the random environmental fluctuations is the correlation time τ_{cor}. It is, so to speak, the memory time of the stochastic process and it is defined for stationary process as:

$$\tau_{cor} = \frac{1}{C(0)} \int_0^\infty C(\tau) d\tau \tag{4.8}$$

The rationale of this definition is easily understood. The right hand side is the area beneath the normalized correlation function $C(\tau) = \frac{E[\delta X_t \delta X_{t+\tau}]}{E[\delta {X_t}^2]}]$ $C(\tau) \ll 1$ and $C(0) = 1$. Intuitively one would say that the process has a long memory, if $C(\tau)$ or $\tilde{C}(\tau)$) decreases only slowly, implying a large area beneath $\tilde{C}(\tau)$. On the other hand, for a process with a short memory, $C(\tau)$ or $\tilde{C}(\tau)$) decreases rapidly, thus giving rise to small area beneath $\tilde{C}(\tau)$. The normalized correlation function is used in order to be able to compare processes with different values for the variance.
A rapidly fluctuating environment can be characterized by the property that the correlation time τ_{cor} of the stochastic process λ_t is much smaller than the typical macroscopic time τ_{macro} of the system:

$$\tau_{cor} \ll \tau_{macro}. \tag{4.9}$$

An alternative way, different from the correlation function, to characterize the dependence relation between the random variables X_t, is based on the fact,

which we quote without proof, that any stationary process can be written as a superposition of oscillations with frequency ν, with random amplitude and phase. The so called frequency spectrum $S(\nu)$ is then a measure for the mean square power with which an oscillation of frequency ν contributes to the process X_t. $S(\nu)$ is just the Fourier transform of the correlation function hence contains the same information on the process:

$$C(\tau) = \int_R e^{i\nu\tau} S(\nu) d\nu. \tag{4.10}$$

Due to a well-known property of the Fourier transform, a narrow frequency spectrum $S(\nu)$ corresponds to a slowly decreasing broad correlation function $C(\tau)$. And vice versa, a broad frequency spectrum is associated with a rapidly decreasing correlation function. This implies that rapid external fluctuations $\tau_{cor} \ll \tau_{macro}$ having a narrow correlation function possess a broad frequency spectrum with an effective band width ν_b defined as:

$$\nu_b = \frac{1}{S(0)} \int_0^\infty S(\nu) d\nu \tag{4.11}$$

which is very large compared to the typical frequency of the system:

$$\nu_b \gg \omega(\bar{X}) \tag{4.12}$$

Typically, the environments of natural systems fulfill this last condition. This feature is easily understood: external noise can be expression of turbulent or chaotic state, a defining property of which is a broad-band spectrum, or the external parameter depends on a multitude of interfering environmental factors, implying that a large number of harmonic modes are " excited " and intervene in its temporary behavior. Therefore in a large class of applications, the environmental fluctuations are very rapid in the sense described above.

4.2.2 The White-Noise Process

If $\tau_{cor} \ll \tau_{macro}$, one is tempted to pass to the limit $\tau_{cor} = 0$. The rationale to adopt this idealization is the following: the memory of the environment is extremely short compared to that of the system. It is therefore reasonable to expect that any effects related to it are barely perceptible in the macroscopic

system. Hence, no qualitative change in the macroscopic behavior should occur if we set the non vanishing but extremely short correlations equal to zero. This means that the environment can be adequately described by a process with independent values at each instant of time, i.e., a so called completely random process. Some circumspection, however, has to be exerted in passing to the limit $\tau_{cor} = 0$ because if we approach the limiting process, having independent values, simply by letting the correlation time go to zero, we shall not only neglect memory effects but at the same time get rid of any effect of the environmental fluctuations. To see this, consider a Gaussian process with an exponentially decreasing correlation function, O-U process. The frequency spectrum of the O-U process is given by:

$$S(\nu) = \frac{1}{2\pi}\int_{\Re} e^{-i\nu\tau}C(\tau)d\tau = \frac{1}{2\pi}\int_{\Re} e^{-i\nu\tau}(\sigma^2/2\gamma)e^{-\gamma|\tau|}d\tau = (\frac{\sigma^2}{2\pi})(\nu^2+\gamma^2)^{-1} \tag{4.13}$$

The correlation time of the O-U process is:

$$\tau_{cor} = \gamma^{-1} \tag{4.14}$$

Hence the limiting $\tau_{cor} \to 0$ corresponds to $\gamma \to \infty$. It is easily seen that in this limit the mean square power with which oscillation of frequency ν contribute to the O-U process X_t vanishes, i.e

$$lim_{\gamma\to\infty}S(\nu) = 0, \quad \nu \in \Re \tag{4.15}$$

This implies that a decrease in the correlation time τ_{cor} without changing the other characteristics of the process leads eventually to a situation in which the random variations have no impact at all on the system, simply because in this limit the total input power $S = 2\int_0^\infty S(\nu)d\nu = \frac{\sigma^2}{2\gamma} = C(0)$ is spread uniformly over infinitely many frequencies. The limit $\tau_{cor} \to 0$ is too simplistic. It implies more than just neglecting the memory of the noise, in fact it is a noiseless limit.

If the external noise with a short memory is to be replaced by an equivalent idealized noise with zero memory, then in the light of the above discussion the appropriate limiting procedure is to couple the decrease in τ_{cor} with an adequate increase in the strength of fluctuations. From (4.13) it follows that

a finite limit is obtained, if concomitant with $\tau_{cor} \to 0$, $\sigma^2 \to \infty$ such that σ^2/γ^2 is a constant and not the variance $\sigma^2/2\gamma$. In the limit $\tau_{cor} \to 0$, $\sigma \to \infty$ such that $\sigma^2\gamma^2 = const = \bar{\sigma}^2$ the frequency spectrum of the O-U process converges to

$$S(\nu) = \frac{\bar{\sigma}^2}{2\pi} \tag{4.16}$$

i.e completely flat spectrum. For its correlation function we obtain in this limit

$$C(\tau) = \bar{\sigma}^2\delta(\tau) \tag{4.17}$$

Here $\delta(\tau)$ denotes the Dirac delta function (zero everywhere except at $\tau = 0$ where it is infinitely high such that $\int_{\Re} \delta(\tau)d\tau = 1$).

As is clear from the frequency spectrum and correlation function, a δ-correlated process has a flat spectrum. This property is at the origin of the name *White noise* for such processes; all frequencies are present with equal power as in white light. The O-U process is a Gaussian process, a property which is conserved in the limiting procedure. For this reason, the limiting process for $\tau_{cor} \to 0$ of the O-U process is known as Gaussian white noise and is in the following denoted $\bar{\sigma}\xi_t$ (where ξ_t is the standard Gaussian white noise with $E[\xi_t] = 0$ and $E[\xi_t\xi_{t+\tau}] = \delta(\tau)$).

Gaussian white noise is an extremely irregular process. It jumps widely around; its realizations are nowhere continuous. Clearly there are other kinds of white noise besides the Gaussian one; it is not difficult to characterize a white-noise process since its defining feature is that it is a completely random process, i.e it has independent values at every instant of time, and has infinite variance. In other words, any process whose correlation function is proportional to a Dirac delta function qualifies as white noise.

It is easy to obtain all possible white noises. Consider a process V_t with stationary independent increments, as for instance, the Wiener process W_t or the Poisson process ν_t. Then the random variables $(V_{t+h} - V_t)/h$ and $(V_{s+h} - V_s)/h$ are independent random variables for h sufficiently small and $t > s$. This property would also be conserved in the limit $h \to 0$ if it could be properly defined. Thus is tempting to think of white noise as the time derivative of a process with stationary independent increments; the Gaussian white noise would be the time derivative of the Wiener process and differ-

entiating the Poisson process would yield, in this spirit, the Poisson white noise.
Hence, the important result is that there is a one to one relation between white-noise processes and ordinary processes with white stationary independent increments namely, "white noise = (d/dt) (processes with stationary independent increments)". Since the latter class of processes is completely known [I.I74], so is then the ensemble of possible white noises. Though Gaussian white noise is so very irregular, it is extremely useful to model rapidly fluctuating phenomena. Not surprisingly, in view of its properties, true white noise of course does not occur in nature. However, as can be seen by their spectra, lots of natural noises are white to a very good approximation.

4.2.3 Phenomenological modeling of macroscopic systems

These considerations put the final touch to the phenomenological modeling of macroscopic systems, subjected to rapidly fluctuating environment. In the idealization of δ-correlated external noise, the system is described by a SDE of the form:

$$\dot{X} = h(X_t) + \lambda g(X_t) + \sigma g(X_t)\xi_t = f_\lambda(X_t) + \sigma g(X_t)\xi_t \tag{4.18}$$

where we have suppressed the bar over σ to denote the intensity of the Gaussian white noise. What are the advantages of neglecting the small memory effects of the environment?
Suppose the following situation: the state of the system at time t has been determined accurately to be x. For the external parameter λ_t only its probability law is known, for instance that it is gaussian distributed. Consider the situation under a more realistic than white noise, e.g. let ξ_t be an O-U process. Then for a short time h into the future, the state of the system will be given by

$$X_{t+h} = x + f_\lambda(x) + \sigma g(x)\xi_t h \tag{4.19}$$

Of course, it would be convenient if the future stochastic evolution of the system could be predicted solely on the basis of the information we possess at the present time t on the state x of the system and on the environmental

conditions as represented by the probability of ξ_t. In mathematical terms, the probability that the system is in state y at some future time t+h should depend only on the present state x and the stationary probability density $P_s(z)$ describing the environment, but not on the past history. Such a situation is the closest stochastic analog to the deterministic situation, where $X(t)$ in (4.4) is completely determined, once the initial condition $X(0)$ is given. This property is a verbal description of the defining feature of Markov processes.

Definition: Markov chain

Let $\chi = (x_1, ..., x_n)$ be the set of a finite number of discrete states. The stochastic process $X = (X_t, t \in \Re^+)$ is a continuous time Markov chain if it satisfies the following Markov property

$$P(X_t = x_j | X_s = x_i) = P(X_t = x_j | X_{r_1} = x_{i_1}, ...X_{r_n} = x_{i_n}, X_s = x_i) \quad (4.20)$$

for $0 \leq r_1 \leq .... \leq r_n < s < t$ and all $x_{i_1}...x_{i_n}, x_i, x_j \in \chi$.

Definition: Markov process

The stochastic process $X = (X_t, t \in \Re^+)$ is a (continuous time continuous state) Markov process if it satisfies the following Markov property:

$$P(X_t \in B | X_s = x) = P(X_t \in B | X_{r_1} = x_1, ...X_{r_n} = x_n, X_s = x) \quad (4.21)$$

for all Borel subsets $B \subset \Re$, time instants $0 \leq r_1 \leq .... \leq r_n \leq s \leq t$ and all $x_1...x_n, x$ for which the conditional probabilities are defined.

For fixed s,x and t the transition probability $P(X_t \in B | X_s = x)$ is a probability measure on the sigma algebra B of Borel subsets of $\Re$ such that

$$P(X_t \in B | X_s = x) = \int_B p(s, x; t, y) dy \quad (4.22)$$

for all $B \in \mathbb{B}$. The quantity $p(s, x; t, .)$ is the transition density.

From the Markov property it follows that

$$p(s, x; t, y) = \int_{-\infty}^{\infty} p(s, x; \tau, z) p(\tau, z; t, y) dz \quad (4.23)$$

for all $s \leq \tau \leq t$ and $x, y \in \Re$. This equation is known as the *Chapman Kolmogorov equation.*

It's important to say that the system can have the above property only if the environment is indeed already completely characterized by its one-dimensional density $p_s(z)$ and not, as is generally the case, by the infinite hierarchy of its n-dimensional probability densities. The only class for which this is true are the processes with independent values at every instant of time, since for completely random processes

$$p(z_1, t_1; ...; z_n, t_n) = \Pi_{i=1}^{n} p_s(z_i). \tag{4.24}$$

So, if the environment had a finite memory, the information of the past would indeed improve our prediction capabilities of the feature stochastic evolution of the system. These heuristic considerations suggest that the system is Markovian if and only if the external fluctuations are white. The following theorem holds: "the process X_t, being a solution of (4.18) is Markovian, if and only if the external noise ξ_t is white". This result explains the importance and appeal of the white-noise idealization. If the system, coupled to a fluctuating environment, can be described by a Markov process, then we have the full arsenal of tools developed to deal with such stochastic processes at our disposition.

4.3 Noise induced non-equilibrium phase transitions

We want now to describe a new class of non equilibrium phase transitions, namely changes in the macroscopic behavior of non linear systems induced by external noise. First of all it's important the choice of systems:

- We shall consider systems spatially homogeneous.
- We shall consider macroscopically large systems and assume they have reached the thermodynamic equilibrium.
- We shall consider systems which can be described by one intensive variable (to have exact analytical results).

Then, the influence of the environment on the macroscopic properties of the system is described on the level of the phenomenological equation via the external parameters λ. If the system is coupled to a fluctuating environment, then these parameters become in turn stochastic quantities. They can be represented by stationary stochastic processes λ_t:

$$\lambda_t = \lambda + \sigma\xi_t \tag{4.25}$$

where λ represents the average state of the environment, ξ_t the fluctuations around λ (ξ_t has zero mean value and intensity σ^2). Including it in the phenomenological description we get the Stochastic differential equation:

$$\dot{X} = f_{\lambda(t)}(X(t)) = h(X_t) + \lambda g(X(t)) + \sigma\xi_t g(X(t)) \tag{4.26}$$

The models for environmental fluctuations can be chosen among the most simple and basic classes of stochastic processes, Gaussian (for continuous varying external parameters) and Poisson processes (for discrete external parameters). Integrating the equation above we get:

$$X_t = X_0 + \int_0^t f_\lambda(X_s)ds + \sigma\int_0^t g(X_s)\xi_s ds \tag{4.27}$$

Formulated in this manner, the question is now how to arrive at the consistent definition of the stochastic integral $\int g(X_s)\xi_s ds$ which is the main source of confusion. The problem is that though a sense can be given to this integral and thus to the SDE (4.26), in spite of the extremely irregular nature of the white noise, there is no unique way to define it, precisely because white noise is so irregular. There are two different ways to define this integral, Ito and Stratonovich, they give different results. Both definitions are based on the heuristic relation that integration of Gaussian white noise yields Brownian motion, which we shall denote by W_t. Therefore the above integral can be written

$$\int g(X_s)\xi_s ds = \int g(X_s)dW_s \tag{4.28}$$

The integral on the right hand side is then defined , as in the case of an ordinary integral, by the limit of the approximating sums

$$\int g(W_s)dW_s = lim \sum g(W_{t_{j-1}})(W_{t_i} - Wt_{i-1}) \tag{4.29}$$

in the Ito sense and in the Stratonovich sense

$$\int g(W_s)dW_s = lim \sum g(\frac{W_{t_{i-1}} + W_{t_i}}{2})(W_{t_i} - Wt_{i-1}). \tag{4.30}$$

So, the only difference is the choice of the evaluation point. Ito chooses the left-hand point $W_{t_{i-1}}$ in the partition of the time interval, whereas Stratonovich opts for the middle point $\frac{(W_{t_{i-1}}+W_{t_i})}{2}$. For an ordinary (deterministic) integral,

$$\int U(X)dX = lim \sum U(\tilde{X}_i)(X_i - X_{i-1}), \tag{4.31}$$

any evaluation point $\tilde{X}_i$, as long as $\tilde{X}_i \in [X_{i-1}, X_i)$ can be chosen; the limit is independent to it. Due to the extremely wild behavior of the Gaussian noise, this is no longer true for the stochastic integral. The limit of the approximating sums depends on the evaluation point; Ito and Stratonovich yield different answers for the same integral:

Ito : $\int_0^t W_s dW_s = \frac{1}{2}(W_t^2 - W_0^2) - \frac{t}{2}$

Stratonovich: $\int_0^t W_s dW_s = \frac{(W_t^2 - W_0^2)}{2}$

Both the Ito and Stratonovich definitions are mathematically correct and can serve as the basis for a consistent calculus.
Systems coupled to a rapidly fluctuating environment can be modeled by Markov processes that are solutions of the stochastic differential equations. The description of (4.26) can be based on:

Ito SDE: $dXt = [h(X_t) + \lambda g(X_t)]dt + \sigma g(X_t)dW_t$

Stratonovich SDE: $dXt = [h(X_t) + \lambda g(X_t)]dt + \sigma g(X) \circ dW_t$

In those two cases, the transition probability density $p(y, t|x)$ can be found using the Fokker Plank equation:

Ito: $\partial_t p(y, t|x) = -\partial_y f_\lambda(y)p(y, t|x) + \frac{\sigma^2}{2}\partial_{yy} g^2(y)p(y, t|x)$

Stratonovich: $\partial_t p(y,t|x) = -\partial_y[f_\lambda(y)+\frac{\sigma^2}{2}g'(y)g(y)]p(y,t|x)+\frac{\sigma^2}{2}\partial_{yy}g^2(y)p(y,t|x)$

4.3.1 Stationary solution of the Fokker-Plank equation (FPE)

Since environment fluctuations can be modeled by a stationary random process, we expect that in general a system subjected to external noise for sufficiently long time will also settle down to stationary behavior. It means that, on time goes to infinity, the system will attain a probability density $p_s(x)$ whose shape does not change any more with time. Now, we shall determine the stationary probability density $p_s(x)$ which characterizes the steady-state behavior of the system under external white noise.
$p_s(x)$ is the stationary solution of the FPE which can be written in the form:

$$\partial t p(x,t|x_0,0) + \partial_x J(x,t|x_0,0) = 0 \tag{4.32}$$

where $J(x,t|x_0,0) = f(x)p(x,t|x_0,0) - \frac{\sigma^2}{2}\partial_x g^2(x)p(x,t|x_0,0)$. The stationary FPE then reads: $\partial_x J_s(x) = 0$ and implies that the stationary probability current is constant on the space $[b_1,b_2]$: $J_s(x) = const$ for $x \in [b_1,b_2]$. In the stationary case, we have the probability current in the interior of the space equal to the current across the boundaries which we call J:

$$J = J_s(x) = J_s(b_1) = J_s(b_2) \tag{4.33}$$

Now,

$$-f(x)p_s(x) + \frac{\sigma^2}{2}\partial_x g^2(x)p_s(x) = -J \tag{4.34}$$

which solving gives

$$p_s(x) = \frac{N}{g^2(x)}exp(\frac{2}{\sigma^2}\int^x \frac{f(u)}{g^2(u)}du) - \frac{2}{\sigma^2 g^2(x)}J\int^x exp(\frac{2}{\sigma^2}\int_z^x \frac{f(u)}{g^2(u)}du)dz \tag{4.35}$$

where N is determined by the normalization condition, J is the probability current at the boundaries of the state space and depends on the nature of the boundaries.

It must be observed that, when the boundaries are natural ($J = 0$) [W.H84] we get

$$p_s(x) = \frac{N}{g^2(x)} exp(\frac{2}{\sigma^2} \int^x \frac{f(u)}{g^2(u)} du) \tag{4.36}$$

To be a stationary probability density, has to be normalizable:

$$N^{-1} = \int_{b_1}^{b_2} \frac{1}{g^2(x)} exp(\frac{2}{\sigma^2} \int^x \frac{f(u)}{g^2(u)} du) < \infty \tag{4.37}$$

If one of the boundaries is attracting, regular or absorbing [W.H84], then $p_s(x) = 0$ for $x \in (b_1, b_2)$, no regular stationary probability density exists.

For a diffusion process corresponding to Stratonovich SDE:

$$dXt = f(X_t)dt + \sigma g(X) \circ dW_t \tag{4.38}$$

the stationary probability density for natural boundaries is:

$$p_s(x) = \frac{N}{g(x)} exp(\frac{2}{\sigma^2} \int^x \frac{f(u)}{g^2(u)} du) \tag{4.39}$$

In general: The stationary behavior of a system describe by SDE

$$dXt = f(X_t)dt + \sigma g(X) dW_t \tag{4.40}$$

is given by:

$$p_s(x) = N g^{-\nu}(x) exp(\frac{2}{\sigma^2} \int^x \frac{f(u)}{g^2(u)} du) \tag{4.41}$$

if $J = 0$, $\nu = 1$ gives the Stratonovich interpretation , $\nu = 2$ the Ito version. It may happen that a SDE interpreted according to Ito admits a stationary solution while interpreted according to Stratonovich it does not, or vice versa, since the formula for $p_s(x)$ differ by a factor $g^{-1}(x)$. If such a discrepancy occurs, in general it signals that the model used to describe the system has some dangerous or pathological features and one has to be doubly careful in justifying the modeling procedure.

Theorem: If the diffusion process X_t is started with a probability density that differs from the stationary one, it will approach the stationary density as time tends to infinity $lim_{t\to\infty} p(x,t) = p_s(x)$.

4.3.2 The neighborhood of deterministic behavior: additive and small multiplicative noise

Consider a non linear macroscopic system which has been coupled with his environment for a sufficiently long time to have settled down to a stationary state. If the surroundings are varying, then the steady states of the systems are zeros of the RHS of the deterministic equation:

$$\dot{X} = h(X) + \lambda g(X) \tag{4.42}$$

Here we shall also suppose that the deterministic system is stable in the sense that the solution $X(t)$ does not blow up to infinity. To be precise, $\forall X_0 \in (b_1, b_2) \exists C < \infty$, dependent on λ, such that

$$|X(t)| \leq C \quad \forall t \tag{4.43}$$

if $X_0 = 0$. This is fulfilled if a $K > 0$ exists such that:

$$h(x) + \lambda g(x) < 0 \quad \forall x > K \tag{4.44}$$

and

$$h(x) + \lambda g(x) > 0 \quad \forall x < -K \tag{4.45}$$

If X is a concentration like variable and has to be non negative, then RHS of (4.42) has to obeys the following condition:

$$h(0) + \lambda g(0) \geq 0 \quad \forall \lambda \tag{4.46}$$

If both b_1, b_2 are finite, we require $h(b_1) + \lambda g(b_1) \geq 0$ and $h(b_2) + \lambda g(b_2) \leq 0$ for all λ. The solution of the first order, one-variable differential equation, is a monotone function with respect to time since $\dot{X}$ takes one and only one well-defined value for every x. Thus (4.43) implies that (4.42) admits only one steady state.

If it admits more than one steady state , then stable and unstable ones alternate. If there are two ore more stable stationary states, then the state space divides in nonoverlapping regions, the "basin of attraction" of the various stable states. This is very easily seen if we write the phenomenological equation in the form

$$\dot{X} = -\partial_X V_\lambda(X), \quad where \;\; V_\lambda(x) = -\int^x [h(z) + \lambda g(z)] dz \tag{4.47}$$

is called the potential of (4.42). The steady states are the extrema of the potential $V_\lambda(x)$ and the normal modes $\omega(\bar{X})$ of the linear stability analysis are given by

$$\omega(\bar{X}) = \partial_{XX} V_\lambda(\bar{X}) \tag{4.48}$$

Hence, the stable steady states correspond to the minima of $V_\lambda(x)$ and the unstable steady states to the maxima.
We want now to analyze how the stationary behavior of a system is modified in a fluctuating environment. In this case, the "state" of the system is given by a random variable.
The system is described by a degenerate random variable of the form

$$X(\omega) = \bar{X}_i \;\; if \; X(0)(\omega) \in A(\bar{X}_i) \tag{4.49}$$

where $A(\bar{X}_i)$ denotes the basin of attraction of the ith steady state. We characterize this (degenerate) random variable by its probability law:

- In the deterministic case: the stationary probability density consist of "delta peaks" centered on the steady state $\bar{X}_i$. The weight of the delta peaks is given by the initial preparation of the system.

- In the stochastic case: external noise has a disorganizing influence. The probability density has a maximum at the coordinate that corresponds to the minimum of the potential and has a certain spread around it, depending on the strength of the external noise. If there is more than one minimum and if there is no effective upper bound on the external fluctuations, then we expect a multimodal probability density with peaks corresponding to the various minima of the potential.

A general picture emerges. The state of the system, i.e. the random variable, is given by an interplay between the dynamics of the system and the external fluctuations.
case 1: the intensity of the white noise is extremely small i.e $\sigma \ll 1$
Defining

$$U(x) = \int^x \frac{f(u)}{g^2(u)} du \tag{4.50}$$

we can write from (4.41) as

$$p_s(x) = Nexp[\frac{2}{\sigma^2}U(\bar{x}_m)]exp[\frac{2}{\sigma^2}[U(x) - U(\bar{x}_m) - \frac{\nu\sigma^2}{2}lng(x)]]. \qquad (4.51)$$

Here $\bar{x}_m$ is the location of the highest maximum of $U(x)$, which we suppose to lie in the interior of the state space (b_1, b_2):

$$U(x) < U(\bar{x}_m) \quad for \ x \neq \bar{x}_m.$$

If σ^2 tends to zero and $x \neq \bar{x}_m$, the second factor becomes exponentially small, so that the dominant contribution to the stationary probability density comes from a neighborhood of the order of σ^2 around the highest maximum of $U(x)$.

case 2: the external noise is additive: $(g(x) = const = c)$

$$U(x) = -\frac{1}{c^2}V_\lambda(x) \qquad (4.52)$$

The highest maximum of $U(x)$ and of the probability density $p_s(x)$ coincides with the position of the deepest potential well for all $\sigma^2, \bar{x}_m = \bar{x}$; no shift occurs.

case 3: the external noise is multiplicative:

$$U(x) \neq -\frac{1}{c^2}V_\lambda(x) \qquad (4.53)$$

The highest maximum of $U(x)$ is not necessarily the one with the deepest potential well in the deterministic description.

Hence, the criterion of absolute stability for the deterministic steady states depends explicitly on the nature of the random perturbations the system is subjected to.

4.3.3 Transition phenomena in a fluctuating environment

We now analyze the stationary behavior of the macroscopic systems for arbitrary noise intensities. What do we mean by a transition in a macroscopic system coupled to a random environment and how do we detect such transitions?

Definition: Transition

A transition occurs precisely at that point in the parameter space, consisting of the mean value of the external noise, its variance its correlation time etc.. where the functional form of the mapping from the sample space Ω into the state space $[b_1, b_2]$ changes qualitatively. This corresponds to a qualitative change in the probability law characterizing the random variable.

In our case, this probability law is given by (4.41), the exact expression for the stationary probability density of a system subjected to Gaussian white noise. How can we detect such qualitative change?

The natural way is look at the deterministic situation for guidance and try to extend the criteria used there to the stochastic case.

- In the deterministic case: a non equilibrium phase transition occur when the potential $V_\lambda(x)$ changes qualitatively. For instance, the number of local extrema changes. This fact has found its precise formulation in catastrophe theory.

- In the stochastic case: is natural to consider the extrema of the stationary probability density $p_s(x)$ as indicators for a transitions. This choice is not only the most direct extension of the deterministic concepts, but also the most appropriate compared with other possibilities that come to mind in the stochastic case as the moments of the distribution.

  Example: Consider the time-dependent Landau equation, often used to describe equilibrium critical phenomena:

  $$dX_t = (\lambda X_t - X_t^3)dt + \sigma dW_t$$

  In the deterministic case, $\sigma = 0$, a critical point occurs at $\lambda = 0$. For λ negative the system has only one steady state, $\bar{x} = 0$, i.e the potential $V_\lambda(x)$ has only one minimum. For λ positive, $\bar{x} = 0$ becomes a maximum of $V_\lambda(x)$ and two minima develop at $\bar{x} = \pm\lambda^{\frac{1}{2}}$, i.e the system now has to stable and one unstable steady states.

  In the stochastic case, which corresponds to additive noise here, the steady state behavior of the system is described by a random variable whose probability law is given by

  $$p_s(x) = Nexp[-V_\lambda(x)/\sigma^2].$$

It is obvious that also in the stochastic case a qualitative change in the steady state occurs at $\lambda = 0$. This transition is accurately reflected by the behavior of the extrema of $p_s(x)$. If however the moment are used, no transition phenomenon is detected. Clearly, it is not the mean value that corresponds to the macroscopic states or phases of the system, but the maxima of $p_s(x)$. This example confirms that the most direct extension of the deterministic concepts as presented above is also the most appropriate. A qualitative change in steady-state behavior is unambiguously reflected in the extrema of the probability density. (The only exception is the transition from a degenerate to a genuine random variable. Here the variance is the best indicator.)

Since a transition occurs if the steady states of the system as given by the random variable changes qualitatively, the extrema of the stationary probability density are merely a practical way to monitor such a qualitative change. The number and position of the extrema of $p_s(x)$ in the stochastic case and $V_\lambda(x)$ in the deterministic case are the most distinguishing features of the steady state behavior of the system.
In summary:

1. A transition occurs when the functional form of the random variable describing the steady state of the system changes qualitatively.

2. This qualitative change is most directly reflected by the extrema of the stationary probability law, except if the transition is due to a change in the nature of boundary.

3. The physical significance of the extrema, apart from being the most appropriate indicator of transition, is their correspondence to the macroscopic phases of the system. The extrema are the order parameter of the transition.

The extrema of $p_s(x)$ are easily found from:

$$[h(x_m) + \lambda g(x_m)] - \nu \frac{\sigma^2}{2} g(x_m) g'(x_m) = 0 \tag{4.54}$$

basic equation for an analysis of the influence of rapid external noise on the steady state behavior of macroscopic non-linear systems.
The basic equation (4.54) contains two terms. The one in brackets, set equal to zero, corresponds to the equation for the deterministic steady states (4.42). The second term describes the influence of external noise. We have again to distinguish between two cases:

1. **Additive noise** ($g(x) = 1$)**:** the influence of the environment fluctuations does not depend on the state of the system. Consequently, the extrema of $p_s(x)$ always coincide with the deterministic steady states, independent of the intensity of the external white noise. Hence, additive external white noise does not modify qualitatively the stationary behavior of one-variable systems.

2. **Multiplicative noise** ($g(x) \neq 1$)**:** the effect of the environment fluctuations does depend on the state of the system. If σ^2 is sufficiently small, then the roots of (4.54) do not differ in number and position from the deterministic steady states. The external noise is not sufficiently strong to change the potential qualitatively. If, however, the intensity σ^2 of the noise increases, then we come to a point where the second term in (4.54) can no longer be neglected. In fact, if σ^2 is sufficiently large, the extrema of $p_s(x)$ can be essentially different in number and position from the deterministic steady state, provided $g(x)$ is nonlinear in a suitable way $f(x) = h(x) + \lambda g(x)$ is a polynomial of degree n and $g'(x)g(x)$ a polynomial of degree m grater than n. When σ^2 crosses a certain threshold value the shape of $p_s(x)$, i.e the random variable describing the stationary behavior of the system, can change drastically; a transition occurs. In addition to the disorganizing effect, which it shares with the additive noise, multiplicative noise can create new states, it can induce new non-equilibrium phase transitions which are no expected from the usual phenomenological descriptions. These are simply called *noise-induced-transitions*.

4.3.4 Time dependent behavior of Fokker-Planck Equations

The preceding sections dealt with the stationary behavior of non linear systems coupled to a fluctuating environment. Sometimes it can be more interesting to observe the transient behavior of such systems instead of the stationary one. This problem is considerably harder than the analysis of stationary behavior and in general no explicit formula for the time dependent solution of the FPE exists, even for one variable systems, in contrast with the stationary solution.
The exact time-dependent solution of a SDE can be easily obtained only if the drift and diffusion coefficients are linear functions. It is thus worthwhile for a study of transient behavior to determine those non linear SDE's which can be transformed into a linear SDE by a bijective change of variable because , for some systems belonging to this class, it is possible to derive the exact time-dependent solution of the corresponding FPE in an explicit manner.

4.4 Numerical simulation of SDE: Eulero-Maruyama method

In my thesis we will work with some SDEs. There are different methods to solve SDEs analytically but we will not see these here. Instead, I will now explain how to apply a simple numerical method to SDE: the Eulero-Maruyama method which is the one I used in my numerical simulations.
A scalar, autonomous SDE can be written in integral form as

$$X_t = X_0 + \int_0^t f(X_s)ds + \int_0^t g(X_s)dW_s, \quad 0 \leq t \leq T. \tag{4.55}$$

Here, f and g are scalar functions and the initial condition X_0 is a random variable. The second integral on the right-hand side of (4.55) is to be taken with respect to Brownian motion, and we assume that the Ito version is used. The solution X_t is a random variable for each t. We do not attempt to explain further what it means for X_t to be a solution to (4.55) instead we define a numerical method for solving it, and we may then regard the

solution X_t as the random variable that arises when we take the zero step size limit in the numerical method.
It is usual to rewrite (4.55) in differential equation form as

$$dX_t = f(X_t)dt + g(X_t)dW_t, \quad X(0) = X_0, \quad 0 \leq t \leq T. \tag{4.56}$$

This is nothing more than a compact way of saying that X_t solves (4.55). To keep with convention, we will emphasize the SDE form (4.56) rather than the integral form (4.55). (Note that we are not allowed to write $\frac{dW_t}{dt}$, since Brownian motion is nowhere differentiable with probability 1.)
If $g = 0$ and X_0 is constant, then the problem becomes deterministic, and (4.56) reduces to the ordinary differential equation $\frac{dX_t}{dt} = f(X_t)$, with $X(0) = X_0$.
To apply a numerical method to (4.56) over $[0, T]$, we first discretize the interval. Let $\Delta t = T/L$ for some positive integer L, and $\tau_j = j\Delta t$. Our numerical approximation will be denoted X_j.
The Eulero Maruyama (EM) method takes the form:

$$X_j = X_{j-1} + f(X_{j-1})\Delta t + g(X_{j-1})(W(\tau_j) - W(\tau_{j-1})), j = 1, 2, ..., L \tag{4.57}$$

To understand where (4.57) comes from, notice from the integral form (4.55) that

$$X(\tau_j) = X(\tau_{j-1}) + \int_{\tau_{j-1}}^{\tau_j} f(X_s)ds + \int_{\tau_{j-1}}^{\tau_j} g(X_s)dW_s. \tag{4.58}$$

Each of the three terms on the right-hand side of (4.57) approximates the corresponding term on the right-hand side of (4.58). We also note that in the deterministic case ($g = 0$ and X_0 constant), (4.57) reduces to Eulero method.

Chapter 5

Bounded noises

Traditionally, stochastic dynamical systems used in the physical sciences have involved Gaussian noise. In recent times, however, it has been recognized that the assumption of Gaussianity is not appropriate in some cases. The Gaussian noise is unbounded, i.e., there exists a positive chance of having very large values. Strictly speaking, this fact contradicts the very nature of a real physical quantity which is always bounded. Studies of dynamical systems with non-Gaussian continuous noise are much more complicated,especially analytically. Although the literature devoted to the study of bounded noises is far more limited than that concerning the Gaussian noise, in recent years a number of interesting works have appeared [TW01, BC05].
Since the noise-induced transitions are dependent on the kind of density of noise adopted [Fue07], we will now consider two different kind of "Bounded Noises". The first is derived by applying a bounded function to a Wiener process, the second through an Ito Stochastic differential equation nonlinear in the diffusion term.
The first bounded noise we consider is the so called sine-Wiener noise [BC05] given by

$$\nu(t) = Bsen(\sqrt{\frac{2}{\tau_{corr}}}W(t)) \tag{5.1}$$

$$W' = \xi(t) \tag{5.2}$$

where B is a constant, τ_{corr} is the correlation time, $\xi(t)$ is a white noise.
The sine-Wiener noise, as it is easy to verify, is such that $< \nu(t) >= 0$

$,< \nu^2(t) >= B^2/2$ and

$$< \nu(t)\nu(t+z) >= \frac{B^2}{2} \exp\left(-\frac{z}{\tau}\right)\left(1 - \exp\left(-4\frac{t}{\tau}\right)\right),$$

where $z \geq 0$.
The second is the Cai-Lin-Suzuki family of noises [CS05, CK04], which is derived by a Langevin equation of the form:

$$\nu'(t) = -\eta\nu + D(\nu)\zeta(t), \tag{5.3}$$

$D(\nu) \geq 0$ is a function such that $D(|B|) = 0$, and $\zeta(t)$ is a gaussian noise with zero mean and unitary variance. We shall further assume that $D(\nu)$ is a symmetric function.
As a consequence, the noise ν is then non-gaussian with zero mean, autocorrelation time $\tau = 1/\eta$ and it satisfies the following bounds: $-B < \nu(t) < B$.
In the particular case [CS05] where

$$D(\nu) = \sqrt{\frac{\eta}{\delta+1}(B^2 - \nu^2)}$$

The stationary density of ν is:

$$P_{st}(\nu) = N\left(1 - \frac{\nu^2}{B^2}\right)_+^{\delta}$$

where N is a normalization constant. Note that the density vanishes for $\nu \leq -B$ and $\nu \geq B$.
Cai Noise we consider is given by:

$$\nu(t) = -\frac{1}{\tau}\nu dt + \frac{1}{\tau}A(B^2 - \nu^2)^{\delta} dW(t) \tag{5.4}$$

$$\nu(0) = \nu_0 \tag{5.5}$$

where τ describes noise's correlation time, B noise's amplitude, A, δ are parameters, $dW(t)$ is a Wiener process.

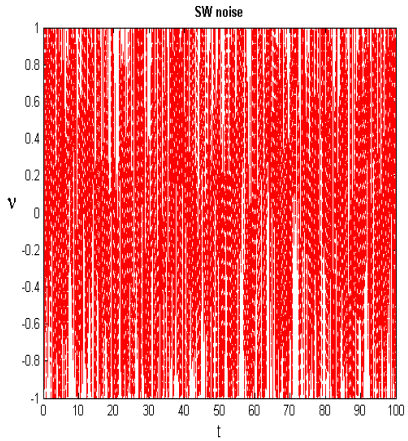

5.1.1 Sine Wiener noise

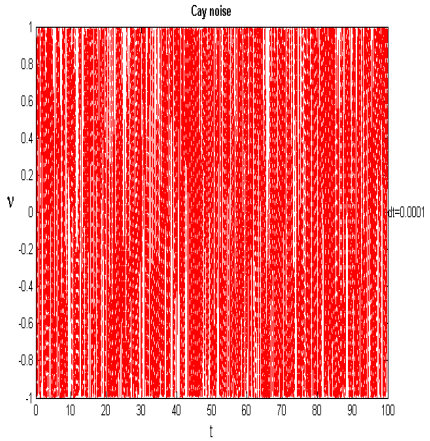

5.1.2 Cai noise

Figure 5.1: Bounded Sine Wiener noise (left figure) and bounded Cai noise (right figure),with amplitude $B = 1$ and correlation time $\tau = 0.1$.

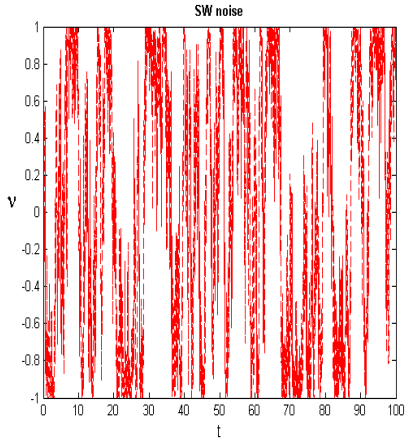

5.2.1 Sine Wiener noise

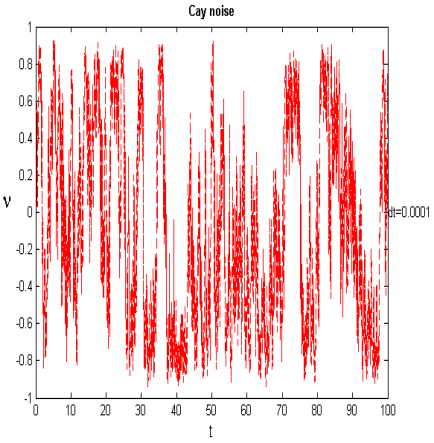

5.2.2 Cai noise

Figure 5.2: Bounded Sine Wiener noise (left figure) and bounded Cai noise (right figure),with amplitude $B = 1$ and correlation time $\tau = 1$.

Chapter 6

Bounded-noise-induced transitions in a tumor-immune system interplay

The objective of my simulations is to investigate the phenomenon of evasion of tumor cells from immune control at a temporal mesoscale. Of course in the very short term if either the tumor is lowly immunogenic or the level of IS is per se slow (i.e because of immunodeficiency [CJ01]) it is obvious that the transformed cells can easily and in short time evade control.
Over the long temporal range not only those slow evolutionary processes but also the IS degradation due to natural senescence [V.A01] can explain long-term evasions. However, middle term evasions are presumably representative of the vast majority of case of immune surveillance failure.
An important factor that has been extensively investigated is the influence of the fluctuations in the proliferation rates of a tumor [W.H84] [W.H77] [A.d07]. Those fluctuations, however, play a dual role since they can also trigger the elimination of the neoplasm.
Given the complexity and multistability of the T-IS interplay, we think that a natural approach is to investigate the role of statistical fluctuations of immune levels that might trigger noise-induced transitions. Moreover , from modeling point of view, the extreme intricacy of the interactions between tumor cells and immune effectors further justifies the inclusion of noise on a

deterministic model of T-IS interplay in order to take into account a plethora of relevant phenomena such as the variable strength of the neoantigens in stimulating the immune response, the expression or absence of expression of molecules needed for T cell activation, the dynamics of Treg cells that generate a state of tolerance to cancer.
In our simulations we have considered the tumor-immune system model already seen in chapter 3 introducing two different kind of "Bounded Noises": Sine Wiener and Cai noise, with parameters values describing more aggressive tumor.
A point to be stressed is that the classical theory of noise induced transitions [W.H84] is an asymptotic theory that refers to the study of the qualitative changes in stationary probability densities: $P_{st}(x) = lim_{t\to\infty}P(x,t)$, where x stands, in biological applications of this theory, for some biological property such as the size of a cellular population, or the viral load or the average activity. Here, of course, we shall assume that x denotes the tumor size. However, whatever asymptotic study might be, if the velocity of convergence of the stationary density is slow,it is in contradiction with the basic fact that living beings have a finite lifespan. Thus the lifespan of the host organisms must be a natural limit to our numerical investigations, which makes the velocity of convergence to $P_{st}(x)$ an essential parameter. If this velocity is slow and the attractor is practically reached in times that are excessively greater than the average lifespan of the organisms in study, one has to investigate the possible qualitative changes of $P(x,t)$ during its transitory, namely at some given realistic times. For this reason we focused here on transitory analysis of $P(x,t)$. Indeed, noise has been introduced on various parameters observing the probability density at time $T = 100$ corresponding , in dimensional time unity, to 3 years about, both in case of Sine Wiener and Cai noise perturbations. It must be observed that all simulations have been done using **Matlab 7.0.4**.
Recall: Kuznetsov model for the interaction between a population of tumor cells and IS cells is given by the equations:

$$x' = x\alpha(1 - bx) - \phi yx \tag{6.1}$$

$$y' = \frac{\beta x}{\eta + x}y - (\mu_0 + \mu_1 x)y + \sigma \tag{6.2}$$

where x describes the number of tumor cells, y the number of IS effectors, α, b, ϕ, β, η, μ_0, μ_1, σ are parameters.

6.1 Perturbation on parameter ϕ

I performed some simulations of the new system, obtained from (6.1), (6.2) simply adding noise ν to the parameter ϕ, in both form of Sine Wiener and Cai:

$$x' = x\alpha(1 - bx) - (\phi + \nu)yx \tag{6.3}$$

$$y' = \frac{\beta x}{\eta + x}y - (\mu_0 + \mu_1 x)y + \sigma \tag{6.4}$$

Before introducing noise, I did some simulations of the deterministic model for parameters values fitted from real data of chimeric mice, aggressive tumor: $\alpha = 1.636$, $b = 0.002$, $\phi = 1$, $\beta = 1.131$, $\eta = 20.19$, $\mu_1 = 10 * (0.00311)$, $\mu_0 = 0.3743$,$\sigma = 0.1181$.
Varying ϕ values I found $\phi_{tangent}$ and $\phi_{eradication}$ which describe, respectively, ϕ values that makes x nullcline tangent to y nullcline and x nullcline go to zero. These values are given by: $\phi_{tangent} = 4.108$ and $\phi_{eradication} = 49.269$(see figures 6.1.1, 6.1.2).

Now Choosing $\phi = 4.2$, close to $\phi_{tangent}$, so that the equilibrium point may be quite metastable, I performed a series of some simulations.

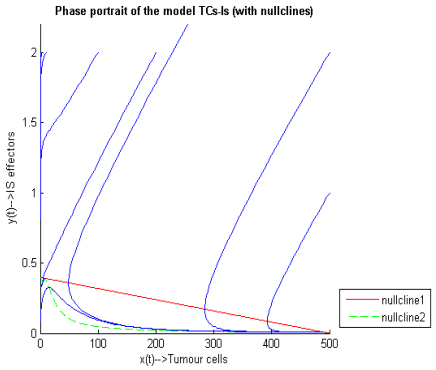

6.1.1 $\phi_{tangent} = 4.108$

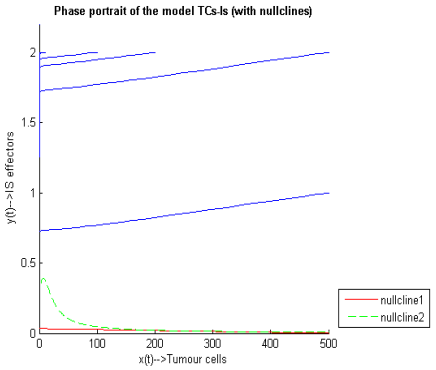

6.1.2 $\phi_{eradication} = 49.269$

The following tables and figures show the results obtained by varying the amplitude of the noise (B) and its correlation time (τ):

SW noise:

Amplitude (B)	Correlation time (τ)	Comments
0.01	0.1	//*
0.01	0.5	//
0.01	1	//
0.01	6	//
0.08	0.1	Evident oscillations
0.08	0.5	Evident oscillations
0.08	1	Evident oscillations
0.08	3	Evident oscillations
0.095	0.1	Evident oscillations
0.095	0.8	Evident oscillations
0.095	3	Evident oscillations
0.1	1	Evident oscillations
0.2	1	Evident oscillations
0.2	2	Evident oscillations
0.2	3	Evident oscillations
0.2	8	Evident oscillations
0.5	1	Evident oscillations
0.8	0.1	Evident oscillations
0.8	1	Evident oscillations
1	1	Evident begins
1.2	1	Evasion
1.4	1	Evasion
1.6	1	Evasion

* No relevant observations.

Cai noise:

Amplitude (B)	Correlation time (τ)	Comments
0.01	0.1	//
0.01	0.5	//
0.01	1	//
0.01	6	//
0.08	0.1	Evident oscillations
0.08	0.5	Evident oscillations
0.08	1	Evident oscillations
0.08	3	Evident oscillations
0.095	0.1	Evident oscillations
0.095	0.8	Evident oscillations
0.095	3	Evident oscillations
0.1	1	Evident oscillations
0.2	1	Evident oscillations
0.2	2	Evident oscillations
0.2	3	Evident oscillations
0.2	8	Evident oscillations
0.5	1	Evident oscillations
0.8	0,1	Evident oscillations
0.8	1	Evident oscillations
1	1	Evasion begins
1.2	1	Evasion begins
1.4	1	Evasion
1.6	1	Evasion

Observations:

Introducing a Sine Wiener noise, for some values of amplitude and correlation time, I can notice a clear evasion from the point of microscopic equilibrium to the macroscopic one as it is evident in the figures (6.3.1) (6.4.1) (6.5.1) (6.6.1) (6.7.1) (6.8.1). Introducing a Cai noise, as well, for some values of amplitude and correlation time, evasion is clear. See figures (6.5.2), (6.6.2) (6.7.2) (6.8.2).

Perturbation on parameter ϕ

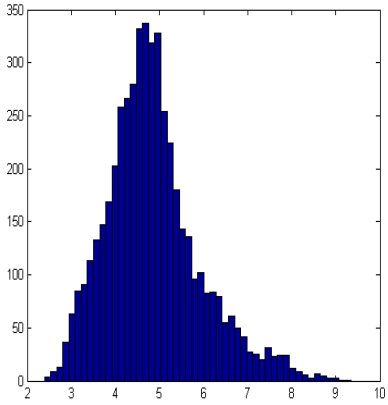

6.1.3 Sine Wiener noise

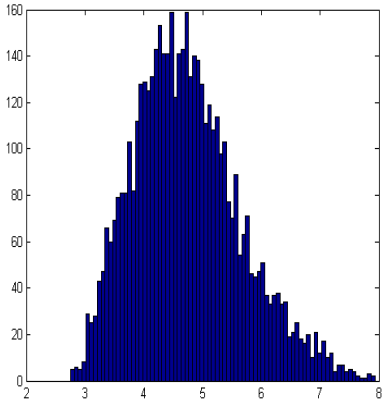

6.1.4 Cai noise

Figure 6.1: X_{final} probability density over 5000 simulations with bounded Sine Wiener noise (left figure) and bounded Cai noise (right figure),with amplitude $B = 1$ and correlation time $\tau = 1$, added on parameter ϕ. Starting values are those of microscopic equilibrium point $(x, y) = (4.83, 0.38)$.

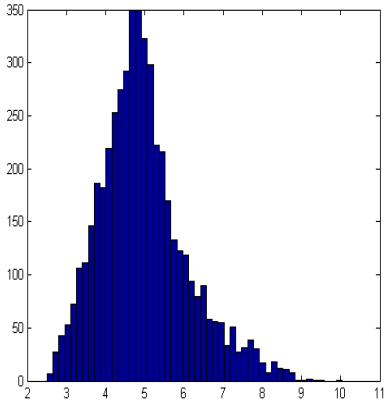

6.2.1 Sine Wiener noise

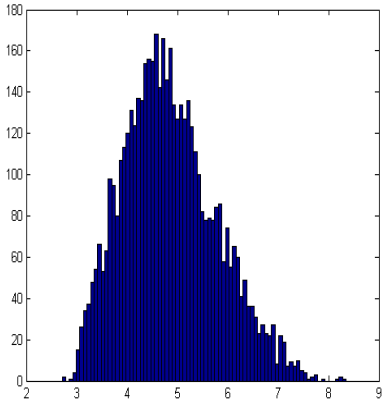

6.2.2 Cai noise

Figure 6.2: X_{final} probability density over 5000 simulations with bounded Sine Wiener noise (left figure) and bounded Cai noise (right figure),with amplitude $B = 1$ and correlation time $\tau = 1$, added on parameter ϕ. Starting values are $(x, y) = (0.1, 2)$.

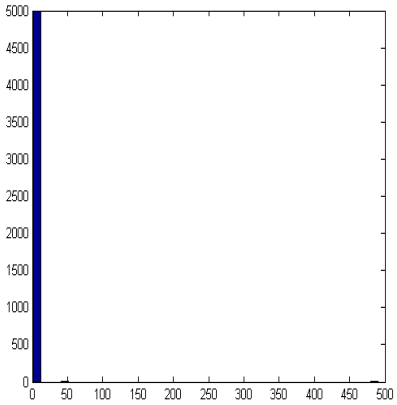

6.3.1 Sine Wiener noise

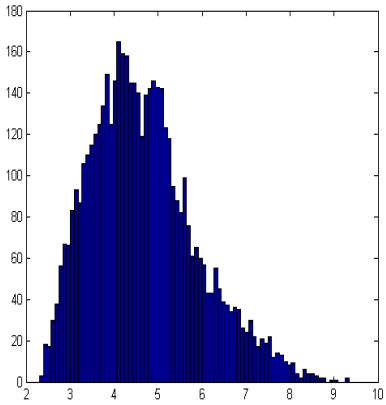

6.3.2 Cai noise

Figure 6.3: X_{final} probability density over 5000 simulations with bounded Sine Wiener noise (left figure) and bounded Cai noise (right figure),with amplitude $B = 1.2$ and correlation time $\tau = 1$, added on parameter ϕ. Starting values are those of microscopic equilibrium point $(x, y) = (4.83, 0.38)$.

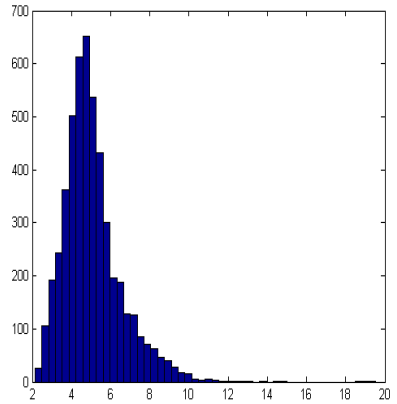

6.4.1 Sine Wiener noise

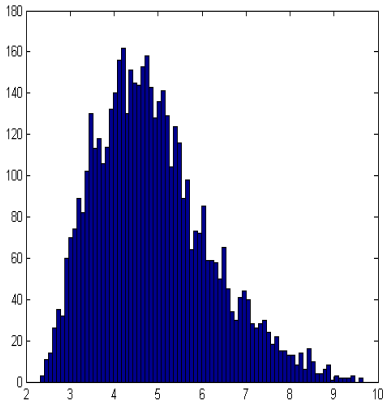

6.4.2 Cai noise

Figure 6.4: X_{final} probability density over 5000 simulations with bounded Sine Wiener noise (left figure) and bounded Cai noise (right figure),with amplitude $B = 1.2$ and correlation time $\tau = 1$, added on parameter ϕ. Starting values are $(x, y) = (0.1, 2)$.

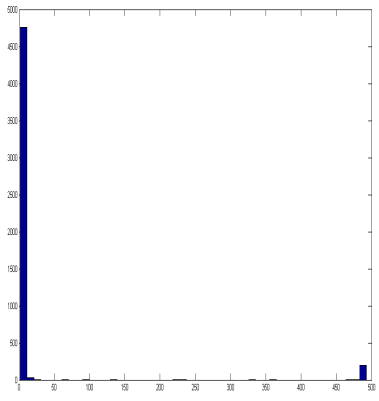

6.5.1 Sine Wiener noise

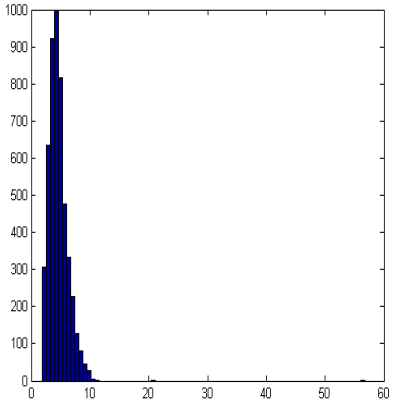

6.5.2 Cai noise

Figure 6.5: X_{final} probability density over 5000 simulations with bounded Sine Wiener noise (left figure) and bounded Cai noise (right figure),with amplitude $B = 1.4$ and correlation time $\tau = 1$, added on parameter ϕ. Starting values are those of microscopic equilibrium point $(x, y) = (4.83, 0.38)$.

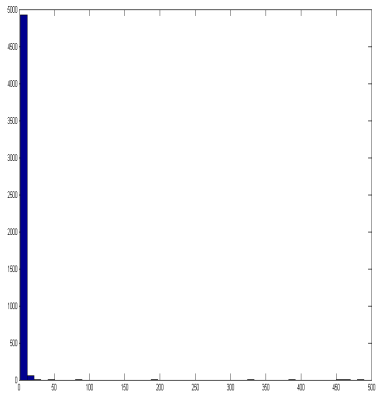

6.6.1 Sine Wiener noise

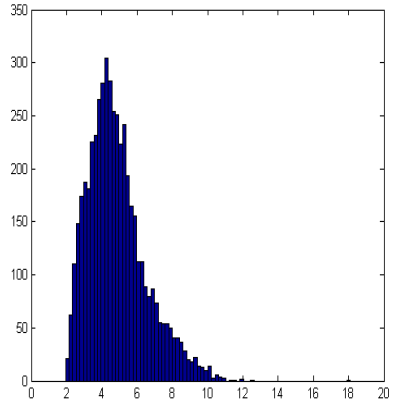

6.6.2 Cai noise

Figure 6.6: X_{final} probability density over 5000 simulations with bounded Sine Wiener noise (left figure) and bounded Cai noise (right figure),with amplitude $B = 1.4$ and correlation time $\tau = 1$, added on parameter ϕ. Starting values are $(x, y) = (0.1, 2)$.

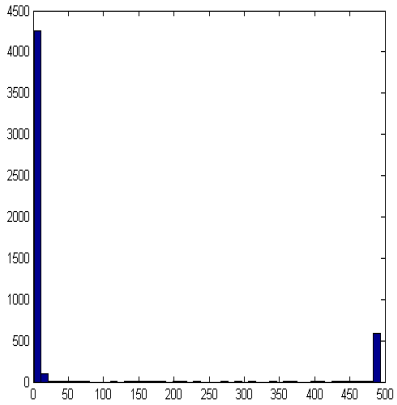

6.7.1 Sine Wiener noise

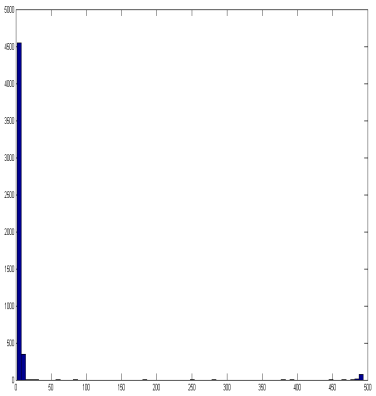

6.7.2 Cai noise

Figure 6.7: X_{final} probability density over 5000 simulations with bounded Sine Wiener noise (left figure) and bounded Cai noise (right figure),with amplitude $B = 1.6$ and correlation time $\tau = 1$, added on parameter ϕ. Starting values are those of microscopic equilibrium point $(x, y) = (4.83, 0.38)$.

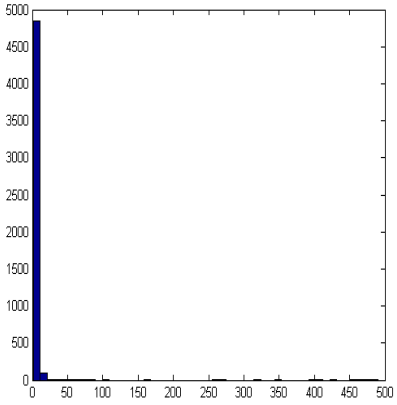

6.8.1 Sine Wiener noise

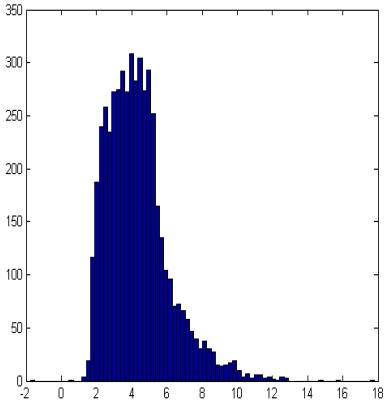

6.8.2 Cai noise

Figure 6.8: X_{final} probability density over 5000 simulations with bounded Sine Wiener noise (left figure) and bounded Cai noise (right figure),with amplitude $B = 1.6$ and correlation time $\tau = 1$, added on parameter ϕ. Starting values are $(x, y) = (0.1, 2)$.

6.2 Perturbation on parameter β

I performed some simulations of the new system obtained from (6.1), (6.2) simply adding noise ν to the parameter β, in both form of Sine Wiener and Cai:

$$x' = x\alpha(1 - bx) - \phi yx \tag{6.5}$$

$$y' = \frac{(\beta + \nu)x}{\eta + x} y - (\mu_0 + \mu_1 x)y + \sigma \tag{6.6}$$

The following tables show the results obtained by varying the amplitude of the noise (B) and its correlation time (τ):

SW noise:

Amplitude (B)	Correlation time (τ)	Comments
1	1	//
1.6	1	//
2	1	//
2	1.2	//
2	2	//
2.5	1	//
2.5	1.2	//
2.5	2	//
3	1	//
3	1.5	//
3	3	//
4	1.5	//
4	2	//
5	2	//
10	3	//
10	8	Evident oscillations
10	10	Evident oscillations
15	3	Evident oscillations
20	3	Evident oscillations

Cai noise:

Amplitude (B)	Correlation time (τ)	Comments
1	1	//
1.6	1	//
2	1	//
2	1.2	//
2	2	//
2.5	1	//
2.5	1.2	//
2.5	2	//
3	1	//
3	1.5	//
3	3	//
4	1.5	//
4	2	//
5	2	//
10	3	//
10	8	Evident oscillations
10	10	Evident oscillations
15	3	Evident oscillations
20	3	Evident oscillations

Observation: Introducing an additive SW / Cai noise to the parameter β there are no relevant changes in the model behavior.

6.3 Perturbation on parameter η

I performed some simulations of the new system obtained from (6.1), (6.2) simply adding noise ν to the parameter η, in both form of Sine Wiener and Cai:

$$x' = x\alpha(1 - bx) - \phi yx \tag{6.7}$$

$$y' = \frac{\beta x}{(\eta + \nu) + x} y - (\mu_0 + \mu_1 x)y + \sigma \tag{6.8}$$

The following tables show the results obtained by varying the amplitude of the noise (B) and its correlation time (τ):

SW noise:

Amplitude (B)	Correlation time (τ)	Comments
1	1	//
1	2	//
1	5	//
1	10	//
2	1	//
2	2	//
2	5	//
2	10	//
5	1	//
5	2	//
5	5	//
5	10	//
10	1	//
10	2	//
10	5	//
10	10	Evident oscillations
20	5	Evident oscillations
20	10	Evident oscillations
30	5	Evident oscillations
30	10	Evident oscillations

Cai noise:

Amplitude (B)	Correlation time (τ)	Comments
1	1	//
1	2	//
1	5	//
1	10	//
2	1	//
2	2	//
2	5	//
2	10	//
5	1	//
5	2	//
5	5	//
5	10	//
10	1	//
10	2	//
10	5	Evident oscillations
10	10	Evident oscillations
20	5	Evident oscillations
20	10	Evident oscillations
30	5	Evident oscillations
30	10	Evident oscillations

Observation: Introducing an additive SW / Cai noise to the parameter η there are no relevant changes in the model behavior.

6.4 Perturbation on parameter σ

I performed some simulations of the new system obtained from (6.1), (6.2) simply adding noise ν to the parameter σ, in both form of Sine Wiener and Cai:

$$x' = x\alpha(1 - bx) - \phi yx \tag{6.9}$$

$$y' = \frac{\beta x}{\eta + x}y - (\mu_0 + \mu_1 x)y + (\sigma + \nu) \tag{6.10}$$

The following tables and figures show the results obtained by varying the amplitude of the noise (B) and its correlation time (τ):

SW noise:

Amplitude (B)	Correlation time (τ)	Comments
0.01	0.1	//
0.01	0.5	//
0.03	0.5	//
0.03	0.8	Evasion begins
0.04	0.2	Evasion begins
0.04	0.4	Evasion
0.05	0.2	Evasion
0.05	0.5	Evasion
0.08	0.1	Evasion
0.08	0.5	Evasion
0.1	0.1	Evasion
0.1	0.5	Evasion
0.1	1	Evasion
0.11	0.1	Evasion
0.118	0.1	Evasion

Cai noise:

Amplitude (B)	Correlation time (τ)	Comments
0.01	0.1	//
0.01	0.5	//
0.03	0.5	//
0.03	0.8	//
0.04	0.2	//
0.04	0.4	//
0.05	0.2	//
0.05	0.5	//
0.08	0.1	//
0.08	0.5	//
0.1	0.1	//
0.1	0.5	//
0.1	1	//
0.11	0.1	//
0.118	0.1	//

Observation: Introducing a Sine Wiener noise, for some values of amplitude and correlation time, I can notice a clear evasion from the point of microscopic equilibrium to the macroscopic one as it is evident in the figures (6.13.1) (6.14.1) (6.15.1) (6.16.1) (6.17.1) (6.18.1) (6.19.1) (6.20.1) (6.21.1) (6.22.1). Introducing a Cai noise, instead, there are no relevant changes in model behavior.

Perturbation on parameter σ

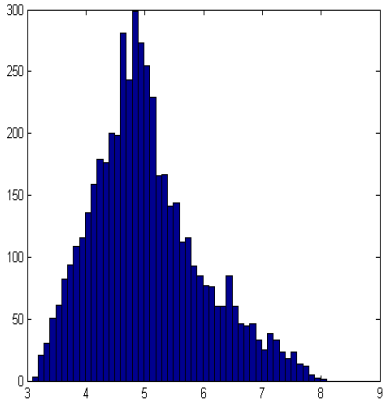

6.9.1 Sine Wiener noise

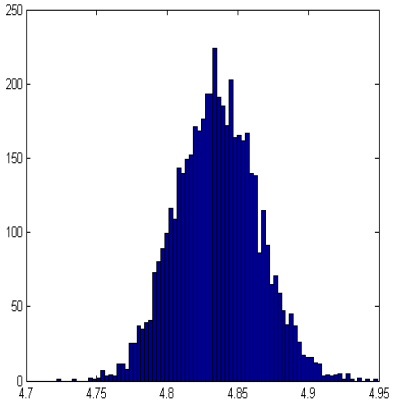

6.9.2 Cai noise

Figure 6.9: X_{final} probability density over 5000 simulations with bounded Sine Wiener noise (left figure) and bounded Cai noise (right figure),with amplitude $B = 0.03$ and correlation time $\tau = 0.8$, added on parameter σ. Starting values are those of microscopic equilibrium point $(x, y) = (4.83, 0.38)$.

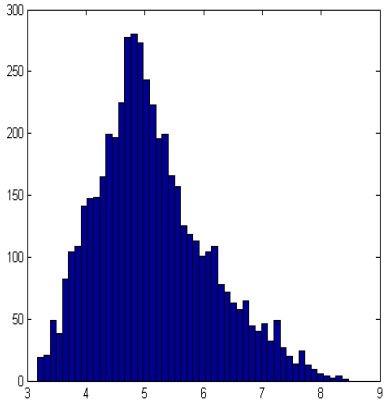

6.10.1 Sine Wiener noise

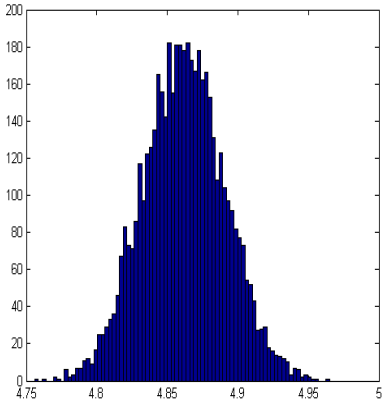

6.10.2 Cai noise

Figure 6.10: X_{final} probability density over 5000 simulations with bounded Sine Wiener noise (left figure) and bounded Cai noise (right figure),with amplitude $B = 0.03$ and correlation time $\tau = 0.8$, added on parameter σ.Starting values are $(x, y) = (0.1, 2)$.

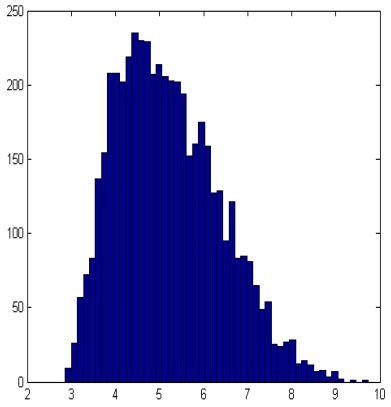

6.11.1 Sine Wiener noise

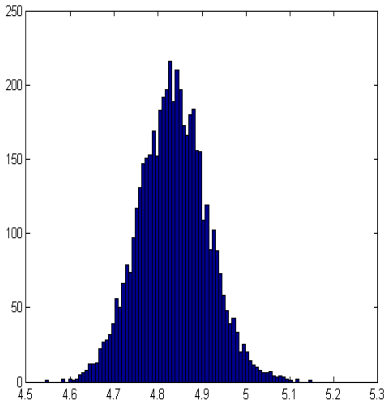

6.11.2 Cai noise

Figure 6.11: X_{final} probability density over 5000 simulations with bounded Sine Wiener noise (left figure) and bounded Cai noise (right figure),with amplitude $B = 0.04$ and correlation time $\tau = 0.2$, added on parameter σ. Starting values are those of microscopic equilibrium point $(x, y) = (4.83, 0.38)$.

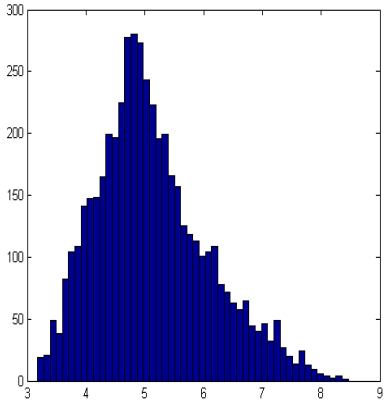

6.12.1 Sine Wiener noise

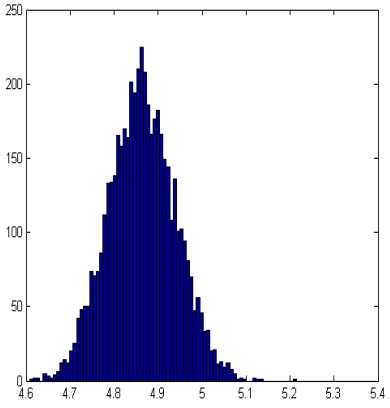

6.12.2 Cai noise

Figure 6.12: X_{final} probability density over 5000 simulations with bounded Sine Wiener noise (left figure) and bounded Cai noise (right figure),with amplitude $B = 0.04$ and correlation time $\tau = 0.2$, added on parameter σ.Starting values are $(x, y) = (0.1, 2)$.

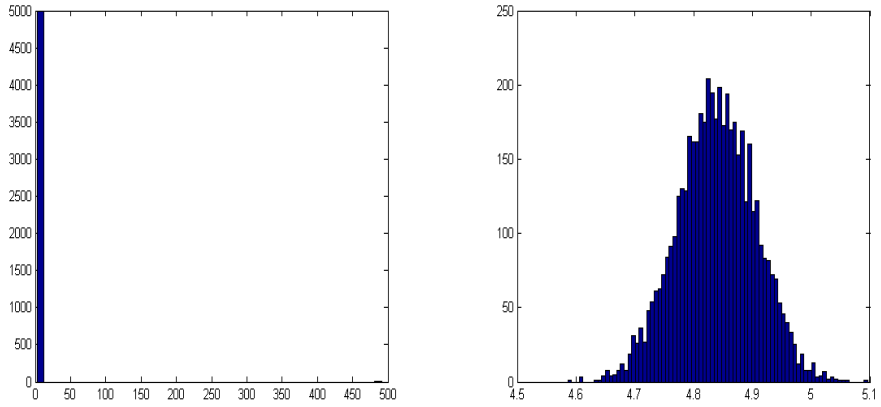

6.13.1 Sine Wiener noise

6.13.2 Cai noise

Figure 6.13: X_{final} probability density over 5000 simulations with bounded Sine Wiener noise (left figure) and bounded Cai noise (right figure),with amplitude $B = 0.04$ and correlation time $\tau = 0.4$, added on parameter σ. Starting values are those of microscopic equilibrium point $(x, y) = (4.83, 0.38)$.

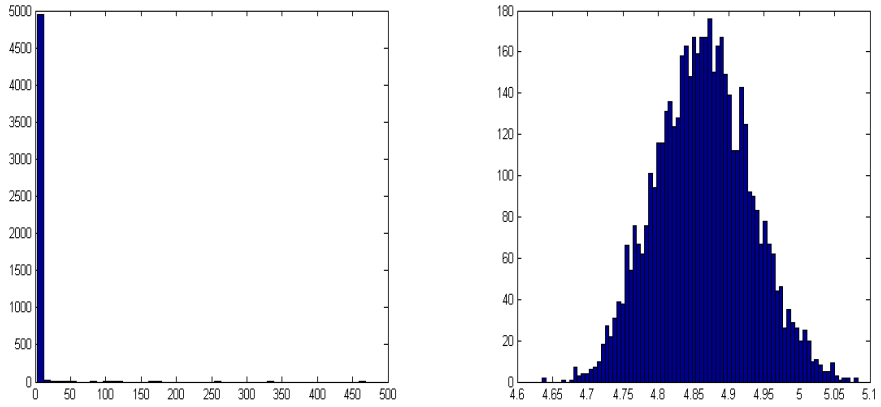

6.14.1 Sine Wiener noise

6.14.2 Cai noise

Figure 6.14: X_{final} probability density over 5000 simulations with bounded Sine Wiener noise (left figure) and bounded Cai noise (right figure),with amplitude $B = 0.04$ and correlation time $\tau = 0.4$, added on parameter σ.Starting values are $(x, y) = (0.1, 2)$.

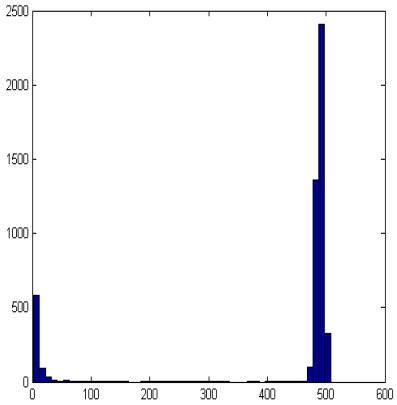

6.15.1 Sine Wiener noise

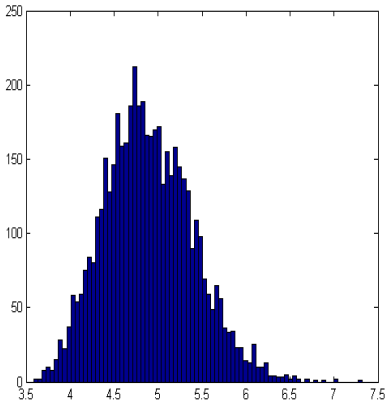

6.15.2 Cai noise

Figure 6.15: X_{final} probability density over 5000 simulations with bounded Sine Wiener noise (left figure) and bounded Cai noise (right figure),with amplitude $B = 0.1$ and correlation time $\tau = 0.1$, added on parameter σ. Starting values are those of microscopic equilibrium point $(x, y) = (4.83, 0.38)$.

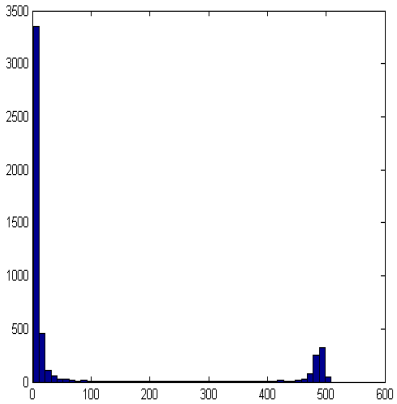

6.16.1 Sine Wiener noise

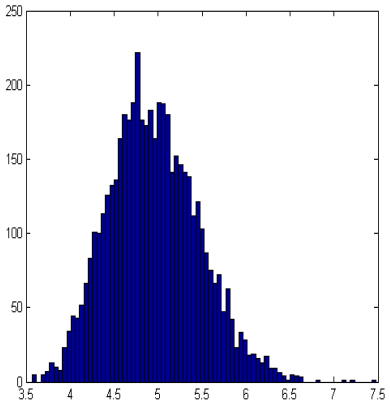

6.16.2 Cai noise

Figure 6.16: X_{final} probability density over 5000 simulations with bounded Sine Wiener noise (left figure) and bounded Cai noise (right figure),with amplitude $B = 0.1$ and correlation time $\tau = 0.1$, added on parameter σ.Starting values are $(x, y) = (0.1, 2)$.

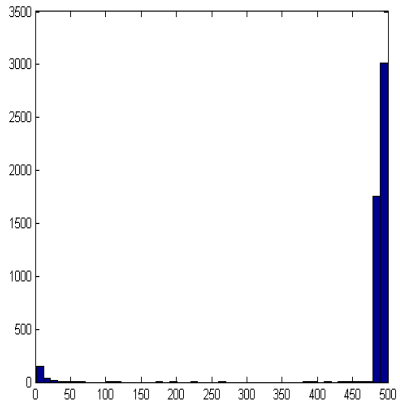

6.17.1 Sine Wiener noise

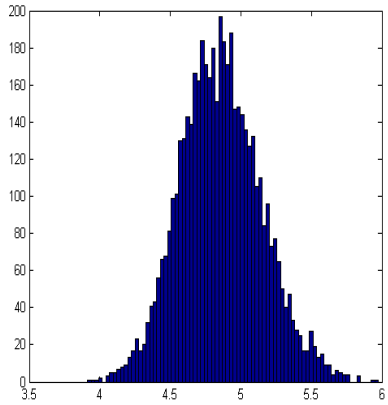

6.17.2 Cai noise

Figure 6.17: X_{final} probability density over 5000 simulations with bounded Sine Wiener noise (left figure) and bounded Cai noise (right figure),with amplitude $B = 0.1$ and correlation time $\tau = 1$, added on parameter σ. Starting values are those of microscopic equilibrium point $(x, y) = (4.83, 0.38)$.

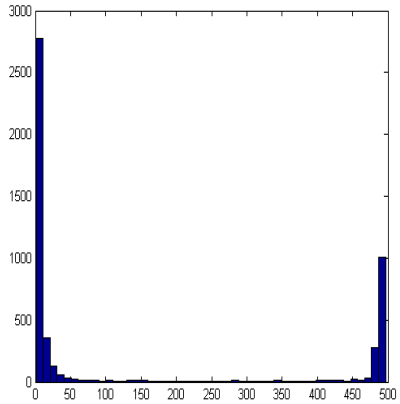

6.18.1 Sine Wiener noise

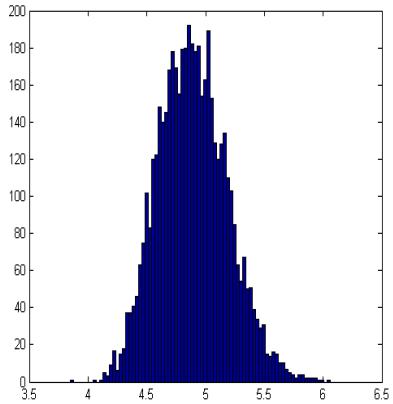

6.18.2 Cai noise

Figure 6.18: X_{final} probability density over 5000 simulations with bounded Sine Wiener noise (left figure) and bounded Cai noise (right figure),with amplitude $B = 0.1$ and correlation time $\tau = 1$, added on parameter σ.Starting values are $(x, y) = (0.1, 2)$.

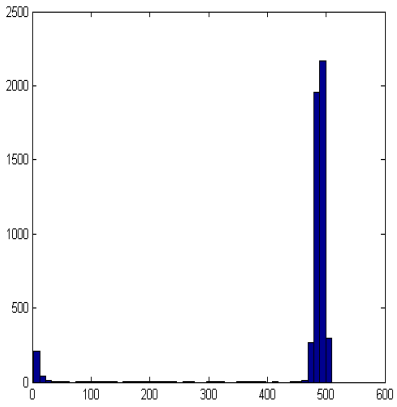

6.19.1 Sine Wiener noise

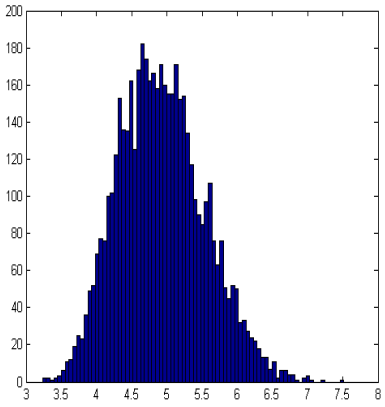

6.19.2 Cai noise

Figure 6.19: X_{final} probability density over 5000 simulations with bounded Sine Wiener noise (left figure) and bounded Cai noise (right figure),with amplitude $B = 0.11$ and correlation time $\tau = 0.1$, added on parameter σ. Starting values are those of microscopic equilibrium point $(x, y) = (4.83, 0.38)$.

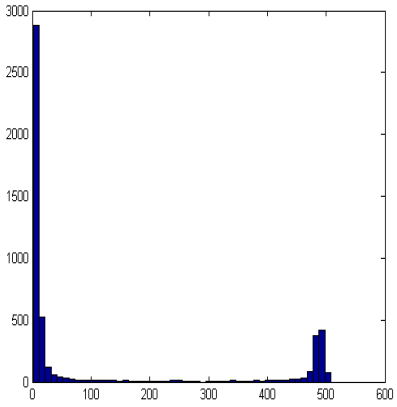

6.20.1 Sine Wiener noise

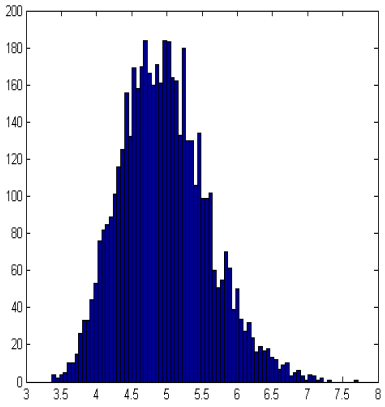

6.20.2 Cai noise

Figure 6.20: X_{final} probability density over 5000 simulations with bounded Sine Wiener noise (left figure) and bounded Cai noise (right figure),with amplitude $B = 0.11$ and correlation time $\tau = 0.1$, added on parameter σ. Starting values are $(x, y) = (0.1, 2)$.

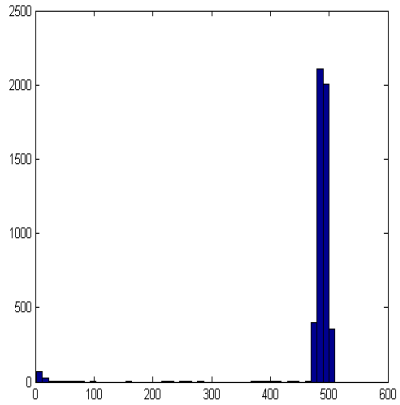

6.21.1 Sine Wiener noise

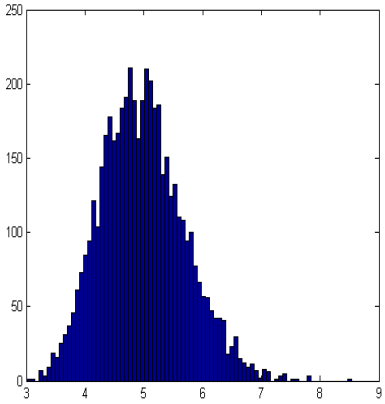

6.21.2 Cai noise

Figure 6.21: X_{final} probability density over 5000 simulations with bounded Sine Wiener noise (left figure) and bounded Cai noise (right figure),with amplitude $B = 0.118$ and correlation time $\tau = 0.1$, added on parameter σ. Starting values are those of microscopic equilibrium point $(x, y) = (4.83, 0.38)$.

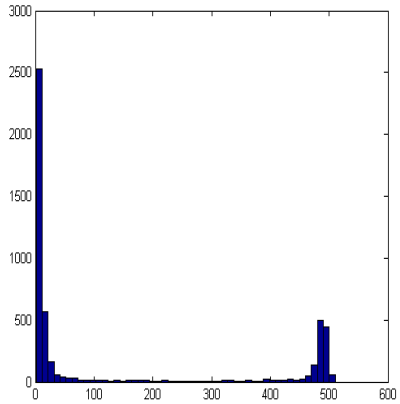

6.22.1 Sine Wiener noise

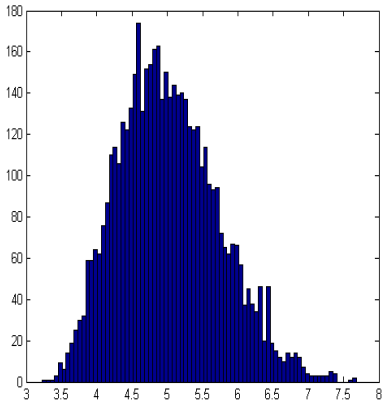

6.22.2 Cai noise

Figure 6.22: X_{final} probability density over 5000 simulations with bounded Sine Wiener noise (left figure) and bounded Cai noise (right figure),with amplitude $B = 0.118$ and correlation time $\tau = 0.1$, added on parameter σ.Starting values are $(x, y) = (0.1, 2)$.

6.5 Other simulations

Clearly, the noise can be inserted in many different ways within the model considered.
Including a multiplicative factor $(1+\nu)$ to the parameter b we get the system:

$$x' = x\alpha(1 - b(1+\nu)x) - \phi yx \tag{6.11}$$

$$y' = \frac{\beta x}{\eta + x}y - (\mu_0 + \mu_1 x)y + \sigma \tag{6.12}$$

The following tables show the results obtained by varying the amplitude of the noise (B) and its correlation time (τ):

SW noise:

Amplitude (B)	Correlation time (τ)	Comments
0.02	0.01	//
0.05	0.01	//
0.05	0.1	//
0.05	1	//
0.08	0.01	//
0.08	0.1	//
0.08	1	//
0.1	0.01	//
0.1	0.1	//
0.1	1	//
0.3	0.05	//
0.3	0.5	//
0.3	2	//
0.5	0.05	//
0.5	0.3	//
0.5	1	//
0.8	0.05	//
0.8	0.5	//
0.8	1	//
1	0.02	//
1	0.3	//
1	1	//
3	0.2	//
3	1	//
3	3	//
5	1	//
5	5	Evident oscillations
10	5	Evident oscillations

Cai noise:

Amplitude (B)	Correlation time (τ)	Comments
0.02	0.01	//
0.05	0.01	//
0.05	0.1	//
0.05	1	//
0.08	0.01	//
0.08	0.1	//
0.08	1	//
0.1	0.01	//
0.1	0.1	//
0.1	1	//
0.3	0.05	//
0.3	0.5	//
0.3	2	//
0.5	0.05	//
0.5	0.3	//
0.5	1	//
0.8	0.05	//
0.8	0.5	//
0.8	1	//
1	0.02	//
1	0.3	//
1	1	//
3	0.2	//
3	1	//
3	3	Evident oscillations
5	1	Evident oscillations
5	5	Evident oscillations
10	5	Evident oscillations

Observation: There are no relevant changes in the model behavior.

Including a multiplicative factor $(1+\nu)$ to x we get the system:

$$x' = x\alpha(1-bx) - \phi yx \tag{6.13}$$

$$y' = \frac{\beta x}{\eta + x(1+\nu)}y - (\mu_0 + \mu_1 x)y + \sigma \tag{6.14}$$

The following tables show the results obtained by varying the amplitude of the noise (B) and its correlation time (τ):

SW noise:

Amplitude (B)	Correlation time (τ)	Comments
0.01	0.01	//
0.01	0.1	//
0.05	0.1	//
0.05	1	//
0.08	1	//
0.08	3	//
0.1	1	//
0.1	3	//
0.5	1	//
0.5	5	//
1	0.1	//
1	1	//

Cai noise:

Amplitude (B)	Correlation time (τ)	Comments
0.01	0.01	//
0.01	0.1	//
0.05	0.1	//
0.05	1	//
0.08	1	//
0.08	3	//
0.1	1	//
0.1	3	//
0.5	1	//
0.5	5	//
1	0.1	//
1	1	//

Observation: There are no relevant changes in the model behavior.

6.6 Conclusions

As we can see from the results, the statistical fluctuations does not make the tumor evade in all cases.
In the case of perturbations on the parameter ϕ , for $B = 1.2, 1.4, 1.6$ and $\tau = 1$ there is transition to bimodality with a considerable probability of tumor explosion in both cases of SW and Cai noise. We recall that the biological meaning of this parameter is the rate of killing tumor cells by the immune system effectors.
The introduction of perturbations on parameter σ shows a behavior that depends on the kind of noise, since there is a remarkable difference between the responses to SW and Cai noises. In the case of SW perturbations, we observed transitions to bimodality with a considerable probability of tumor explosion for noise amplitude and correlation time values: $B = 0.03$,$\tau = 0.8$; $B = 0.04, \tau = 0.2, 0.4$; $B = 0.05, \tau = 0.2, 0.5$; $B = 0.08, \tau = 0.1, 0.5$; $B = 0.1, \tau = 0.1, 0.5$; $B = 0.11, \tau = 0.1$; $B = 0.118, \tau = 0.1$. Using Cai noise, on the contrary, there are not relevant changes in model behavior. We recall that the biological meaning of the parameter σ is the local influx of immune system effectors.
Clearly, transitions depend on the noise model adopted. These observation, confirming the biological intuition, suggest that SW fluctuations easily induce immunoevasion while Cai fluctuations are generally filtered out or have small effects.
In the case of perturbations on parameter β, η and other simulations there are not relevant changes on model behavior.
In conclusion, our results seem to show that these perturbations may contribute to triggering the tumor escape but-generally speaking-not so easy. We showed that limiting the analysis at finite significant time (T=100), the transition to larger values is not reached if the oscillation B of the noise is too small or if the autocorrelation time τ is small.

Chapter 7

Non-clonal resistance to chemotherapy induced by its stochastical fluctuations

We have seen in the previous chapter that, introducing a bounded noise-band stochastic perturbation in a model of tumor-immune system interplay may dramatically modify the behavior of its solutions. The above mentioned analysis was in absence of the delivery of therapies, and was valid for highly to moderately immunogenic tumors, which are able to trigger the action of the immune system. Here we study a quite opposite case: the introduction of bounded perturbation in a simple but realistic novel mathematical model of tumor growth in presence of the delivering of a constant continuous chemotherapy.

The large rate of relapses during chemotherapeutic treatments of tumors is generally explained through the paradigm Clonal Resistance (CR).[1] However, in last decade, a number of biophysical investigations [JTT99, DC01, Jai01] revealed that a significant fraction of cases of resistance to therapy is actually linked to phenomena that may, broadly speaking, be defined as physical resistance (PR) to drugs. Perhaps the most important among these phenomena are: a limited ability of the drug to penetrate into the tumoral tissue because

[1] Clonal Resistance: the emergence through fast mutations of drug-insensitive cells in a tumor under chemotherapy.[DG09]

of a poor or nonlinear diffusivity [AT09] and the anomalous binding of the drug molecule to the surface of tumor cells or to extracellular matrix [GJ00]. This means that resistance cannot only be imputed to a sort of Darwinian evolution of the cancerous population through the birth of new clones, but also to the pharmacodynamics of the molecules of the drugs in the tumor.
Here we want to stress two possible different ways of insurgence of resistance due to a nonlinear population interplay with noise. The presence of multiple equilibria in the model, can make the stochastic bounded fluctuations that affect both the carrying capacity of the tumor or the drug level in the blood, cause the transition from a low equilibrium to a far larger value, not compatible with the life of the host. We propose to frame the above phenomena as a new and non-clonal kind of resistance to chemotherapy.

7.1 Model of tumor growth in presence of chemotherapy

Let us consider a tumor - solid or non-solid - whose size (biomass, number of viable cells, etc..) at time t is denoted as X, and which is growing according to a classical growth law [Whe98]:

$$X' = f\left(\frac{X}{K}\right) X,$$

where $K > 0$ and $f(u)$ is a decreasing function of u for which $f(1) = 0$. The value K is usually called *carrying capacity*, which depends on the available nutrients and/or space, for which the tumor cells compete. Another important parameter is the value $\alpha = f(0)$, which we shall call "the baseline growth rate" (BGR), which can be read as a measure of the intrinsic growth rate of the tumor, in absence of any competition. Of course, since $f(u)$ is decreasing, the BGR is also the maximal growth rate.
Two well known growth laws are the Gompertz law where $f(X) = pLog(K/X)$, and the generalized logistic $f(X) = \alpha(1 - (X/K)^a)$ with $a > 0$. Note that in the Gompertz case, the BGR is infinite, which is not realistic.
Let the tumor be under the delivering of a cytotoxic therapy with a drug whose blood concentration, denoted by $c(t)$, may be periodic or constant.

Which is the effect of $c(t)$ on the tumor growth? The log-kill hypothesis [H.E86] prescribes that the rate of tumor cells killing is proportional to the product $c(t)X(t)$:

$$X' = f\left(\frac{X}{K}\right)X - \gamma c(t)X(t). \tag{7.1}$$

In the case of a bounded intrinsic growth rate, i.e. $f(0) < \infty$, the condition $< c(t) >> f(0)/\gamma$ implies that $X(t) \to 0$, independently from $X(0) > 0$.
However, since seventies Norton and Simon [L.Na, L.Nb] stressed as a potential pitfall of the log-kill hypothesis the fact that the relative killing rate is simply taken proportional to $c(t)$. According to the log-kill hypothesis, the same drug concentration is indeed able to kill the same relative number of cells per unit time independently of the tumor burden. Moreover, the absolute velocity of regression caused by $c(t)$ would be greater in the larger tumors. This is often unrealistic. On the contrary, in clinics it is often observed that the effort to make a large tumor regress is considerable greater, whereas hystologically similar tumors of small volumes are curable using the same delivered quantity of the chemotherapeutic agent. A possible cause of this fact is the development of clones of cells that are resistant to the delivered agent. However, since the reduced drug effectiveness may also be present in the very first phases of a therapy, Norton and Simon [L.Na, L.Nb] summarized this observation, by assuming that the parameter γ is not constant but it is a decreasing function of X: $\gamma(X)$, with $\gamma'(X) < 0$, leading to the following non-logkill model:

$$X' = f\left(\frac{X}{K}\right)X - \gamma(X)c(t)X, \qquad X(0) = X_0. \tag{7.2}$$

In particular, Norton and Simon proposed that $\gamma(X)$ be proportional to $f(X/K)$ [L.Na, L.Nb], which we shall not assume here. We thus consider generic decreasing $\gamma(X)$.
It is trivial to verify that if $\langle c(t)\rangle > \alpha/\gamma(0)$ then the tumor free equilibrium $X_e = 0$ is locally stable, whereas in case of constant continuous infusion, $c(t) = C$, if $\gamma(X)C > f(X/K)$ then the tumor free equilibrium $X_e = 0$ is globally stable. In the general case, since $\gamma(K) > f(1) = 0$, if $\alpha > \gamma(0)C$ there will be an odd number N of equilibria : $X_1(C,K)$,...,$X_N(C,K)$. It is easy matter to verify that the odd-numbered equilibria, $X_1(C,K)$,... $X_N(C,K)$

are locally stable, whereas the even numbered points $X_2(C,K)$,...,$X_{N-1}(C,)$ are unstable. By varying C or K one may get one ore more hysteresis bifurcations.
Let us suppose that $\gamma(X)C$ be such that three equilibria are present. Then standard analysis reveals that $X_1(C,K)$ and $X_3(C,K)$ will be locally stable and $X_2(C,K)$ will be unstable, and it follows that $X(t) \to X_1(C,K)$ for all $X_0 \in (0, X_2(C,K))$. This means that the chemotherapy, although it does not eliminate the neoplasm, is at least able to control the tumor size keeping it at a low level. This result might seem a good suboptimal result in absence of insurgence of clonal resistance.

7.2 Bounded noises introduction in the model

Apart from the clonal resistance, we shall show that the target tumor may equally escape from the therapeutic control through stochastic fluctuation of either the carrying capacity or the drug concentration.
As far as the carrying capacity K is, this parameter summarizes many important phenomena related to the availability of nutrients. For example, in case of solid tumors K depends on the growth of the neoplasia-induced vessels, whose rate constant are unlikely constant. Moreover, the growth of tumor depends on the general energy intake of the host organism etc..
As a consequence we shall assume that the carrying capacity is a function of time that oscillates around an average value $K_m > 0$:

$$K(t) = K_m(1 + \nu_K(t)) > 0. \tag{7.3}$$

where $\nu_K(t)$ is a noise. We will consider both Sine Wiener and Cai noise.
As far as the chemotherapy is concerned, therapies that guarantee a constant drug density profile as well as effectiveness do not exist in the reality, since the drug concentration will be affected by stochastic oscillations:

$$c(t) = C_m(1 + \nu_C(t)) > 0, \tag{7.4}$$

where $\nu_C(t)$ is a noise and C_m is the average value of the drug concentration profile.

Thus, here we shall study the following stochastic equation:

$$X' = f\left(\frac{X}{K_m(1+\nu_K(t))}\right)X - \gamma(X)C_m(1+\nu_C(t))X. \tag{7.5}$$

The noisy nature of one or both the carrying capacity and the drug density in conjunction with the inherent bistability of the tumor-therapy system, thus, suggests that there might be the insurgence of noise-induced transitions from the "small" steady state $X_1(C_m, K_m)$ toward the macroscopic equilibrium state $X_3(C_m, K)$, as in other important bistable systems.

These transition would be caused by the presence of hysteresis bifurcations that, as it is well known [J.H91], are characterized by the existence of two values of the bifurcation parameter such that infinitesimal changes in the value of this parameter imply that the behavior of the solution has a sudden change. This means that near those two points the behavior of the system is extremely sensitive to any kind of perturbations. As a result the treatment requires that the fluctuations be explicitly incorporated into the model [W.H84, W.H77].

These observations led Horsthemke and Lefever to define the theory of noise-induced transitions (NIT) [W.H84] that investigate the phase transitions induced by zero-mean noises in non-equilibrium systems. Such transitions depend on the characteristics of the noise, such as its variance, and have the effect of changing the nature of the stationary probability density function of state variables, for example from unimodal to bimodal, or vice-versa. The NIT theory is of the utmost interest in biomedicine, since "in-vivo the environmental situations are... extremely complex and thus likely to present important fluctuations" [R.L79].

A classical approach consists in assuming that the stochastic perturbations are gaussian white or colored noises. This, however, is an inappropriate solution in our case for two reasons.

The first reason is that the system in study depends nonlinearly from one of the two stochastically perturbed parameters: the carrying capacity K.

The second reason involves the fluctuations affecting C. Indeed, let us consider the model (7.8) with $\nu_K(t) = 0$ and let us allow that $\nu_C(t)$ is a gaussian noise, implying:

$$dX = F(X/K)dt - \gamma(X)C_m(dt + \xi(t)\sqrt{dt}),$$

where $\xi(t)$ are Gaussian random numbers.
Since the noise is unbounded, there will be a non-null probability that $C_m(dt+\xi(t)\sqrt{dt}) < 0$.
In other words, there would be a non-null probability that a cytotoxic-chemotherapy may add neoplastic cells to its target tumor, which is a non-sense. As a consequence the gaussian noise should be avoided to investigate the effects of fluctuations of chemotherapy. Note that also extremely large killing rates per time units are not possible, which precludes not only gaussian noises, but also lognormal noises.
For these reasons, we shall assume that both $\nu_K(t)$ and $\nu_C(t)$ are bounded noises, i.e. that it exists a $B > 0$ such that $|\nu(t)| < B < +\infty$.
Since the noise-induced transitions are dependent on the kind of density of noise adopted [Fue07], we shall assume two kind of bounded noise: The sine-Wiener noise and The Cai noise [CS05].
To make as simple as possible our model, in our simulations we shall assume that the tumor growth law, in absence of therapies, a generalized logistic law: $f(X/K) = \alpha(1-(X/K)^a)$, where $0 < a \leq 1$. As far as $\gamma(x)$ is concerned, in absence of experimental data that may suggest some biologically plausible $\gamma(X)$, we used in our simulation a Hill-like function, which is ubiquitary in biological modelling, and which in our case reads:

$$\gamma(X) = A\frac{1}{1+\left(\frac{X}{X^*}\right)^n},$$

where $0 < X_* < K$ is a typical size tuning the action of the chemotherapy, and $n > 0$ is a parameter that tunes the shape of the function (e.g. for $n >> 1$ and $X \geq 0$ it holds: $\gamma(X) \approx Heaviside(X^* - X)$). The parameter A embeds the baseline effectiveness of the drug dose profile $c(t)$ for small size tumors. Moreover, we shall non-dimensionalize the model by assuming that $K_m = 1$ and that $\alpha = 1$, i.e. we assume that the reference size is the average carrying capacity and that the reference time unit is the characteristic time of growth of the tumor for small tumor size (where $X' \approx \alpha X$).
A major point to be stressed is that the classical theory of noise induced transitions [W.H84] is an asymptotic theory that refers to the study of the qualitative changes in stationary probability densities: $P_{st}(x) = lim_{t\to\infty}P(x,t)$. However, whatever asymptotic study might be, if the velocity of convergence

of the stationary density is slow,it is in contradiction with the basic fact that living beings have a finite lifespan. Thus the lifespan of the host organisms must be a natural limit to our numerical investigations, which makes the velocity of convergence to $P_{st}(x)$ an essential parameter. If this velocity is slow and the attractor is practically reached in times that are excessively greater than the average lifespan of the organisms in study, one has to investigate the possible qualitative changes of $P(x,t)$ during its transitory, namely at some given realistic times. For this reason we focused here on transitory analysis of $P(x,t)$. Indeed, noise has been introduced on carrying capacity and drug concentration observing the probability density at time $T = 66$ corresponding , in dimensional time unity, to 1 year about, both in case of Sine Wiener and Cai noise perturbations. It must be observed that all simulations have been done using **Matlab 7.0.4**.

7.3 Numerical simulations

In our simulations we considered as reference host organism for the tumor the mouse (lifespan is 3 years about and in average tumor growth times is in days). Namely, since the average lifespan of a mice is 3 years, since tumors are diseases of later ages, and, finally, chemotherapies have a finite length, we shall calculate the stationary density at one year. Since the time-dimensional baseline growth rate of lymphoma in chimeric mice is 0.18 $days^{-1}$, we shall consider the transitory behaviors at $t = 66$ adimensional time units.
We considered 4 different sets of parameters and calculated the transitory density at one year starting from the microscopic equilibrium point.

These are the sets considered:
1set: $a = 1$, $X^* = 0.25$, $n = 6$, $X_0 = 0.105$
2set: $a = 1$, $X^* = 0.25$, $n = 10$, $X_0 = 0.100$
3set: $a = 2/3$, $X^* = 0.262$, $n = 2$, $X_0 = 0.045$
4set: $a = 1.1$, $X^* = 0.25$, $n = 10$, $X_0 = 0.123$

Bounded SW and Cai noise on carrying capacity

The first step in my numerical simulations is given by the introduction of Sine Wiener / Cai noise on the carrying capacity: K(t). Hence we shall study the following stochastic equation:

$$X' = f\left(\frac{X}{K_m(1+\nu_K(t))}\right)X - \gamma(X)C_m X. \tag{7.6}$$

The following tables and figures show the results obtained by varying the amplitude of the noise (B) and its correlation time (τ):

SW noise:

Amplitude (B)	Correlation time (τ)	1 set*	2 set	3 set	4 set
0.01	0.1	//	//	//	//
0.01	1	//	//	//	//
0.01	5	//	//	//	//
0.08	0.1	//	//	//	//
0.08	1	//	//	//	//
0.08	5	//	//	//	//
0.1	0.1	//	//	//	//
0.1	1	//	//	//	//
0.1	5	//	//	//	//
0.2	0.1	//	//	//	//
0.2	1	Evasion	//	//	//
0.2	5	Evasion	//	//	//
0.3	0.1	//	//	//	//
0.3	1	Evasion	//	Evasion	//
0.3	5	Evasion	//	Evasion	Evasion
0.4	0.1	//	//	//	//
0.4	1	Evasion	//	Evasion	//
0.45	0.1	Evasion	//	//	//
0.5	0.1	Evasion	//	//	//
0.5	1	Evasion	//	Evasion	Evasion
0.5	5	Evasion	//	Evasion	Evasion
0.8	1	Evasion	Evasion	Evasion	Evasion

Cai noise:

Amplitude (B)	Correlation time (τ)	1 set	2 set	3 set	4 set
0.01	0.1	//	//	//	//
0.01	1	//	//	//	//
0.01	5	//	//	//	//
0.08	0.1	//	//	//	//
0.08	1	//	//	//	//
0.08	5	//	//	//	//
0.1	0.1	//	//	//	//
0.1	1	//	//	//	//
0.1	5	//	//	//	//
0.2	0.1	//	//	//	//
0.2	1	//	//	//	//
0.2	5	//	//	//	//
0.3	0.1	//	//	//	//
0.3	1	//	//	//	//
0.3	5	//	//	//	//
0.4	0.1	//	//	//	//
0.4	1	//	//	//	//
0.45	0.1	//	//	//	//
0.5	0.1	//	//	//	//
0.5	1	Evasion	//	//	Evasion
0.5	5	Evasion	//	//	//
0.8	1	Evasion	//	Evasion	Evasion

*1 set: $a = 1$, $X^* = 0.25$, $n = 6$, $X_0 = 0.105$
2 set: $a = 1$, $X^* = 0.25$, $n = 10$, $X_0 = 0.100$
3 set: $a = 2/3$, $X^* = 0.262$, $n = 2$, $X_0 = 0.045$
4 set: $a = 1.1$, $X^* = 0.25$, $n = 10$, $X_0 = 0.123$

Observations:

Introducing a SW noise, for some values of amplitude and correlation time, I can notice a clear evasion from the point of microscopic equilibrium to the macroscopic one (see figures). Introducing a Cai noise, as well, for some values of amplitude and correlation time, evasion is clear.

Perturbation on carrying capacity K

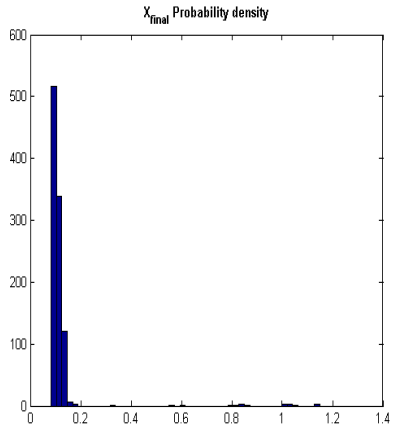

7.1.1 Sine Wiener noise

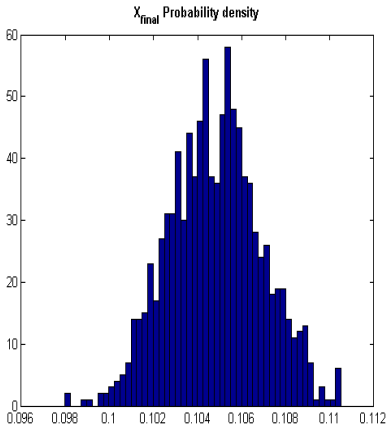

7.1.2 Cai noise

Figure 7.1: X_{final} probability density over 1000 simulations with bounded Sine Wiener noise (left figure) and bounded Cai noise (right figure),with amplitude $B = 0.2$ and correlation time $\tau = 1$, added on carrying capacity. Starting value is the microscopic equilibrium point $x = 0.105$.

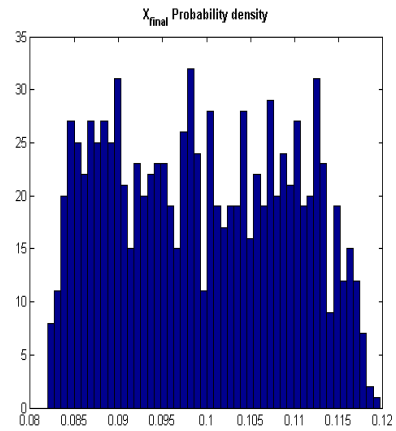

7.2.1 Sine Wiener noise

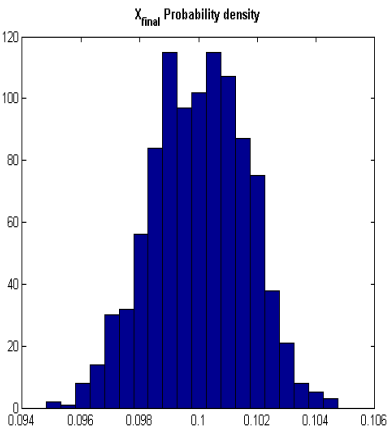

7.2.2 Cai noise

Figure 7.2: X_{final} probability density over 1000 simulations with bounded Sine Wiener noise (left figure) and bounded Cai noise (right figure),with amplitude $B = 0.2$ and correlation time $\tau = 1$, added on carrying capacity. Starting value is the microscopic equilibrium point $x = 0.1$.

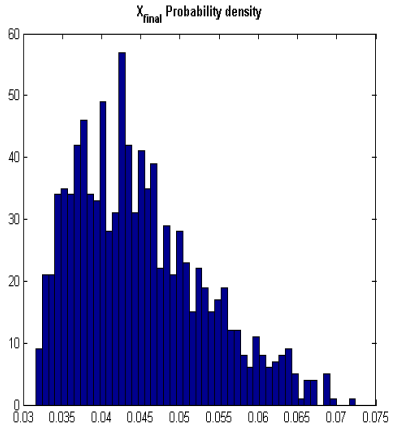

7.3.1 Sine Wiener noise

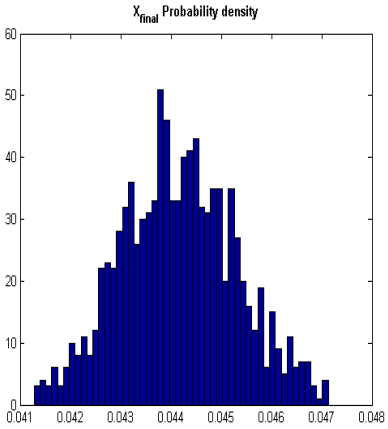

7.3.2 Cai noise

Figure 7.3: X_{final} probability density over 1000 simulations with bounded Sine Wiener noise (left figure) and bounded Cai noise (right figure),with amplitude $B = 0.2$ and correlation time $\tau = 1$, added on carrying capacity. Starting value is the microscopic equilibrium point $x = 0.045$.

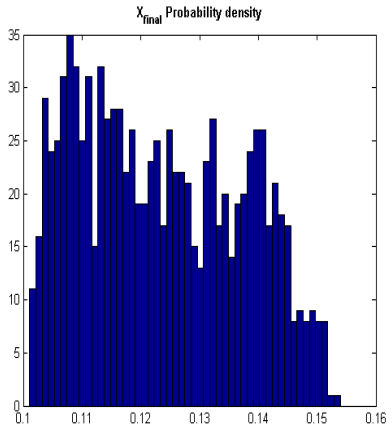

7.4.1 Sine Wiener noise

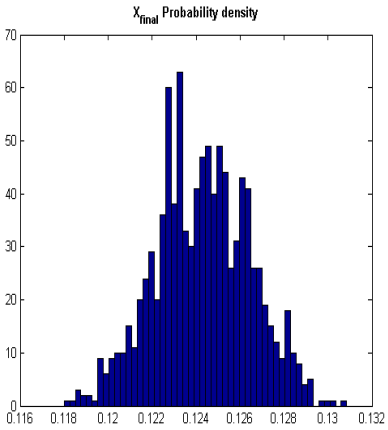

7.4.2 Cai noise

Figure 7.4: X_{final} probability density over 1000 simulations with bounded Sine Wiener noise (left figure) and bounded Cai noise (right figure),with amplitude $B = 0.2$ and correlation time $\tau = 1$, added on carrying capacity. Starting value is the microscopic equilibrium point $x = 0.123$.

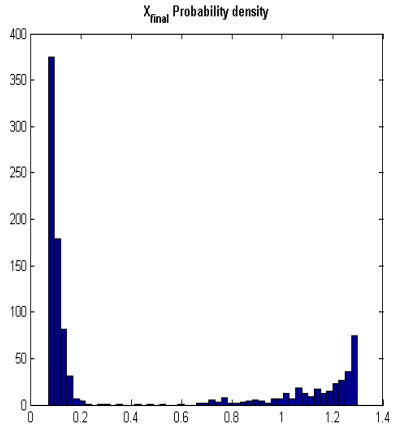

7.5.1 Sine Wiener noise

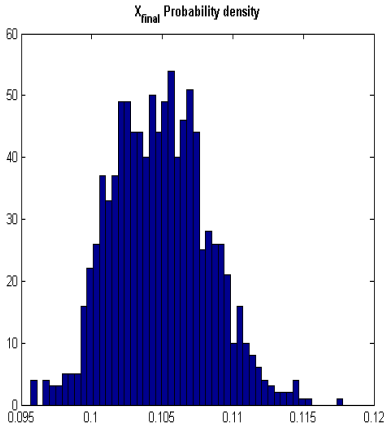

7.5.2 Cai noise

Figure 7.5: X_{final} probability density over 1000 simulations with bounded Sine Wiener noise (left figure) and bounded Cai noise (right figure),with amplitude $B = 0.3$ and correlation time $\tau = 5$, added on carrying capacity. Starting value is the microscopic equilibrium point $x = 0.105$.

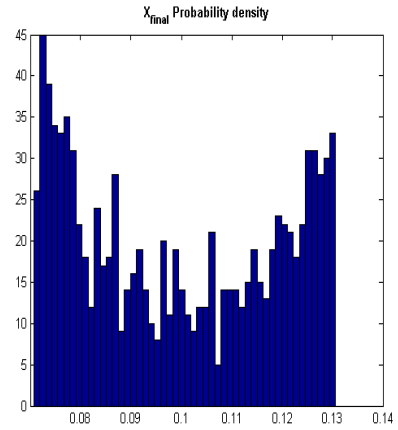

7.6.1 Sine Wiener noise

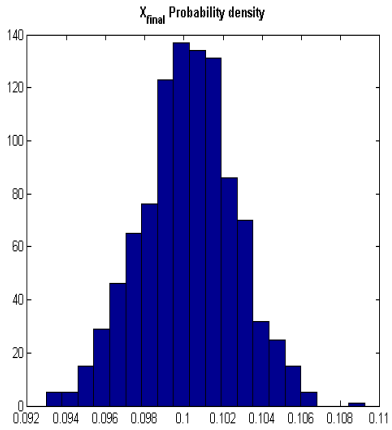

7.6.2 Cai noise

Figure 7.6: X_{final} probability density over 1000 simulations with bounded Sine Wiener noise (left figure) and bounded Cai noise (right figure),with amplitude $B = 0.3$ and correlation time $\tau = 5$, added on carrying capacity. Starting value is the microscopic equilibrium point $x = 0.1$.

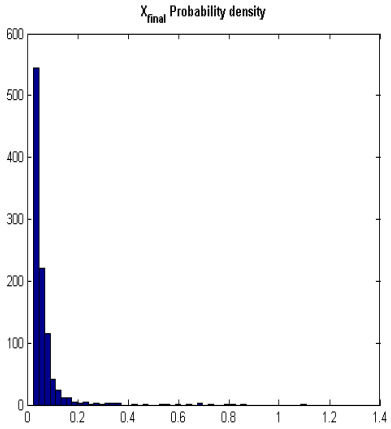

7.7.1 Sine Wiener noise

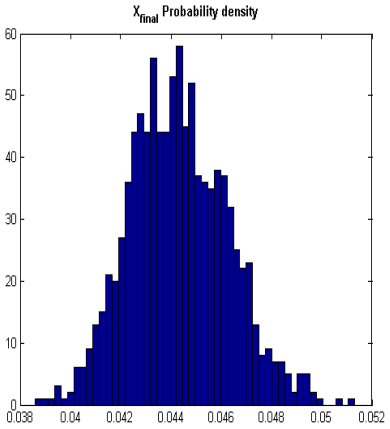

7.7.2 Cai noise

Figure 7.7: X_{final} probability density over 1000 simulations with bounded Sine Wiener noise (left figure) and bounded Cai noise (right figure),with amplitude $B = 0.3$ and correlation time $\tau = 5$, added on carrying capacity. Starting value is the microscopic equilibrium point $x = 0.045$.

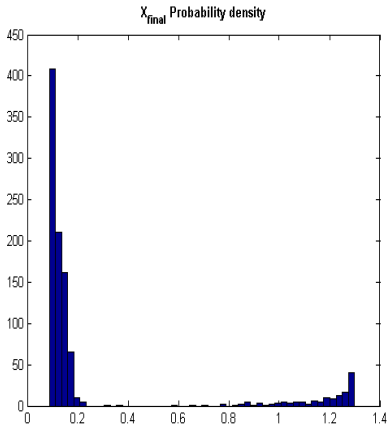

7.8.1 Sine Wiener noise

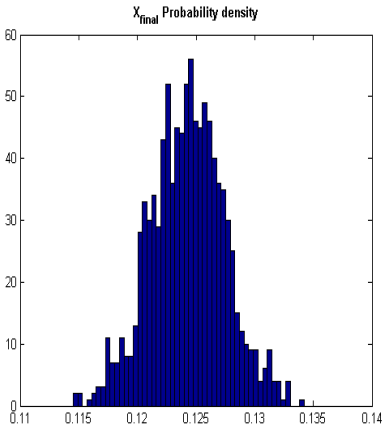

7.8.2 Cai noise

Figure 7.8: X_{final} probability density over 1000 simulations with bounded Sine Wiener noise (left figure) and bounded Cai noise (right figure),with amplitude $B = 0.3$ and correlation time $\tau = 5$, added on carrying capacity. Starting value is the microscopic equilibrium point $x = 0.123$.

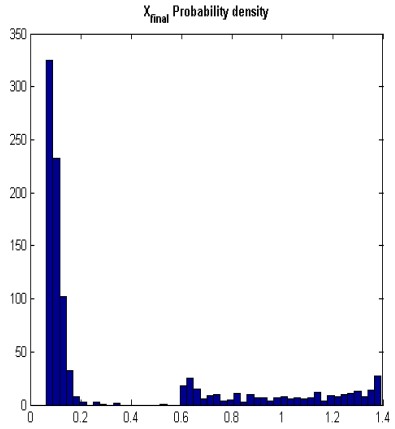

7.9.1 Sine Wiener noise

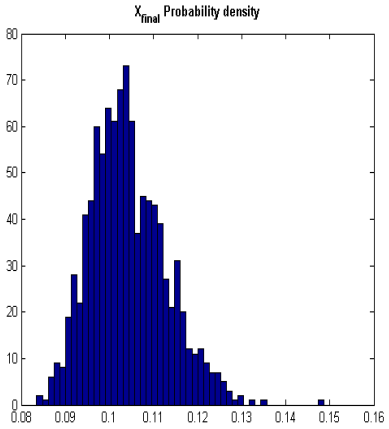

7.9.2 Cai noise

Figure 7.9: X_{final} probability density over 1000 simulations with bounded Sine Wiener noise (left figure) and bounded Cai noise (right figure),with amplitude $B = 0.4$ and correlation time $\tau = 1$, added on carrying capacity. Starting value is the microscopic equilibrium point $x = 0.105$.

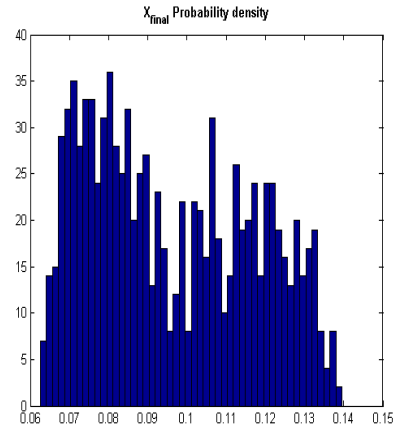

7.10.1 Sine Wiener noise

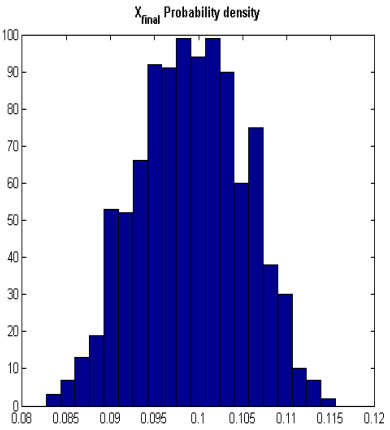

7.10.2 Cai noise

Figure 7.10: X_{final} probability density over 1000 simulations with bounded Sine Wiener noise (left figure) and bounded Cai noise (right figure),with amplitude $B = 0.4$ and correlation time $\tau = 1$, added on carrying capacity. Starting value is the microscopic equilibrium point $x = 0.1$.

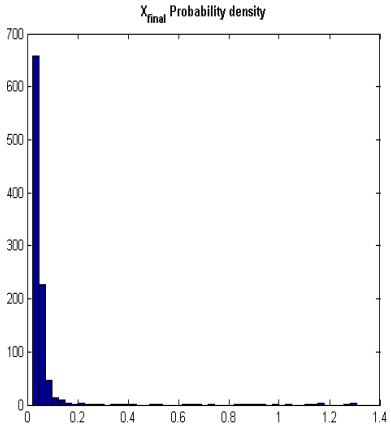

7.11.1 Sine Wiener noise

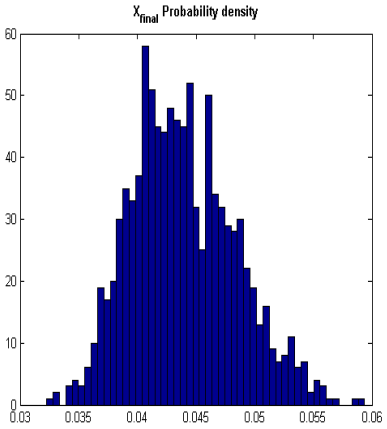

7.11.2 Cai noise

Figure 7.11: X_{final} probability density over 1000 simulations with bounded Sine Wiener noise (left figure) and bounded Cai noise (right figure),with amplitude $B = 0.4$ and correlation time $\tau = 1$, added on carrying capacity. Starting value is the microscopic equilibrium point $x = 0.045$.

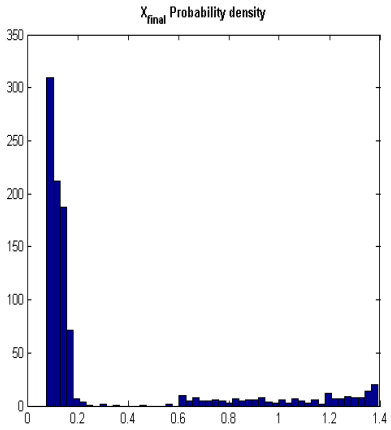

7.12.1 Sine Wiener noise

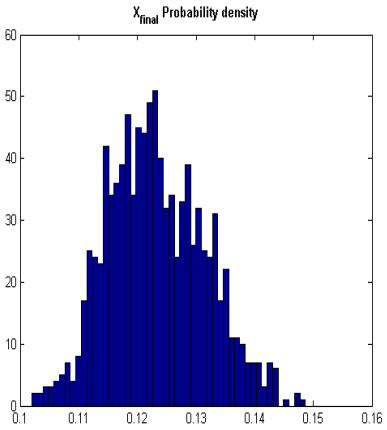

7.12.2 Cai noise

Figure 7.12: X_{final} probability density over 1000 simulations with bounded Sine Wiener noise (left figure) and bounded Cai noise (right figure),with amplitude $B = 0.4$ and correlation time $\tau = 1$, added on carrying capacity. Starting value is the microscopic equilibrium point $x = 0.123$.

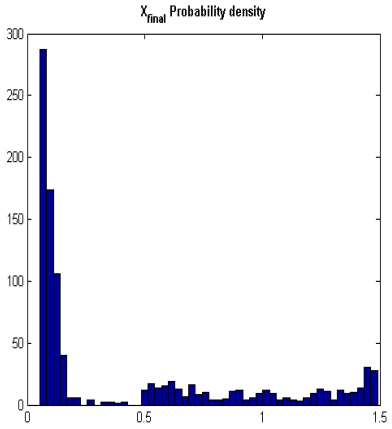

7.13.1 Sine Wiener noise

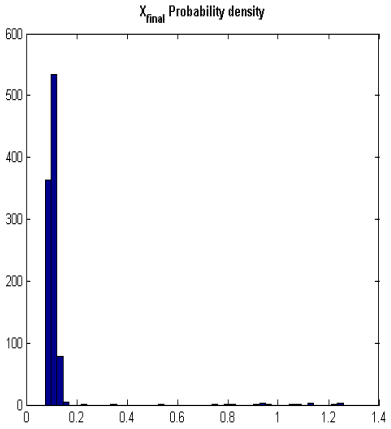

7.13.2 Cai noise

Figure 7.13: X_{final} probability density over 1000 simulations with bounded Sine Wiener noise (left figure) and bounded Cai noise (right figure),with amplitude $B = 0.5$ and correlation time $\tau = 1$, added on carrying capacity. Starting value is the microscopic equilibrium point $x = 0.105$.

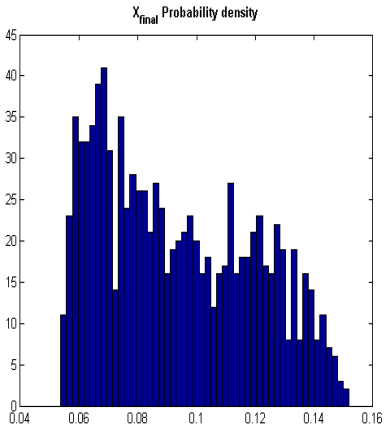

7.14.1 Sine Wiener noise

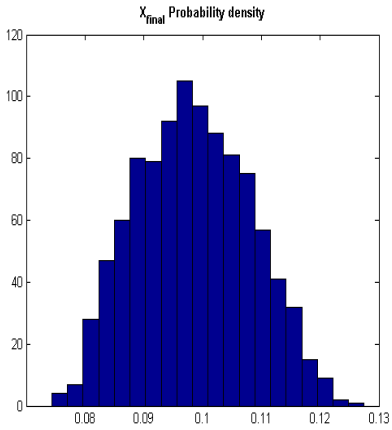

7.14.2 Cai noise

Figure 7.14: X_{final} probability density over 1000 simulations with bounded Sine Wiener noise (left figure) and bounded Cai noise (right figure),with amplitude $B = 0.5$ and correlation time $\tau = 1$, added on carrying capacity. Starting value is the microscopic equilibrium point $x = 0.1$.

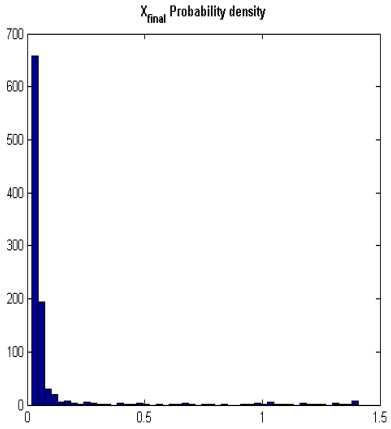

7.15.1 Sine Wiener noise

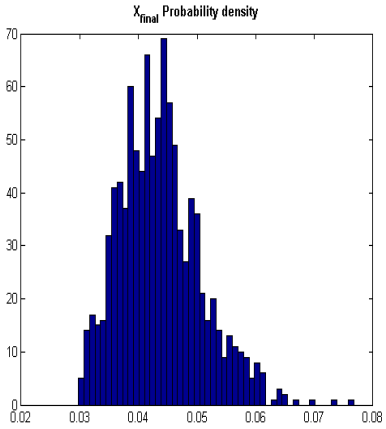

7.15.2 Cai noise

Figure 7.15: X_{final} probability density over 1000 simulations with bounded Sine Wiener noise (left figure) and bounded Cai noise (right figure),with amplitude $B = 0.5$ and correlation time $\tau = 1$, added on carrying capacity. Starting value is the microscopic equilibrium point $x = 0.045$.

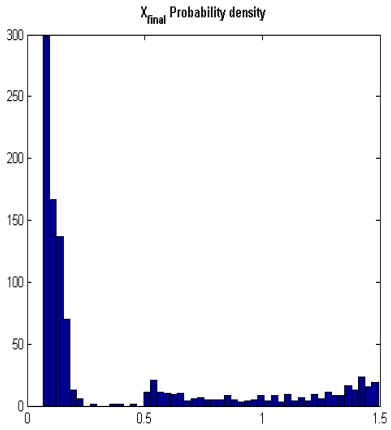

7.16.1 Sine Wiener noise

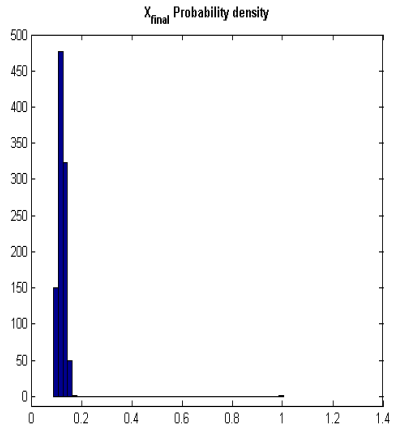

7.16.2 Cai noise

Figure 7.16: X_{final} probability density over 1000 simulations with bounded Sine Wiener noise (left figure) and bounded Cai noise (right figure),with amplitude $B = 0.5$ and correlation time $\tau = 1$, added on carrying capacity. Starting value is the microscopic equilibrium point $x = 0.123$.

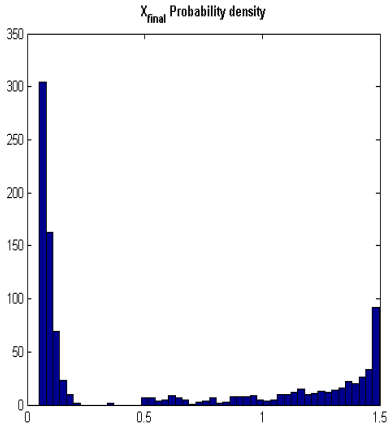

7.17.1 Sine Wiener noise

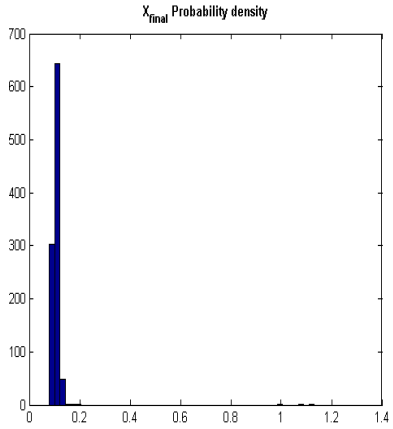

7.17.2 Cai noise

Figure 7.17: X_{final} probability density over 1000 simulations with bounded Sine Wiener noise (left figure) and bounded Cai noise (right figure),with amplitude $B = 0.5$ and correlation time $\tau = 5$, added on carrying capacity. Starting value is the microscopic equilibrium point $x = 0.105$.

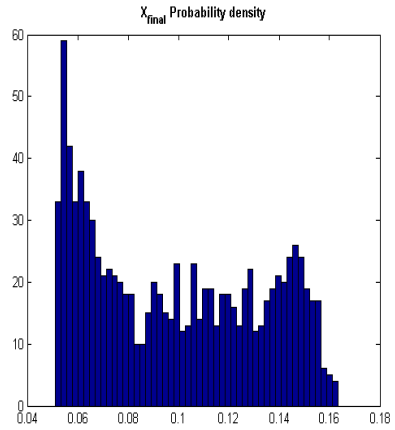

7.18.1 Sine Wiener noise

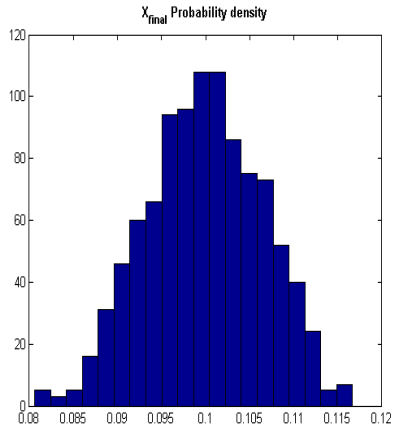

7.18.2 Cai noise

Figure 7.18: X_{final} probability density over 1000 simulations with bounded Sine Wiener noise (left figure) and bounded Cai noise (right figure),with amplitude $B = 0.5$ and correlation time $\tau = 5$, added on carrying capacity. Starting value is the microscopic equilibrium point $x = 0.1$.

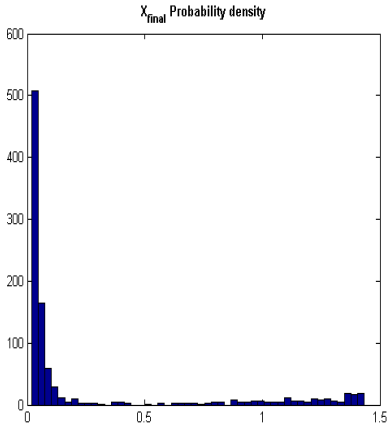

7.19.1 Sine Wiener noise

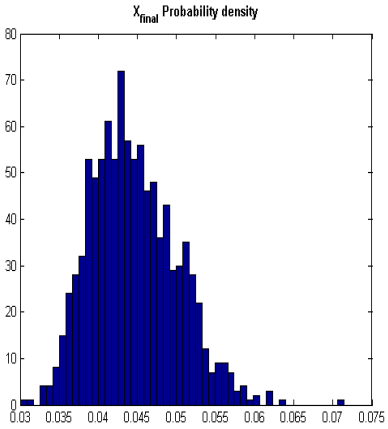

7.19.2 Cai noise

Figure 7.19: X_{final} probability density over 1000 simulations with bounded Sine Wiener noise (left figure) and bounded Cai noise (right figure),with amplitude $B = 0.5$ and correlation time $\tau = 5$, added on carrying capacity. Starting value is the microscopic equilibrium point $x = 0.045$.

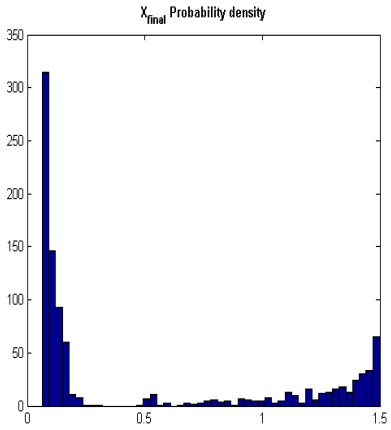

7.20.1 Sine Wiener noise

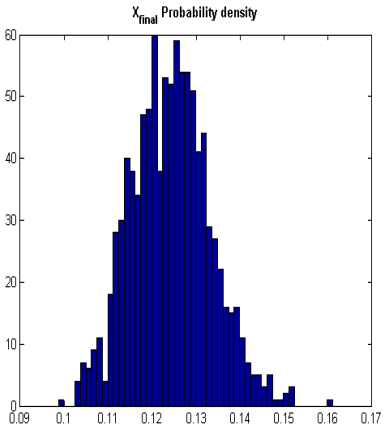

7.20.2 Cai noise

Figure 7.20: X_{final} probability density over 1000 simulations with bounded Sine Wiener noise (left figure) and bounded Cai noise (right figure),with amplitude $B = 0.5$ and correlation time $\tau = 5$, added on carrying capacity. Starting value is the microscopic equilibrium point $x = 0.123$.

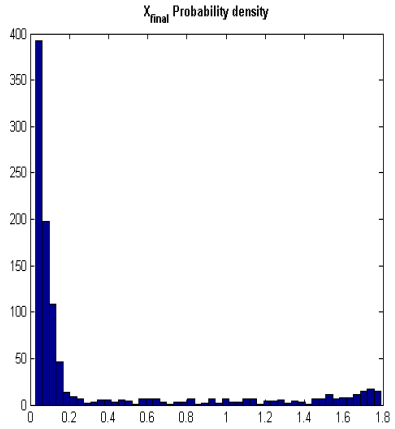

7.21.1 Sine Wiener noise

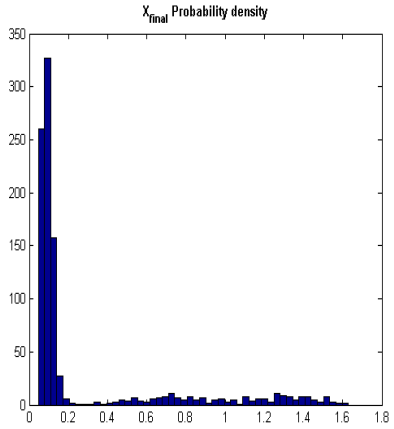

7.21.2 Cai noise

Figure 7.21: X_{final} probability density over 1000 simulations with bounded Sine Wiener noise (left figure) and bounded Cai noise (right figure),with amplitude $B = 0.8$ and correlation time $\tau = 1$, added on carrying capacity. Starting value is the microscopic equilibrium point $x = 0.105$.

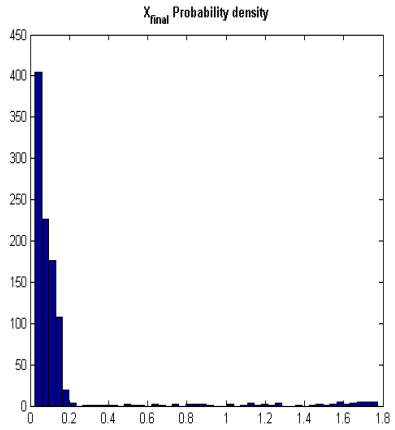

7.22.1 Sine Wiener noise

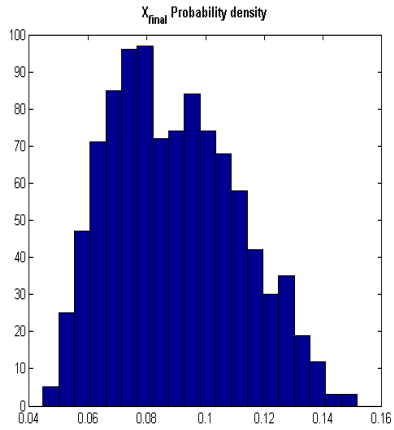

7.22.2 Cai noise

Figure 7.22: X_{final} probability density over 1000 simulations with bounded Sine Wiener noise (left figure) and bounded Cai noise (right figure),with amplitude $B = 0.8$ and correlation time $\tau = 1$, added on carrying capacity. Starting value is the microscopic equilibrium point $x = 0.1$.

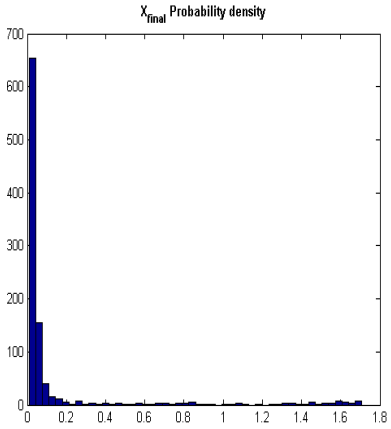

7.23.1 Sine Wiener noise

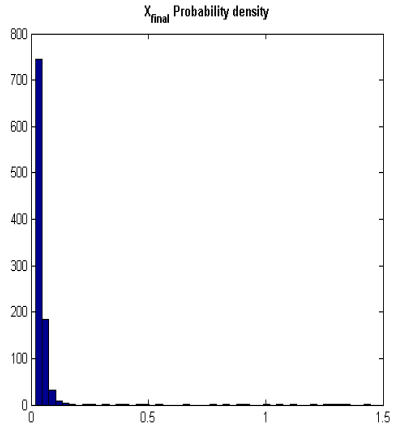

7.23.2 Cai noise

Figure 7.23: X_{final} probability density over 1000 simulations with bounded Sine Wiener noise (left figure) and bounded Cai noise (right figure),with amplitude $B = 0.8$ and correlation time $\tau = 1$, added on carrying capacity. Starting value is the microscopic equilibrium point $x = 0.045$.

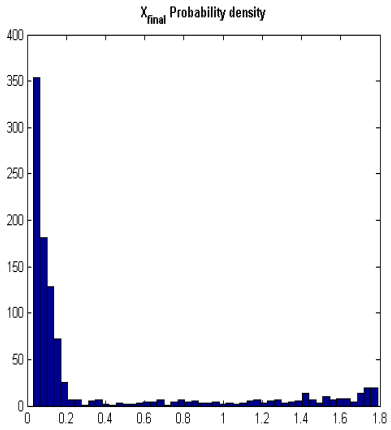

7.24.1 Sine Wiener noise

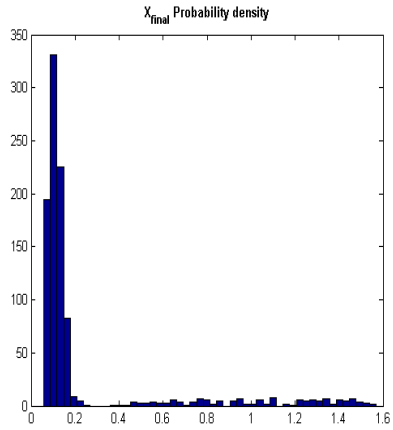

7.24.2 Cai noise

Figure 7.24: X_{final} probability density over 1000 simulations with bounded Sine Wiener noise (left figure) and bounded Cai noise (right figure),with amplitude $B = 0.8$ and correlation time $\tau = 1$, added on carrying capacity. Starting value is the microscopic equilibrium point $x = 0.123$.

Bounded SW and Cai noise on the drug concentration

The second step in my numerical simulations is given by the introduction of Sine Wiener / Cai noise on drug concentration: C(t). Hence we shall study the following stochastic equation:

$$X' = f\left(\frac{X}{K_m}\right) X - \gamma(X) C_m (1 + \nu_C(t)) X. \tag{7.7}$$

The following tables and figures show the results obtained by varying the amplitude of the noise (B) and its correlation time (τ):

SW noise:

Amplitude (B)	Correlation time (τ)	1 set	2 set	3 set	4 set
0.001	0.1	//	//	//	//
0.001	1	//	//	//	//
0.01	0.1	//	//	//	//
0.01	1	//	//	//	//
0.03	0.1	//	//	//	//
0.03	1	Evasion	//	//	//
0.04	0.1	//	//	//	//
0.04	1	Evasion	//	Evasion	Evasion
0.05	0.1	Evasion	//	//	//
0.05	1	Evasion	//	Evasion	Evasion
0.08	0.1	Evasion	//	Evasion	Evasion
0.08	1	Evasion	Evasion	Evasion	Evasion
0.1	1	Evasion	Evasion	Evasion	Evasion
0.15	1	Evasion	Evasion	Evasion	Evasion
0.2	1	Evasion	Evasion	Evasion	Evasion
0.3	1	Evasion	Evasion	Evasion	Evasion
0.5	1	Evasion	Evasion	Evasion	Evasion

Cai noise:

Amplitude (B)	Correlation time (τ)	1 set	2 set	3 set	4 set
0.001	0.1	//	//	//	//
0.001	1	//	//	//	//
0.01	0.1	//	//	//	//
0.01	1	//	//	//	//
0.03	0.1	//	//	//	//
0.03	1	//	//	//	//
0.04	0.1	//	//	//	//
0.04	1	//	//	//	//
0.05	0.1	//	//	//	//
0.05	1	//	//	//	//
0.08	0.1	//	//	//	//
0.08	1	//	//	//	//
0.1	1	//	//	//	//
0.15	1	Evasion	//	//	//
0.2	1	Evasion	//	Evasion	Evasion
0.3	1	Evasion	Evasion	Evasion	Evasion
0.5	1	Evasion	Evasion	Evasion	Evasion

Observations:

Introducing a Sine Wiener noise, for some values of amplitude and correlation time, I can notice a clear evasion from the point of microscopic equilibrium to the macroscopic one as it is evident in the following figures. Introducing a Cai noise, as well, for some values of amplitude and correlation time, evasion is clear.

Perturbation on drug concentration C

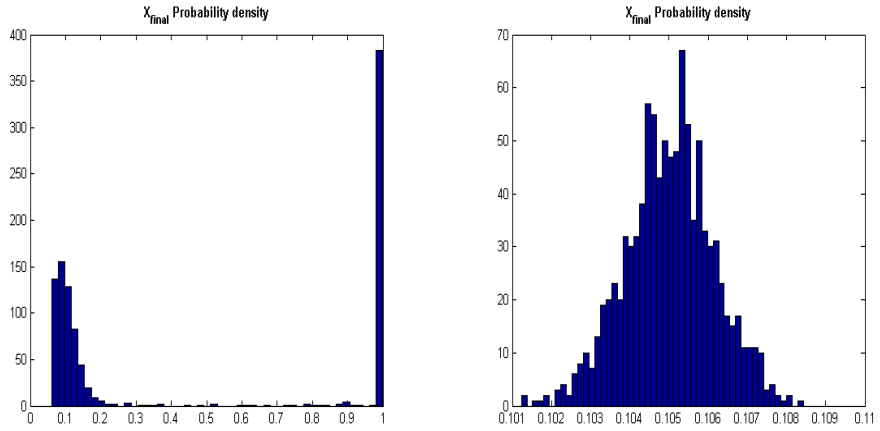

7.25.1 Sine Wiener noise

7.25.2 Cai noise

Figure 7.25: X_{final} probability density over 1000 simulations with bounded Sine Wiener noise (left figure) and bounded Cai noise (right figure),with amplitude $B = 0.05$ and correlation time $\tau = 1$, added on drug concentration. Starting value is the microscopic equilibrium point $x = 0.105$.

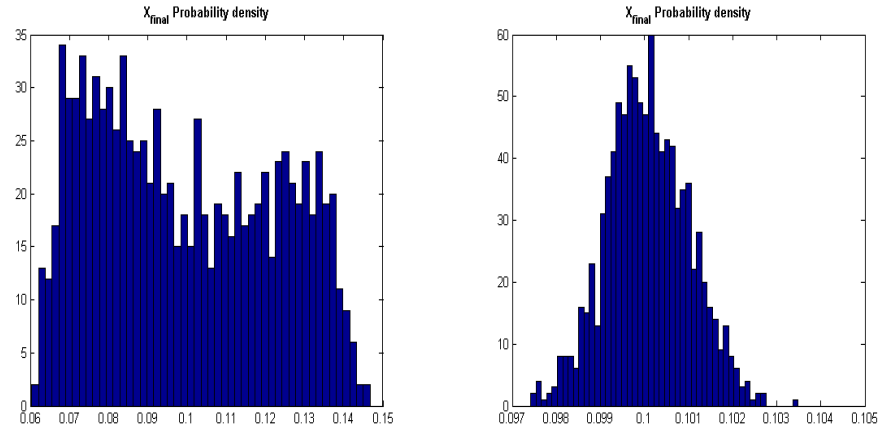

7.26.1 Sine Wiener noise

7.26.2 Cai noise

Figure 7.26: X_{final} probability density over 1000 simulations with bounded Sine Wiener noise (left figure) and bounded Cai noise (right figure),with amplitude $B = 0.05$ and correlation time $\tau = 1$, added on drug concentration. Starting value is the microscopic equilibrium point $x = 0.1$.

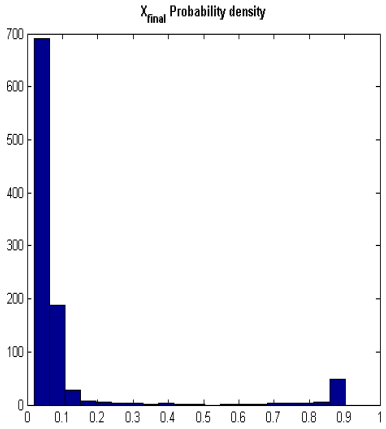

7.27.1 Sine Wiener noise

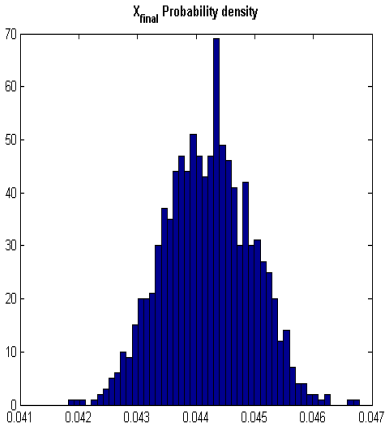

7.27.2 Cai noise

Figure 7.27: X_{final} probability density over 1000 simulations with bounded Sine Wiener noise (left figure) and bounded Cai noise (right figure),with amplitude $B = 0.05$ and correlation time $\tau = 1$, added on drug concentration. Starting value is the microscopic equilibrium point $x = 0.045$.

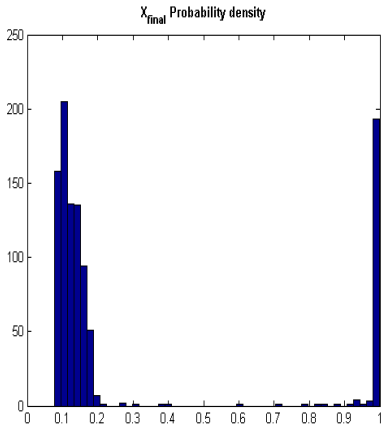

7.28.1 Sine Wiener noise

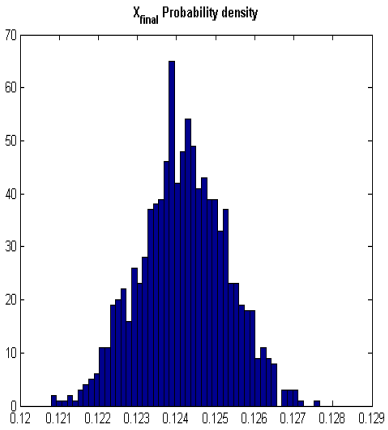

7.28.2 Cai noise

Figure 7.28: X_{final} probability density over 1000 simulations with bounded Sine Wiener noise (left figure) and bounded Cai noise (right figure),with amplitude $B = 0.05$ and correlation time $\tau = 1$, added on drug concentration. Starting value is the microscopic equilibrium point $x = 0.123$.

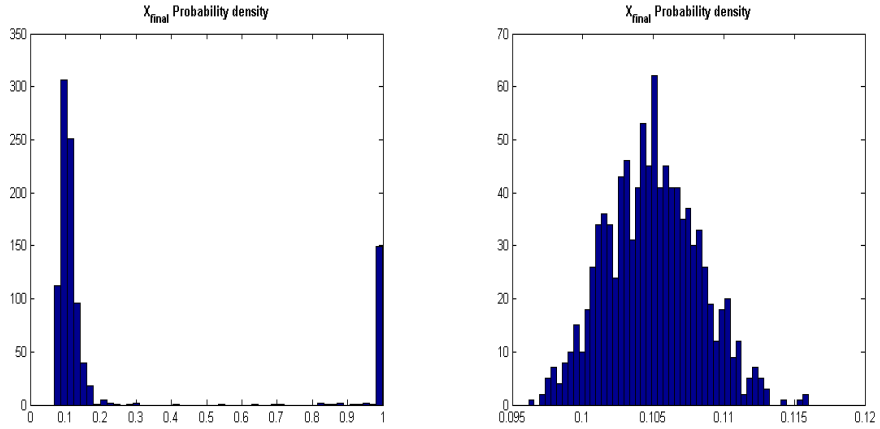

7.29.1 Sine Wiener noise

7.29.2 Cai noise

Figure 7.29: X_{final} probability density over 1000 simulations with bounded Sine Wiener noise (left figure) and bounded Cai noise (right figure),with amplitude $B = 0.08$ and correlation time $\tau = 0, 1$, added on drug concentration. Starting value is the microscopic equilibrium point $x = 0.105$.

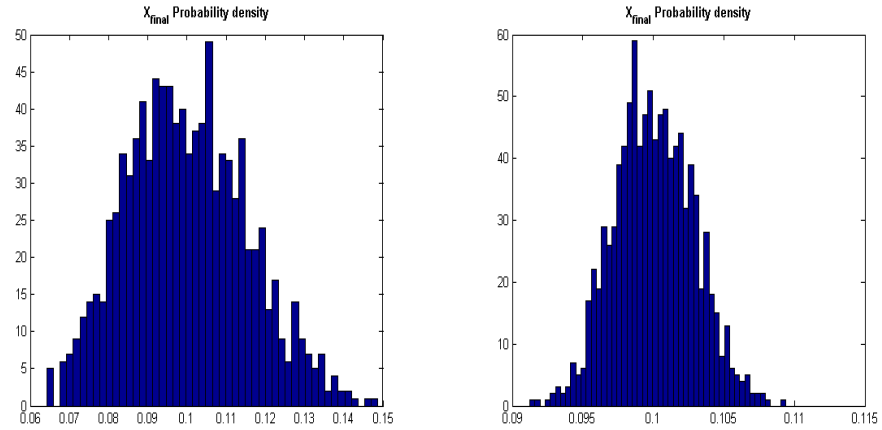

7.30.1 Sine Wiener noise

7.30.2 Cai noise

Figure 7.30: X_{final} probability density over 1000 simulations with bounded Sine Wiener noise (left figure) and bounded Cai noise (right figure),with amplitude $B = 0.08$ and correlation time $\tau = 0, 1$, added on drug concentration. Starting value is the microscopic equilibrium point $x = 0.1$.

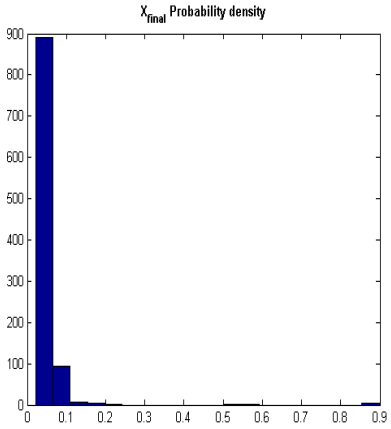

7.31.1 Sine Wiener noise

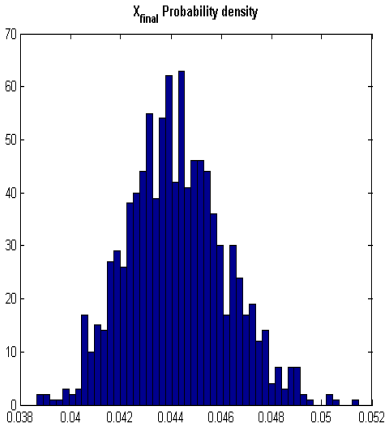

7.31.2 Cai noise

Figure 7.31: X_{final} probability density over 1000 simulations with bounded Sine Wiener noise (left figure) and bounded Cai noise (right figure),with amplitude $B = 0.08$ and correlation time $\tau = 0, 1$, added on drug concentration. Starting value is the microscopic equilibrium point $x = 0.045$.

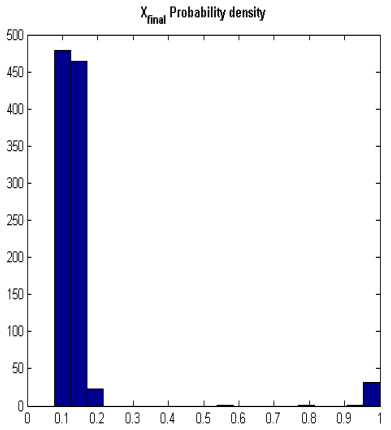

7.32.1 Sine Wiener noise

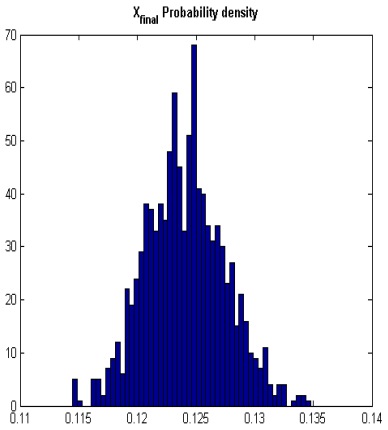

7.32.2 Cai noise

Figure 7.32: X_{final} probability density over 1000 simulations with bounded Sine Wiener noise (left figure) and bounded Cai noise (right figure),with amplitude $B = 0.08$ and correlation time $\tau = 0, 1$, added on drug concentration. Starting value is the microscopic equilibrium point $x = 0.123$.

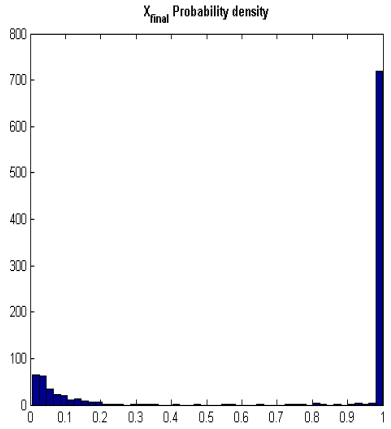

7.33.1 Sine Wiener noise

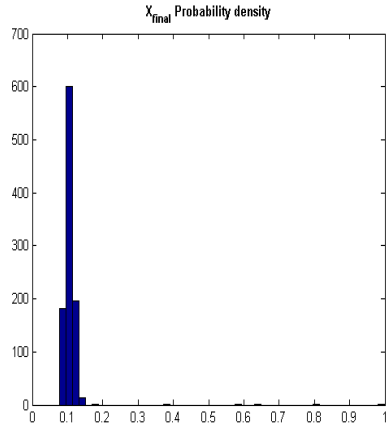

7.33.2 Cai noise

Figure 7.33: X_{final} probability density over 1000 simulations with bounded Sine Wiener noise (left figure) and bounded Cai noise (right figure),with amplitude $B = 0.15$ and correlation time $\tau = 1$, added on drug concentration. Starting value is the microscopic equilibrium point $x = 0.105$.

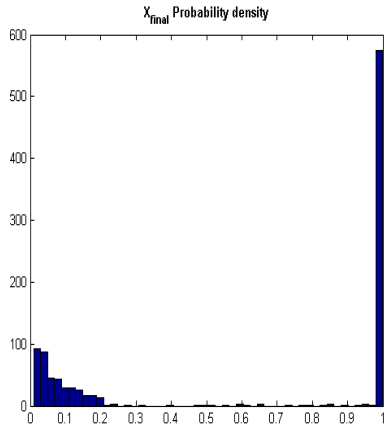

7.34.1 Sine Wiener noise

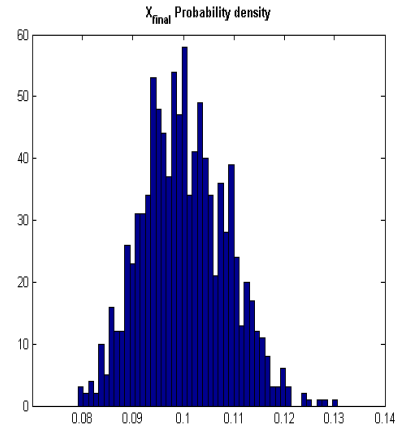

7.34.2 Cai noise

Figure 7.34: X_{final} probability density over 1000 simulations with bounded Sine Wiener noise (left figure) and bounded Cai noise (right figure),with amplitude $B = 0.15$ and correlation time $\tau = 1$, added on drug concentration. Starting value is the microscopic equilibrium point $x = 0.1$.

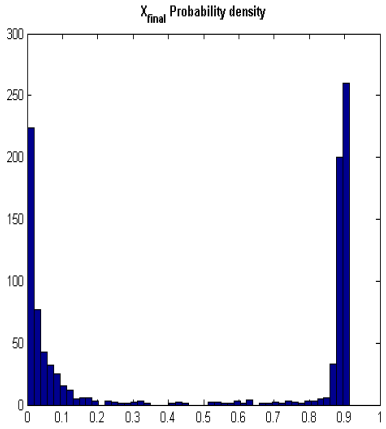

7.35.1 Sine Wiener noise

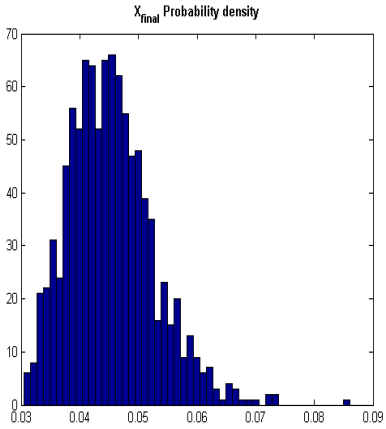

7.35.2 Cai noise

Figure 7.35: X_{final} probability density over 1000 simulations with bounded Sine Wiener noise (left figure) and bounded Cai noise (right figure),with amplitude $B = 0.15$ and correlation time $\tau = 1$, added on drug concentration. Starting value is the microscopic equilibrium point $x = 0.045$.

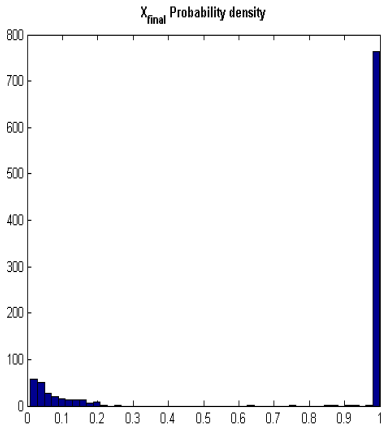

7.36.1 Sine Wiener noise

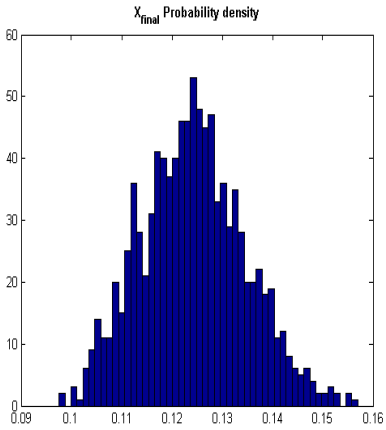

7.36.2 Cai noise

Figure 7.36: X_{final} probability density over 1000 simulations with bounded Sine Wiener noise (left figure) and bounded Cai noise (right figure),with amplitude $B = 0.15$ and correlation time $\tau = 1$, added on drug concentration. Starting value is the microscopic equilibrium point $x = 0.123$.

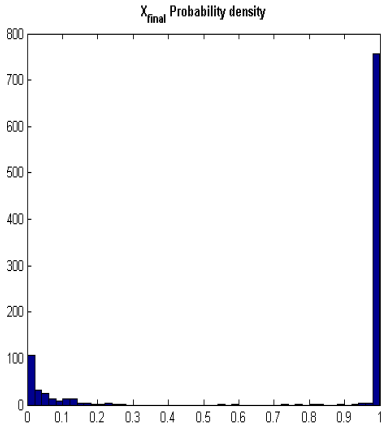

7.37.1 Sine Wiener noise

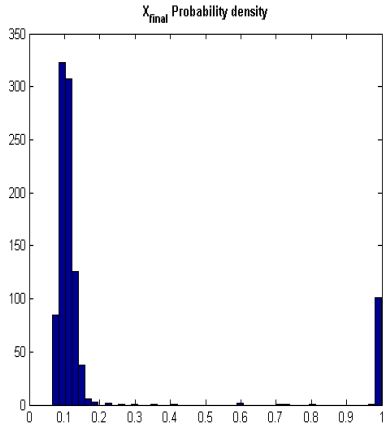

7.37.2 Cai noise

Figure 7.37: X_{final} probability density over 1000 simulations with bounded Sine Wiener noise (left figure) and bounded Cai noise (right figure),with amplitude $B = 0.2$ and correlation time $\tau = 1$, added on drug concentration. Starting value is the microscopic equilibrium point $x = 0.105$.

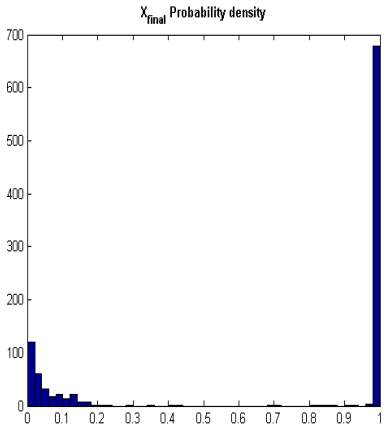

7.38.1 Sine Wiener noise

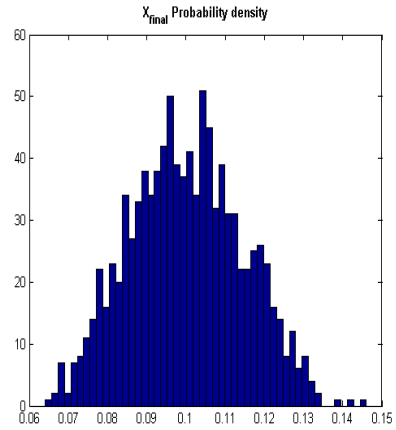

7.38.2 Cai noise

Figure 7.38: X_{final} probability density over 1000 simulations with bounded Sine Wiener noise (left figure) and bounded Cai noise (right figure),with amplitude $B = 0.2$ and correlation time $\tau = 1$, added on drug concentration. Starting value is the microscopic equilibrium point $x = 0.1$.

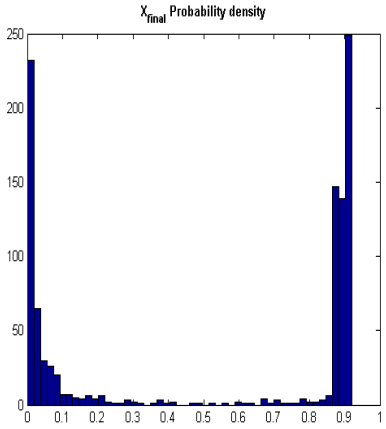

7.39.1 Sine Wiener noise

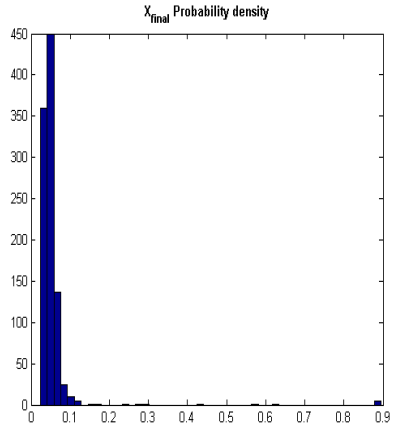

7.39.2 Cai noise

Figure 7.39: X_{final} probability density over 1000 simulations with bounded Sine Wiener noise (left figure) and bounded Cai noise (right figure),with amplitude $B = 0.2$ and correlation time $\tau = 1$, added on drug concentration. Starting value is the microscopic equilibrium point $x = 0.045$.

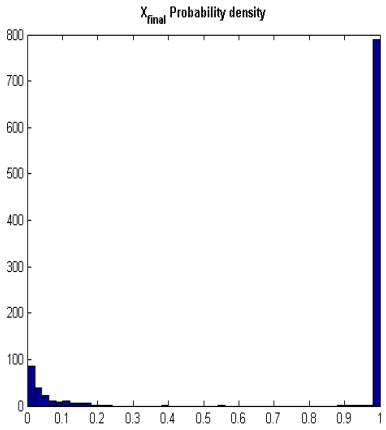

7.40.1 Sine Wiener noise

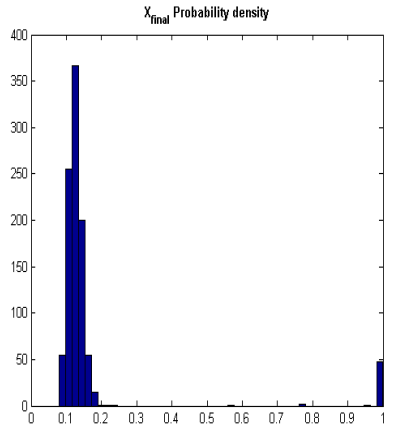

7.40.2 Cai noise

Figure 7.40: X_{final} probability density over 1000 simulations with bounded Sine Wiener noise (left figure) and bounded Cai noise (right figure),with amplitude $B = 0.2$ and correlation time $\tau = 1$, added on drug concentration. Starting value is the microscopic equilibrium point $x = 0.123$.

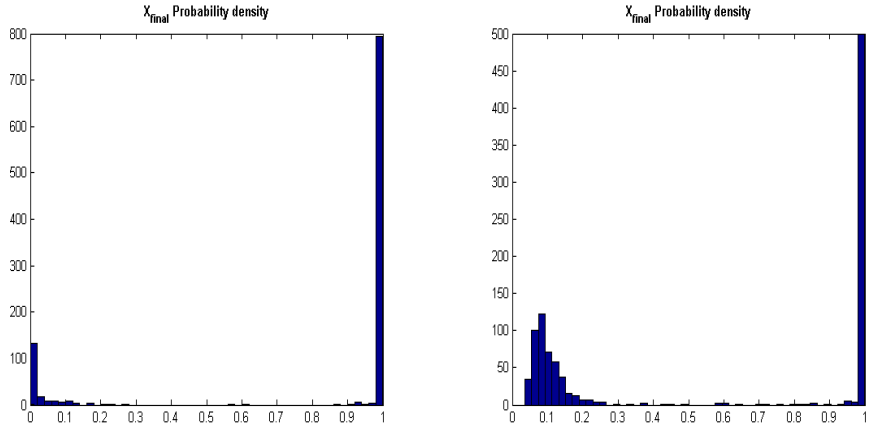

7.41.1 Sine Wiener noise

7.41.2 Cai noise

Figure 7.41: X_{final} probability density over 1000 simulations with bounded Sine Wiener noise (left figure) and bounded Cai noise (right figure),with amplitude $B = 0.3$ and correlation time $\tau = 1$, added on drug concentration. Starting value is the microscopic equilibrium point $x = 0.105$.

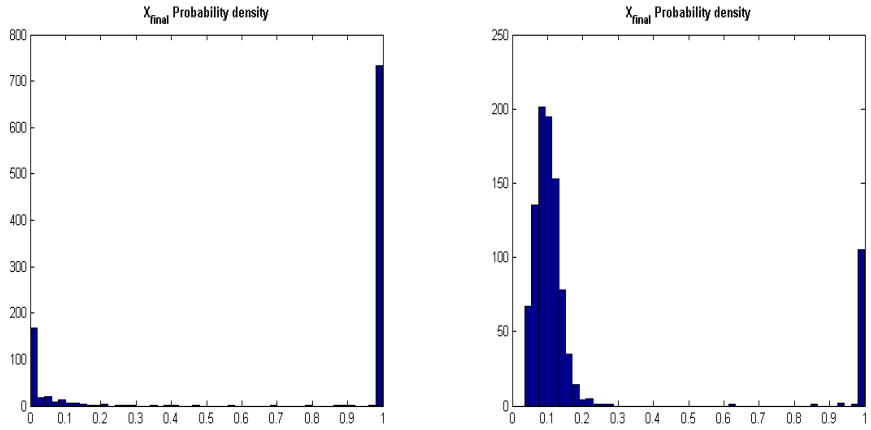

7.42.1 Sine Wiener noise

7.42.2 Cai noise

Figure 7.42: X_{final} probability density over 1000 simulations with bounded Sine Wiener noise (left figure) and bounded Cai noise (right figure),with amplitude $B = 0.3$ and correlation time $\tau = 1$, added on drug concentration. Starting value is the microscopic equilibrium point $x = 0.1$.

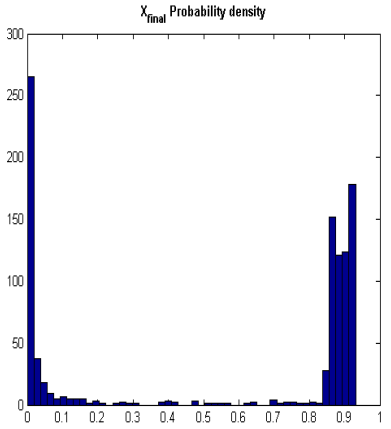

7.43.1 Sine Wiener noise

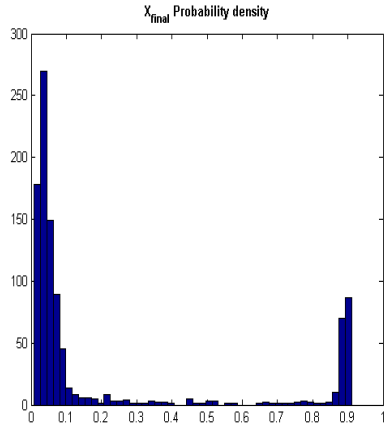

7.43.2 Cai noise

Figure 7.43: X_{final} probability density over 1000 simulations with bounded Sine Wiener noise (left figure) and bounded Cai noise (right figure),with amplitude $B = 0.3$ and correlation time $\tau = 1$, added on drug concentration. Starting value is the microscopic equilibrium point $x = 0.045$.

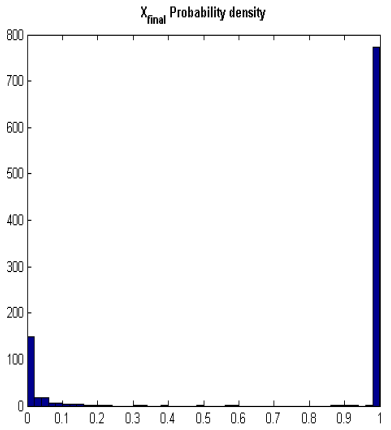

7.44.1 Sine Wiener noise

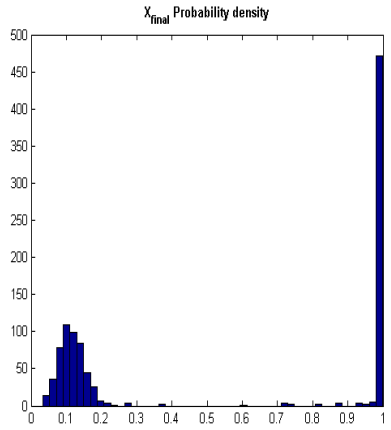

7.44.2 Cai noise

Figure 7.44: X_{final} probability density over 1000 simulations with bounded Sine Wiener noise (left figure) and bounded Cai noise (right figure),with amplitude $B = 0.3$ and correlation time $\tau = 1$, added on drug concentration. Starting value is the microscopic equilibrium point $x = 0.123$.

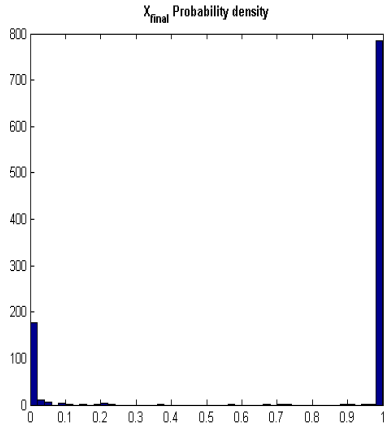

7.45.1 Sine Wiener noise

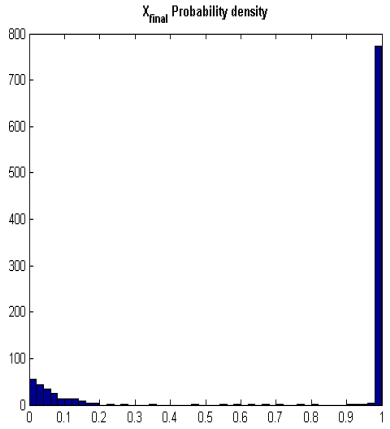

7.45.2 Cai noise

Figure 7.45: X_{final} probability density over 1000 simulations with bounded Sine Wiener noise (left figure) and bounded Cai noise (right figure),with amplitude $B = 0.5$ and correlation time $\tau = 1$, added on drug concentration. Starting value is the microscopic equilibrium point $x = 0.105$.

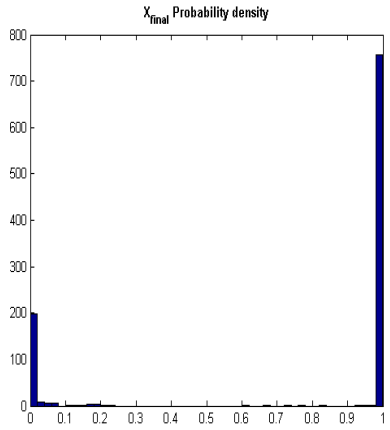

7.46.1 Sine Wiener noise

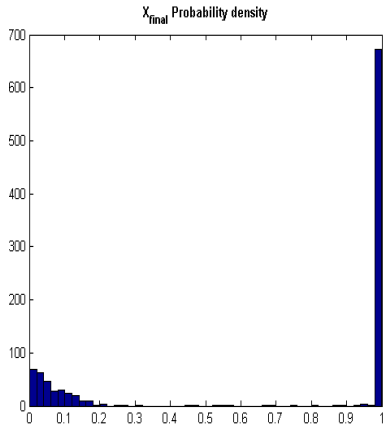

7.46.2 Cai noise

Figure 7.46: X_{final} probability density over 1000 simulations with bounded Sine Wiener noise (left figure) and bounded Cai noise (right figure),with amplitude $B = 0.5$ and correlation time $\tau = 1$, added on drug concentration. Starting value is the microscopic equilibrium point $x = 0.1$.

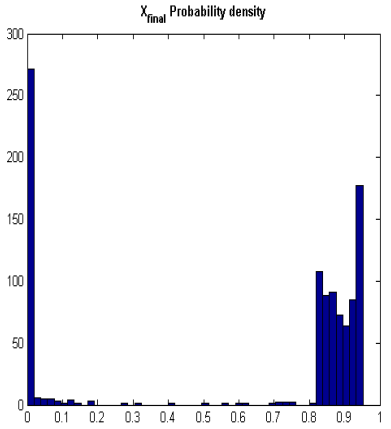

7.47.1 Sine Wiener noise

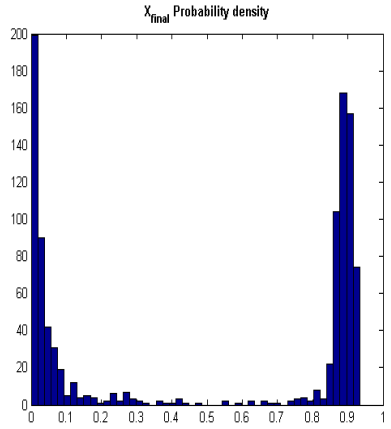

7.47.2 Cai noise

Figure 7.47: X_{final} probability density over 1000 simulations with bounded Sine Wiener noise (left figure) and bounded Cai noise (right figure),with amplitude $B = 0.5$ and correlation time $\tau = 1$, added on drug concentration. Starting value is the microscopic equilibrium point $x = 0.045$.

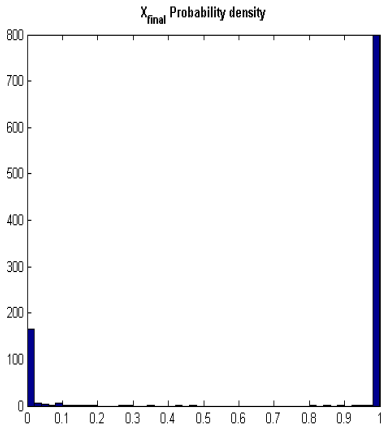

7.48.1 Sine Wiener noise

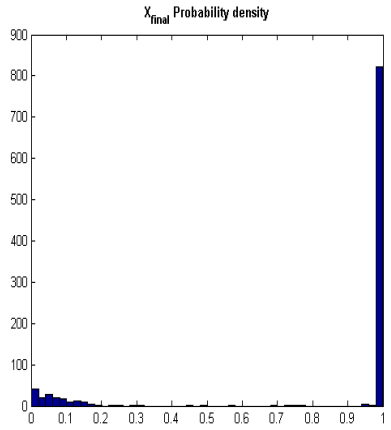

7.48.2 Cai noise

Figure 7.48: X_{final} probability density over 1000 simulations with bounded Sine Wiener noise (left figure) and bounded Cai noise (right figure),with amplitude $B = 0.5$ and correlation time $\tau = 1$, added on drug concentration. Starting value is the microscopic equilibrium point $x = 0.123$.

Bounded SW and Cai noise in both carrying capacity and drug density

The last step in my numerical simulations is given by the introduction of Sine Wiener / Cai noise on both carrying capacity K(t) and drug concentration C(t). Hence we shall study the following stochastic equation:

$$X' = f\left(\frac{X}{K_m(1+\nu_K(t))}\right)X - \gamma(X)C_m(1+\nu_C(t))X. \tag{7.8}$$

The following tables and figures show the results obtained by varying the amplitude of the noise (B) and its correlation time (τ):

SW noise:

B_c	B_k	τ_c	τ_k	1 set	2 set	3 set	4 set
0.01	0.01	0.1	0.1	//	//	//	//
0.01	0.01	1	1	//	//	//	//
0.01	0.01	1	5	//	//	//	//
0.02	0.02	1	1	//	//	//	//
0.02	0.02	1	1	//	//	//	//
0.02	0.02	1	5	//	//	//	//
0.03	0.03	0.1	0.1	//	//	//	//
0.03	0.03	1	1	Evasion	//	Evasion	//
0.05	0.05	0.1	0.1	Evasion	//	//	//
0.05	0.05	1	1	Evasion	//	Evasion	Evasion
0.05	0.05	1	5	Evasion	//	Evasion	Evasion
0.1	0.04	1	0.1	Evasion	Evasion	Evasion	Evasion
0.2	0.04	1	0.1	Evasion	Evasion	Evasion	Evasion

Cai noise:

B_c	B_k	τ_c	τ_k	1 set	2 set	3 set	4 set
0.01	0.01	0.1	0.1	//	//	//	//
0.01	0.01	1	1	//	//	//	//
0.01	0.01	1	5	//	//	//	//
0.02	0.02	1	1	//	//	//	//
0.02	0.02	1	1	//	//	//	//
0.02	0.02	1	5	//	//	//	//
0.03	0.03	0.1	0.1	//	//	//	//
0.03	0.03	1	1	//	//	//	//
0.05	0.05	0.1	0.1	//	//	//	//
0.05	0.05	1	1	//	//	//	//
0.05	0.05	1	5	//	//	//	//
0.1	0.04	1	0.1	//	//	//	//
0.2	0.04	1	0.1	Evasion	//	Evasion	Evasion

Perturbation on carrying capacity K and drug concentration C

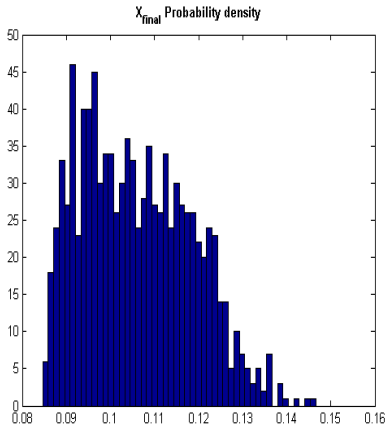

7.49.1 Sine Wiener noise

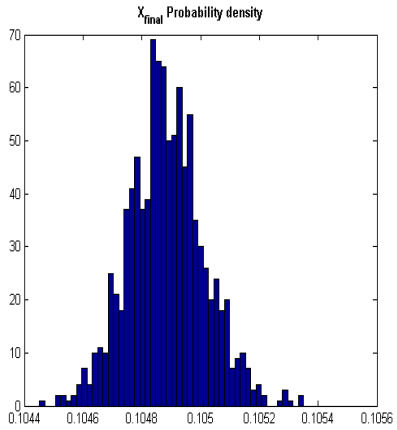

7.49.2 Cai noise

Figure 7.49: X_{final} probability density over 1000 simulations with bounded Sine Wiener noise (left figure) and bounded Cai noise (right figure)added on carrying capacity, with amplitude $B_k = 0.02$ and correlation time $\tau_k = 5$, and drug concentration, with amplitude $B_c = 0.02$ and correlation time $\tau_c = 1$,. Starting value is the microscopic equilibrium point $x = 0.105$.

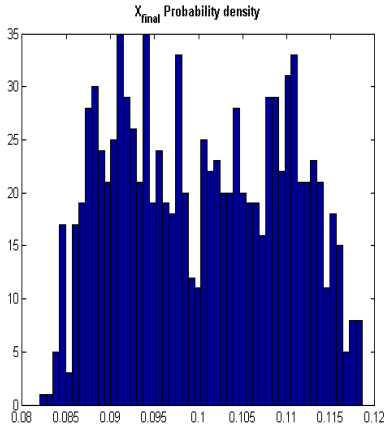

7.50.1 Sine Wiener noise

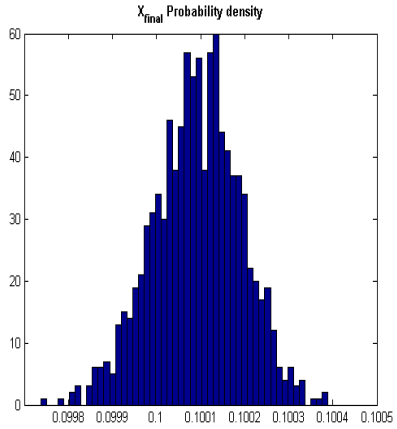

7.50.2 Cai noise

Figure 7.50: X_{final} probability density over 1000 simulations with bounded Sine Wiener noise (left figure) and bounded Cai noise (right figure)added on carrying capacity, with amplitude $B_k = 0.02$ and correlation time $\tau_k = 5$, and drug concentration, with amplitude $B_c = 0.02$ and correlation time $\tau_c = 1$. Starting value is the microscopic equilibrium point $x = 0.1$.

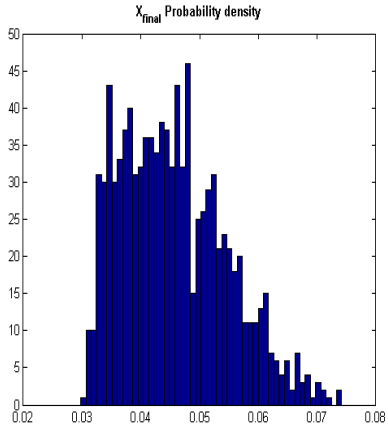

7.51.1 Sine Wiener noise

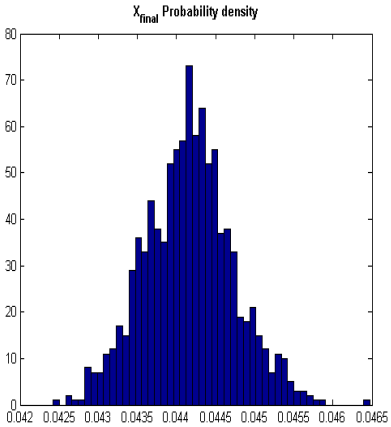

7.51.2 Cai noise

Figure 7.51: X_{final} probability density over 1000 simulations with bounded Sine Wiener noise (left figure) and bounded Cai noise (right figure)added on carrying capacity, with amplitude $B_k = 0.02$ and correlation time $\tau_k = 5$, and drug concentration, with amplitude $B_c = 0.02$ and correlation time $\tau_c = 1$. Starting value is the microscopic equilibrium point $x = 0.045$.

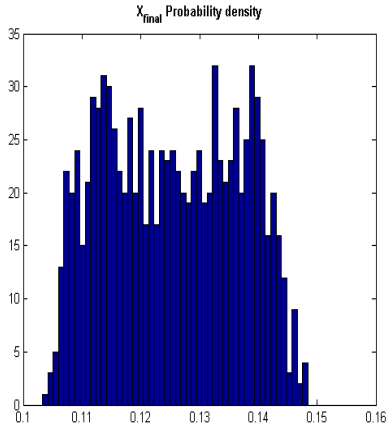

7.52.1 Sine Wiener noise

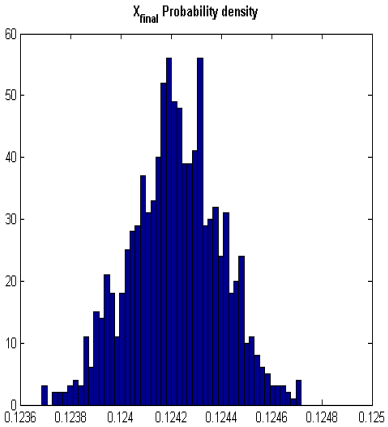

7.52.2 Cai noise

Figure 7.52: X_{final} probability density over 1000 simulations with bounded Sine Wiener noise (left figure) and bounded Cai noise (right figure)added on carrying capacity, with amplitude $B_k = 0.02$ and correlation time $\tau_k = 5$, and drug concentration, with amplitude $B_c = 0.02$ and correlation time $\tau_c = 1$. Starting value is the microscopic equilibrium point $x = 0.123$.

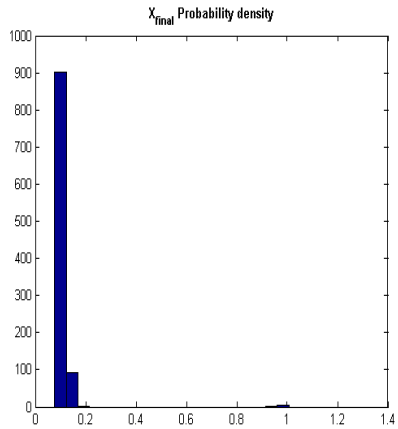

7.53.1 Sine Wiener noise

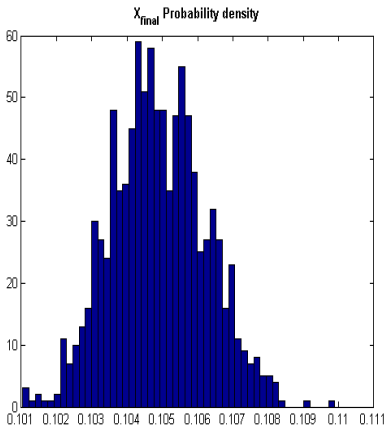

7.53.2 Cai noise

Figure 7.53: X_{final} probability density over 1000 simulations with bounded Sine Wiener noise (left figure) and bounded Cai noise (right figure)added on carrying capacity, with amplitude $B_k = 0.05$ and correlation time $\tau_k = 0.1$, and drug concentration, with amplitude $B_c = 0.05$ and correlation time $\tau_c = 0.1$,. Starting value is the microscopic equilibrium point $x = 0.105$.

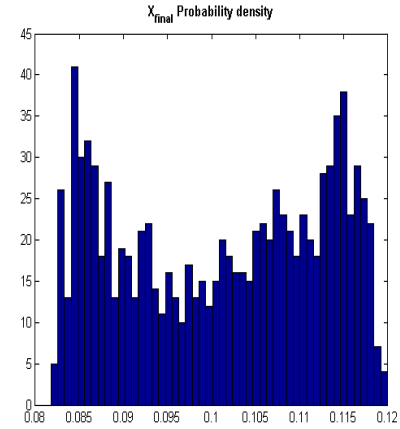

7.54.1 Sine Wiener noise

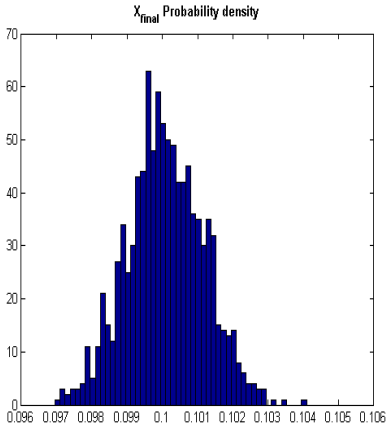

7.54.2 Cai noise

Figure 7.54: X_{final} probability density over 1000 simulations with bounded Sine Wiener noise (left figure) and bounded Cai noise (right figure)added on carrying capacity, with amplitude $B_k = 0.05$ and correlation time $\tau_k = 0.1$, and drug concentration, with amplitude $B_c = 0.05$ and correlation time $\tau_c = 0, 1$. Starting value is the microscopic equilibrium point $x = 0.1$.

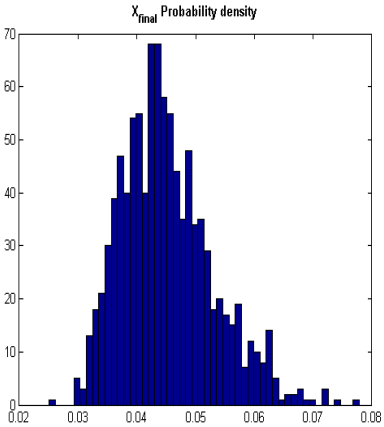

7.55.1 Sine Wiener noise

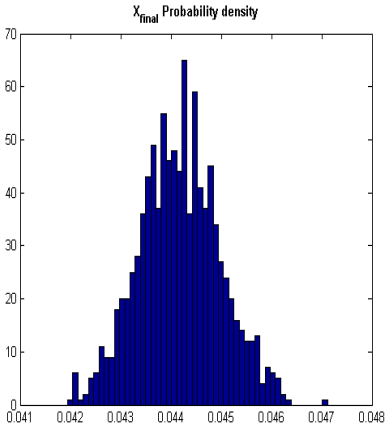

7.55.2 Cai noise

Figure 7.55: X_{final} probability density over 1000 simulations with bounded Sine Wiener noise (left figure) and bounded Cai noise (right figure)added on carrying capacity, with amplitude $B_k = 0.05$ and correlation time $\tau_k = 0.1$, and drug concentration, with amplitude $B_c = 0.05$ and correlation time $\tau_c = 0.1$. Starting value is the microscopic equilibrium point $x = 0.045$.

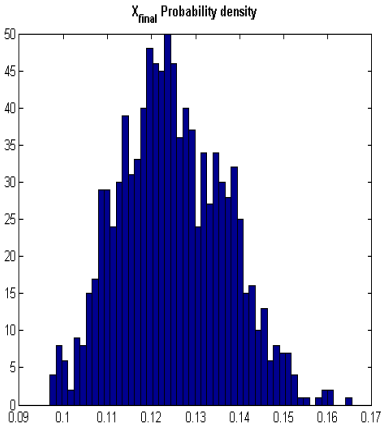

7.56.1 Sine Wiener noise

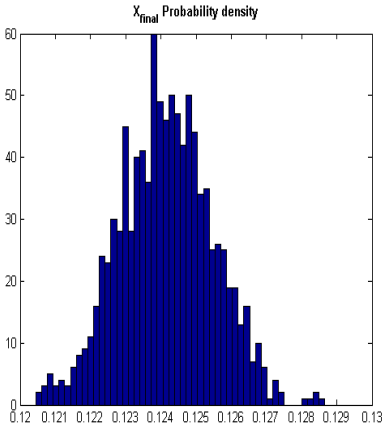

7.56.2 Cai noise

Figure 7.56: X_{final} probability density over 1000 simulations with bounded Sine Wiener noise (left figure) and bounded Cai noise (right figure)added on carrying capacity, with amplitude $B_k = 0.05$ and correlation time $\tau_k = 0.1$, and drug concentration, with amplitude $B_c = 0.05$ and correlation time $\tau_c = 0.1$. Starting value is the microscopic equilibrium point $x = 0.123$.

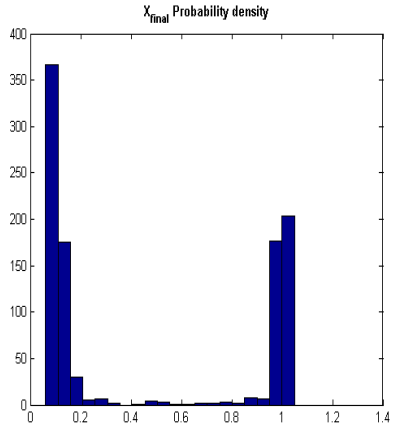

7.57.1 Sine Wiener noise

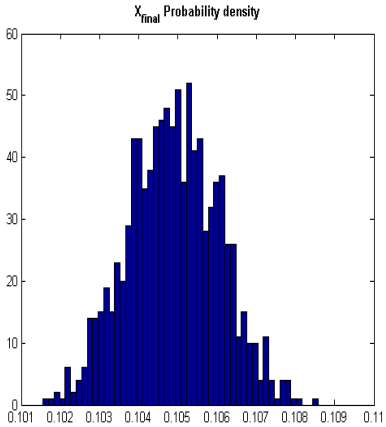

7.57.2 Cai noise

Figure 7.57: X_{final} probability density over 1000 simulations with bounded Sine Wiener noise (left figure) and bounded Cai noise (right figure)added on carrying capacity, with amplitude $B_k = 0.05$ and correlation time $\tau_k = 1$, and drug concentration, with amplitude $B_c = 0.05$ and correlation time $\tau_c = 1$,. Starting value is the microscopic equilibrium point $x = 0.105$.

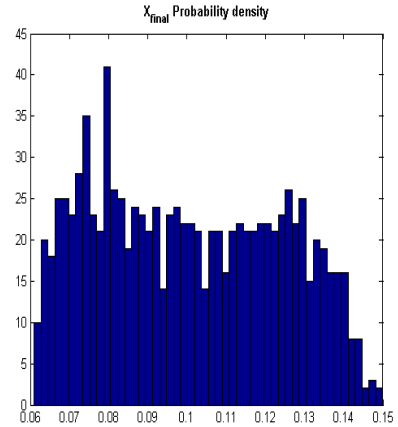

7.58.1 Sine Wiener noise

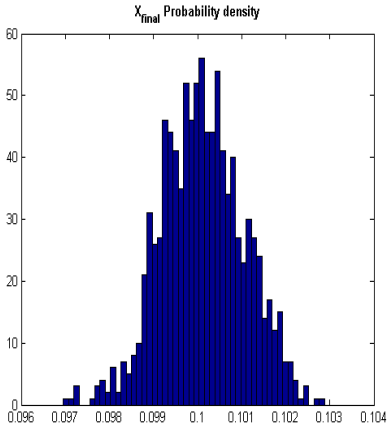

7.58.2 Cai noise

Figure 7.58: X_{final} probability density over 1000 simulations with bounded Sine Wiener noise (left figure) and bounded Cai noise (right figure)added on carrying capacity, with amplitude $B_k = 0.05$ and correlation time $\tau_k = 1$, and drug concentration, with amplitude $B_c = 0.05$ and correlation time $\tau_c = 1$. Starting value is the microscopic equilibrium point $x = 0.1$.

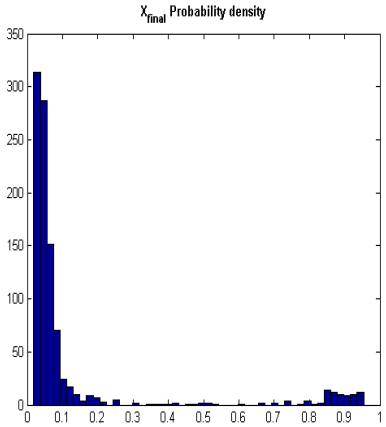

7.59.1 Sine Wiener noise

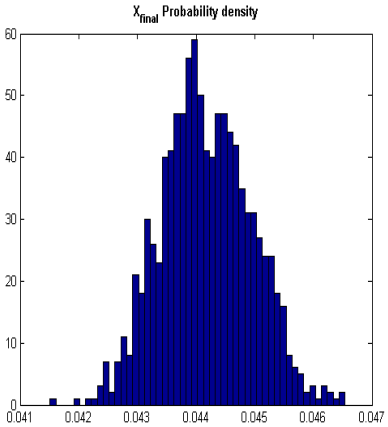

7.59.2 Cai noise

Figure 7.59: X_{final} probability density over 1000 simulations with bounded Sine Wiener noise (left figure) and bounded Cai noise (right figure)added on carrying capacity, with amplitude $B_k = 0.05$ and correlation time $\tau_k = 1$, and drug concentration, with amplitude $B_c = 0.05$ and correlation time $\tau_c = 1$. Starting value is the microscopic equilibrium point $x = 0.045$.

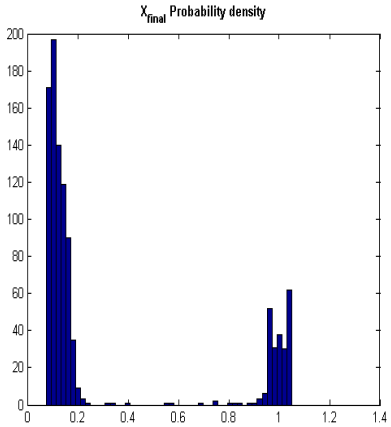

7.60.1 Sine Wiener noise

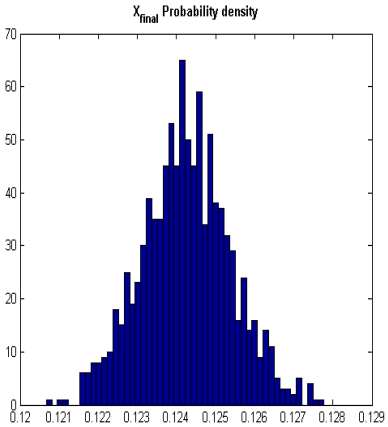

7.60.2 Cai noise

Figure 7.60: X_{final} probability density over 1000 simulations with bounded Sine Wiener noise (left figure) and bounded Cai noise (right figure)added on carrying capacity, with amplitude $B_k = 0.05$ and correlation time $\tau_k = 1$, and drug concentration, with amplitude $B_c = 0.05$ and correlation time $\tau_c = 1$. Starting value is the microscopic equilibrium point $x = 0.123$.

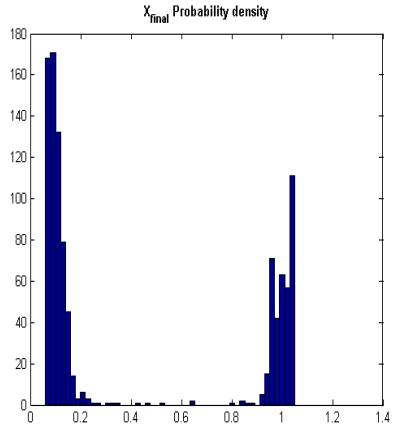

7.61.1 Sine Wiener noise

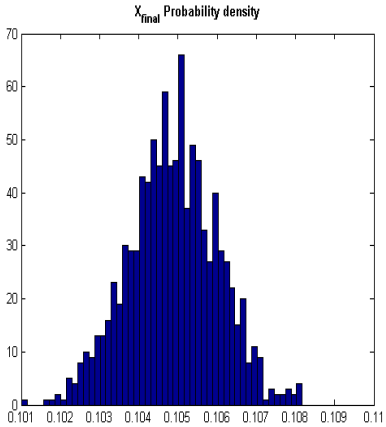

7.61.2 Cai noise

Figure 7.61: X_{final} probability density over 1000 simulations with bounded Sine Wiener noise (left figure) and bounded Cai noise (right figure)added on carrying capacity, with amplitude $B_k = 0.05$ and correlation time $\tau_k = 5$, and drug concentration, with amplitude $B_c = 0.05$ and correlation time $\tau_c = 1$,. Starting value is the microscopic equilibrium point $x = 0.105$.

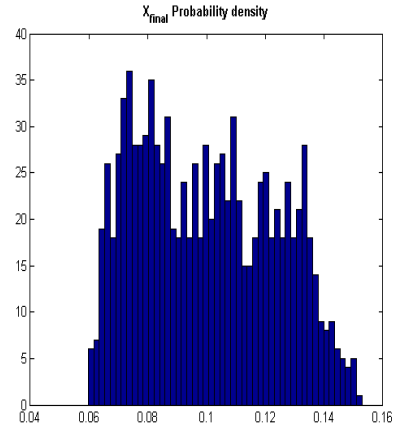

7.62.1 Sine Wiener noise

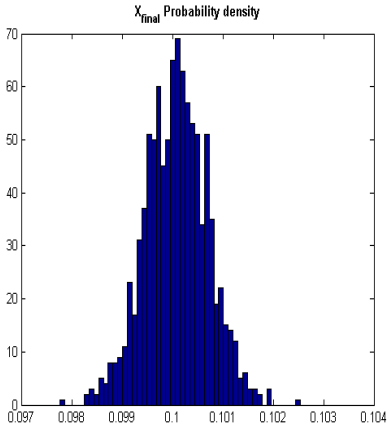

7.62.2 Cai noise

Figure 7.62: X_{final} probability density over 1000 simulations with bounded Sine Wiener noise (left figure) and bounded Cai noise (right figure)added on carrying capacity, with amplitude $B_k = 0.05$ and correlation time $\tau_k = 5$, and drug concentration, with amplitude $B_c = 0.05$ and correlation time $\tau_c = 1$. Starting value is the microscopic equilibrium point $x = 0.1$.

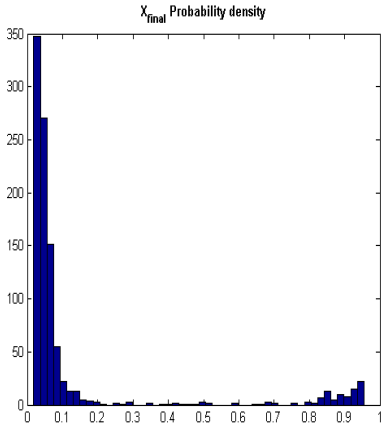

7.63.1 Sine Wiener noise

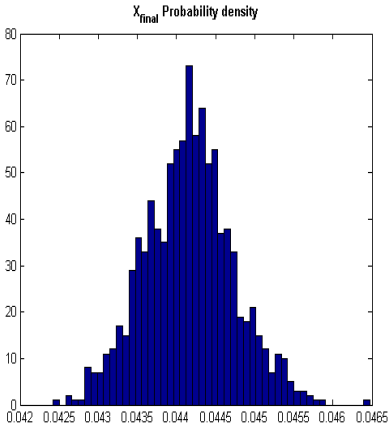

7.63.2 Cai noise

Figure 7.63: X_{final} probability density over 1000 simulations with bounded Sine Wiener noise (left figure) and bounded Cai noise (right figure)added on carrying capacity, with amplitude $B_k = 0.05$ and correlation time $\tau_k = 5$, and drug concentration, with amplitude $B_c = 0.05$ and correlation time $\tau_c = 1$. Starting value is the microscopic equilibrium point $x = 0.045$.

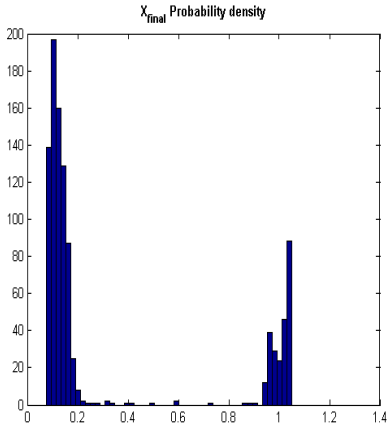

7.64.1 Sine Wiener noise

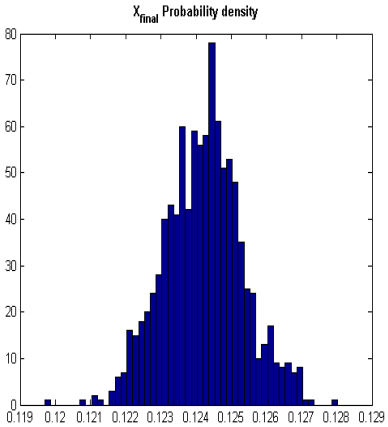

7.64.2 Cai noise

Figure 7.64: X_{final} probability density over 1000 simulations with bounded Sine Wiener noise (left figure) and bounded Cai noise (right figure)added on carrying capacity, with amplitude $B_k = 0.05$ and correlation time $\tau_k = 5$, and drug concentration, with amplitude $B_c = 0.05$ and correlation time $\tau_c = 1$. Starting value is the microscopic equilibrium point $x = 0.123$.

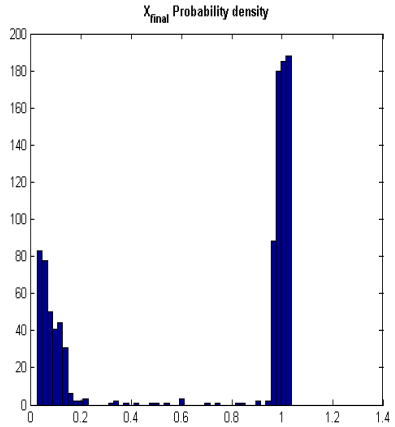

7.65.1 Sine Wiener noise

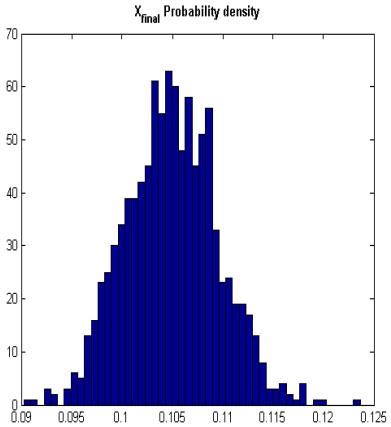

7.65.2 Cai noise

Figure 7.65: X_{final} probability density over 1000 simulations with bounded Sine Wiener noise (left figure) and bounded Cai noise (right figure)added on carrying capacity, with amplitude $B_k = 0.04$ and correlation time $\tau_k = 0.1$, and drug concentration, with amplitude $B_c = 0.1$ and correlation time $\tau_c = 1$,. Starting value is the microscopic equilibrium point $x = 0.105$.

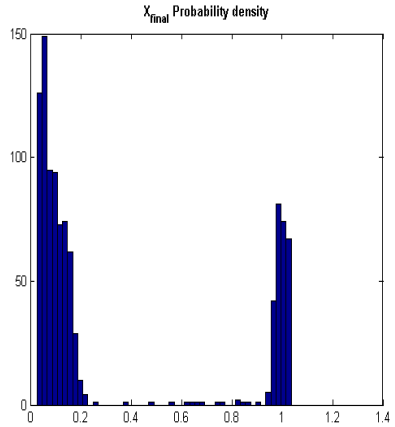

7.66.1 Sine Wiener noise

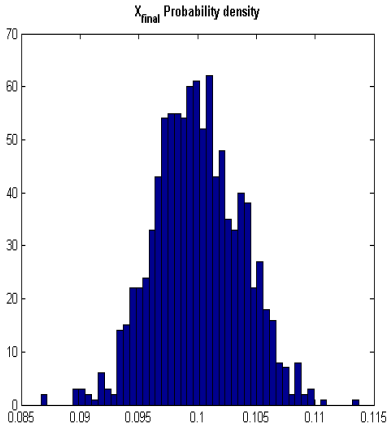

7.66.2 Cai noise

Figure 7.66: X_{final} probability density over 1000 simulations with bounded Sine Wiener noise (left figure) and bounded Cai noise (right figure)added on carrying capacity, with amplitude $B_k = 0.04$ and correlation time $\tau_k = 0, 1$, and drug concentration, with amplitude $B_c = 0.1$ and correlation time $\tau_c = 1$. Starting value is the microscopic equilibrium point $x = 0.1$.

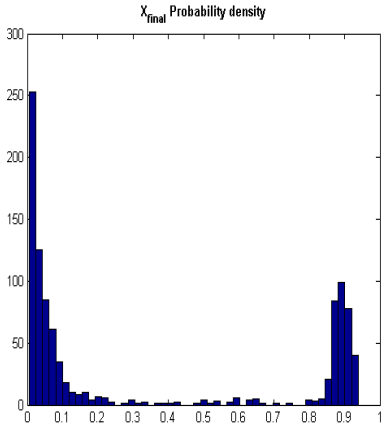

7.67.1 Sine Wiener noise

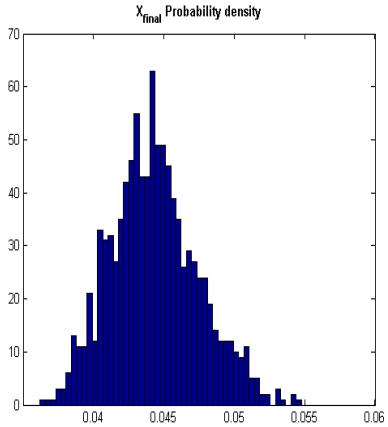

7.67.2 Cai noise

Figure 7.67: X_{final} probability density over 1000 simulations with bounded Sine Wiener noise (left figure) and bounded Cai noise (right figure)added on carrying capacity, with amplitude $B_k = 0.04$ and correlation time $\tau_k = 0, 1$, and drug concentration, with amplitude $B_c = 0.1$ and correlation time $\tau_c = 1$. Starting value is the microscopic equilibrium point $x = 0.045$.

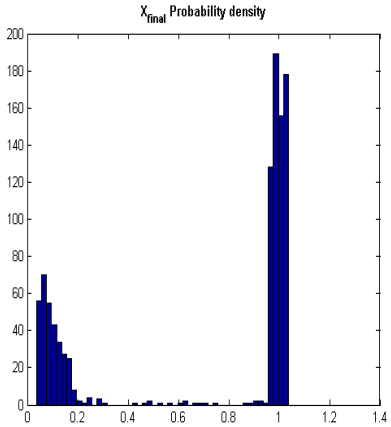

7.68.1 Sine Wiener noise

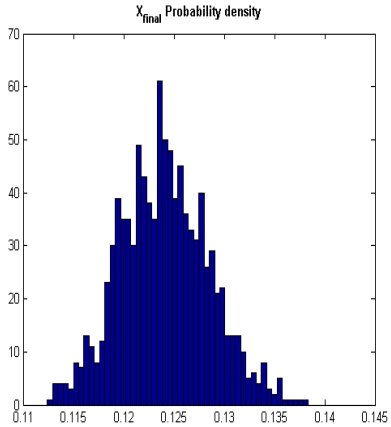

7.68.2 Cai noise

Figure 7.68: X_{final} probability density over 1000 simulations with bounded Sine Wiener noise (left figure) and bounded Cai noise (right figure)added on carrying capacity, with amplitude $B_k = 0.04$ and correlation time $\tau_k = 0, 1$, and drug concentration, with amplitude $B_c = 0.1$ and correlation time $\tau_c = 1$. Starting value is the microscopic equilibrium point $x = 0.123$.

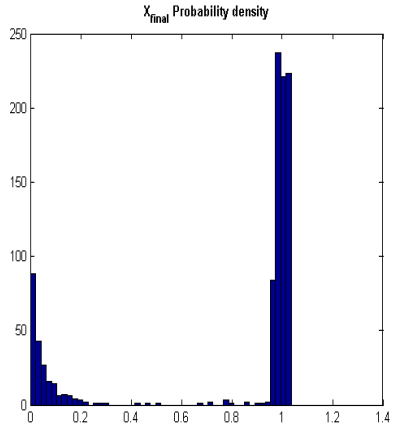

7.69.1 Sine Wiener noise

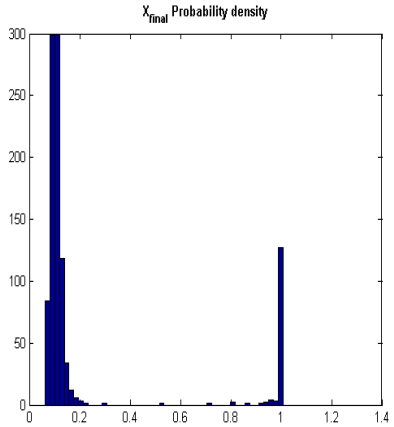

7.69.2 Cai noise

Figure 7.69: X_{final} probability density over 1000 simulations with bounded Sine Wiener noise (left figure) and bounded Cai noise (right figure)added on carrying capacity, with amplitude $B_k = 0.04$ and correlation time $\tau_k = 0.1$, and drug concentration, with amplitude $B_c = 0.2$ and correlation time $\tau_c = 1$,. Starting value is the microscopic equilibrium point $x = 0.105$.

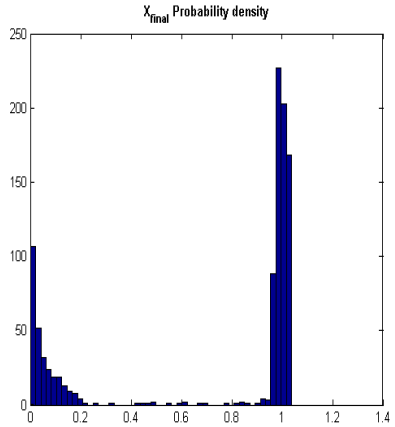

7.70.1 Sine Wiener noise

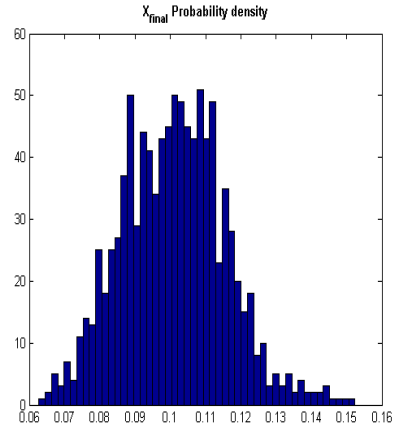

7.70.2 Cai noise

Figure 7.70: X_{final} probability density over 1000 simulations with bounded Sine Wiener noise (left figure) and bounded Cai noise (right figure)added on carrying capacity, with amplitude $B_k = 0.04$ and correlation time $\tau_k = 0, 1$, and drug concentration, with amplitude $B_c = 0.2$ and correlation time $\tau_c = 1$. Starting value is the microscopic equilibrium point $x = 0.1$.

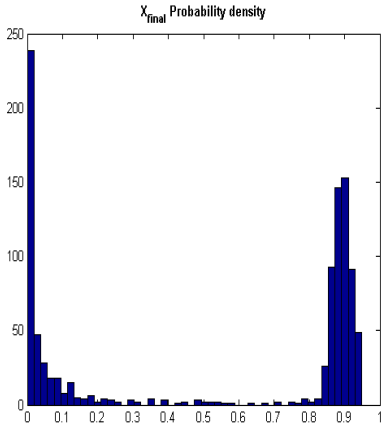

7.71.1 Sine Wiener noise

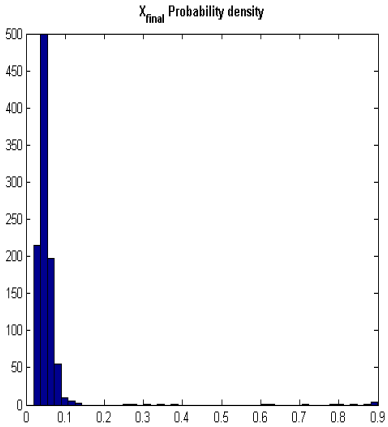

7.71.2 Cai noise

Figure 7.71: X_{final} probability density over 1000 simulations with bounded Sine Wiener noise (left figure) and bounded Cai noise (right figure)added on carrying capacity, with amplitude $B_k = 0.04$ and correlation time $\tau_k = 0, 1$, and drug concentration, with amplitude $B_c = 0.2$ and correlation time $\tau_c = 1$. Starting value is the microscopic equilibrium point $x = 0.045$.

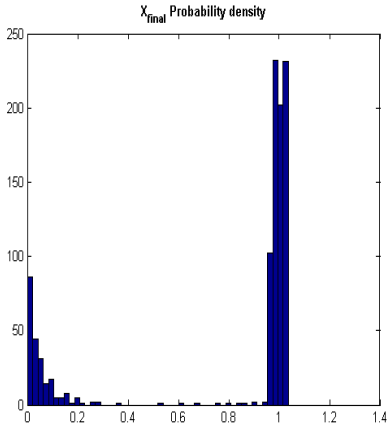

7.72.1 Sine Wiener noise

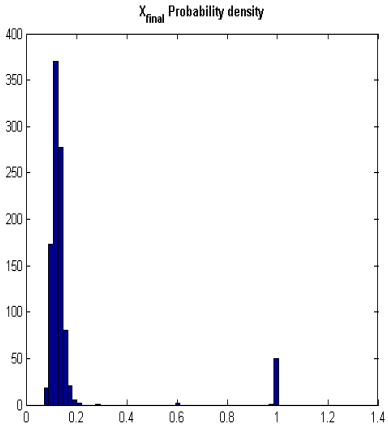

7.72.2 Cai noise

Figure 7.72: X_{final} probability density over 1000 simulations with bounded Sine Wiener noise (left figure) and bounded Cai noise (right figure)added on carrying capacity, with amplitude $B_k = 0.04$ and correlation time $\tau_k = 0, 1$, and drug concentration, with amplitude $B_c = 0.2$ and correlation time $\tau_c = 1$. Starting value is the microscopic equilibrium point $x = 0.123$.

7.4 Conclusions

As we can see from the results, the statistical fluctuations does not make the tumor evade in all cases.
In the case of perturbations on the *carrying capacity* we may summarize as follows the results of our simulations for the various parametric sets:

- **1 set:** In the case of SW noise, starting from equilibrium point $X_0 = 0.105$ for $B = 0.2, \tau = 1, 5$; $B = 0.3, \tau = 1, 5$; $B = 0.4, \tau = 1$; $B = 0.45, \tau = 0, 1$; $B = 0.5, \tau = 0.1, 1, 5$; $B = 0.8, \tau = 1$ there is transition to bimodality with a considerable probability of tumor explosion. In the case of Cai noise we observe transition only for $B = 0.5, \tau = 1, 5$; $B = 0.8, \tau = 1$.

- **2 set:** In the case of SW noise, starting from equilibrium point $X_0 = 0.100$ for $B = 0.8, \tau = 1$ there is transition to bimodality with a considerable probability of tumor explosion. In the case of Cai noise we do not observe transition in any case.

- **3 set:** In the case of SW noise, starting from equilibrium point $X_0 = 0.045$ for $B = 0.3, \tau = 1, 5$; $B = 0.4, \tau = 1$; $B = 0.5, \tau = 1, 5$; $B = 0.8, \tau = 1$ there is transition to bimodality with a considerable probability of tumor explosion. In the case of Cai noise we observe transition only for $B = 0.8, \tau = 1$.

- **4 set:** In the case of SW noise, starting from equilibrium point $X_0 = 0.123$ for $B = 0.3, \tau = 5$; $B = 0.5, \tau = 1, 5$; $B = 0.8, \tau = 1$ there is transition to bimodality with a considerable probability of tumor explosion. In the case of Cai noise we observe transition only for $B = 0.5, \tau = 1$; $B = 0.8, \tau = 1$.

Similarly, in the case of perturbations on the *drug concentration* we have that:

- **1 set:** In the case of SW noise, starting from equilibrium point $X_0 = 0.105$ for $B = 0.03, \tau = 1$; $B = 0.04, \tau = 1$; $B = 0.05, \tau = 0.1, 1$; $B = 0, 08, \tau = 0.1, 1$; $B = 0.1, \tau = 1$; $B = 0.15, \tau = 1$; $B = 0.2, \tau = 1$; $B = 0.3, \tau = 1$; $B = 0.5, \tau = 1$, there is transition to bimodality with a considerable probability of tumor explosion. In the case of Cai noise we observe transition only for $B = 0.15, \tau = 1$; $B = 0.2, \tau = 1$; $B = 0.3, \tau = 1$; $B = 0.5, \tau = 1$.

- **2 set:** In the case of SW noise, starting from equilibrium point $X_0 = 0.100$ for $B = 0, 08, \tau = 0.1, 1$; $B = 0.1, \tau = 1$; $B = 0.15, \tau = 1$; $B = 0.2, \tau = 1$; $B = 0.3, \tau = 1$; $B = 0.5, \tau = 1$, there is transition to bimodality with a considerable probability of tumor explosion. In the case of Cai noise we observe transition only for $B = 0.3, \tau = 1$; $B = 0.5, \tau = 1$.

- **3 set:** In the case of SW noise, starting from equilibrium point $X_0 = 0.045$ for $B = 0.04, \tau = 1$; $B = 0.05, \tau = 1$; $B = 0, 08, \tau = 0.1, 1$; $B = 0.1, \tau = 1$; $B = 0.15, \tau = 1$; $B = 0.2, \tau = 1$; $B = 0.3, \tau = 1$; $B = 0.5, \tau = 1$, there is transition to bimodality with a considerable probability of tumor explosion. In the case of Cai noise we observe transition only for $B = 0.2, \tau = 1$; $B = 0.3, \tau = 1$; $B = 0.5, \tau = 1$.

- **4 set:** In the case of SW noise, starting from equilibrium point $X_0 = 0.045$ for $B = 0.04, \tau = 1$; $B = 0.05, \tau = 1$; $B = 0, 08, \tau = 0.1, 1$; $B = 0.1, \tau = 1$; $B = 0.15, \tau = 1$; $B = 0.2, \tau = 1$; $B = 0.3, \tau = 1$; $B = 0.5, \tau = 1$, there is transition to bimodality with a considerable probability of tumor explosion. In the case of Cai noise we observe transition only for $B = 0.2, \tau = 1$; $B = 0.3, \tau = 1$; $B = 0.5, \tau = 1$.

Clearly, transitions depend on the noise model adopted and also on the initial point considered. This observation also holds by considering stochastic perturbations on both carrying capacity and drug density.
From a biological point of view, we may say that:

- The stochastic fluctuations that unavoidably arise in the tumor microenvironment, which are modeled by means of bounded noises perturbing the tumoral carrying capacity, may cause the escape of the tumor from the control imposed by the chemotherapy;
- Stochastic oscillations in chemotherapy level joined with nonlinear tumor size-dependent effectiveness of the delivered agent may induce tumor relapse;
- Synergistic effects are possible;

Note that none of the above mechanisms is related to emergence of resistent clones in the tumor cells population.
In conclusion, our results seem to show that stochastic perturbations may contribute to triggering the tumor escape, although less easily than one might predict by assuming a Gaussian noise. Also here, as in our immuno-oncological simulations, one can observe that, limiting the analysis at finite significant time (T=66), the transition to larger values is not reached if the oscillation B of the noise is too small or if the autocorrelation time τ is small.

Thanks

Se all'inizio di questa avventura qualcuno avesse voluto puntare sulla mia riuscita.. gli avrei dato del pazzo. Ma sono tenace e determinata e poi, si sa, con certe persone affianco si arriva proprio dappertutto.
Questa tesi rappresenta il coronamento del mio percorso universitario, profondo, a volte burrascoso, difficile a tratti ma comunque bello ed interessante. Beh certo ho sudato 2000 camicie ma che dite non ne é valsa la pena?
Ringrazio prima di tutti la mia famiglia, mamma, babbo, Gio, nonna Franci e nonno Giorgio che mi amano e mi sostengono sempre e comunque.
Ringrazio il professor Mirko Degli Esposti e il Dr. Alberto d'Onofrio per l'aiuto profondo, il sostegno e la pazienza.
Ringrazio i miei zii tutti per esserci e farmi star bene.
Ringrazio la Zia Mary perché é una potenza.
Ringrazio l'Ili che é la coinquilina piú bella del mondo e ci deve credere.
Rngrazio l'Alis perché l'anno vissuto con lei mi ha fatto crescere e imparare.
Ringrazio Pallu e Durham per l'amicizia e l'Erasmus, unico e irripetibile.
Ringrazio Ilaria (nonché Il prof.) che é la cuoca e l'amica che tutti vorrebbero.
Ringrazio Teresa (la vamp) che con il suo carisma e la sua determinazione é un vulcano.
Ringrazio Chiara perché é speciale.
Ringrazio Marta e Gloria per le studiate, le partite a carte e le cenette nella casetta sotto le torri.
RIngrazio Miki ottimo amico, FONDAMENTALE.
Ringrazio le amiche di una vita: Claudia, Elisa, Martina, Betta, Matilde, Sofia, Virginia, Chiara.. per esserci sempre.
Ringrazio Mattia che é il mio migliore amico, e lo sará sempre.

Ringrazio la Crosti per il suo sorriso contagioso e per essere sempre se stessa.
Ringrazio Case Bruciate e i suoi abitanti che mi hanno reso grezza e campagnola ma a cui voglio bene da sempre.
Ringrazio Jack, Albi, Max, Met, Paffi, Masca, Mike, Filo C., Filo M., Pasquá e Vito perché Plastic Fantastic Band e Co é una squadra furtissimi.
Ringrazio la Julius, Vali, Ponsi, Luna, Giadi, Niko, Benni, Bea che ho scoperto da poco ma che adoro.
Ringrazio Mike per le innumerevoli serate e le risate fatte con le "perle dell'Ili".
Ringrazio tutti quelli che ho dimenticato di scrivere.
Ringrazio Bologna per le sue luci che tutti ci invidiano, per il cibo, le persone, le torri e la puzza in via petroni.
Ringrazio me stessa perché ce l'ho messa tutta.
Per questi anni meravigliosi... Grazie.

Bibliography

[A.d05] A.d'Onofrio. A general framework for modeling tumor-immune system competition and immunotherapy: Mathematical analysis and biomedical inferences. *Physica D*, 208:220–235, 2005.

[A.d07] A.d'onofrio. Chaos,solitons fractals. 31 ,261, 2007.

[A.M94] A.M.Parfitt. Gompertzian growth curve in parathyroid tumours; further evidence for the set point hypothesis. *Cell Prolif*, 30:341–649, 1994.

[AT09] ER Edelman AR Tzafriri, AD Levin. *Cell Proliferation*, 42:348–363, 2009.

[BC05] RB Bobryk and A. Chrzeszczyk. *Physica A*, 358:263–272, 2005.

[B.J70] B.J.Kennedy. Cyclic leukocyte oscillations in chronic myelogenous leukemia during hydroxyurea theraphy. *Blood*, 35:751–760, 1970.

[C.A07] C.Archambeau. A short introduction to diffusion processes and ito calulus. 2007.

[CC91] T.Kwembe C. Calderon. Modeling tumor growth. *Math.Biosci.*, 103:97–114, 1991.

[CJ01] Jr. et al. C.A. Janeway. Immunobiology. 2001.

[CK04] G. Q. Lin Cai and Y. K. *Physical Review E*, 54,299, 2004.

[CM89] R.Demicheli R.Foroni A.Ingrosso G.Pratesi C.Soranzo and M.Tortoreto. An exponential-gompertizan description of lovo cell tumor growth from in vivo and in vitro data. *Cancer.Res.*, 49:6543–6546, 1989.

[CS05] Cai and Suzuki. *Nol. Dyn.*, 45,95, 2005.

[DC01] IF Tannock DSM Cowan. *International Journal of Cancer*, 91:120–125, 2001.

[DG09] D.Trk and G.Szakcs. Curr. opin. in drug discovery and dev. 12, 2009.

[DH09] Heller Orians Purves D.Sadava and Hillis. *BIOLOGIA 3 Evoluzione e la biodiversita'*, volume 1-2. Zanichelli, 2009.

[D.K98] J.C.Panetta D.Kirschner. Modeling immunotheraphy of the tumor-immune interaction. *J.Math.Biol.*, 37:235–252, 1998.

[d'O10] Alberto d'Onofrio. Bounded-noise-induced transitions in a tumor-immune system interplay. *Physical Review*, E 81, 2010.

[Edi03] S.A.Agarwala(Guest Editor). New applications of cancer immunotheraphy. *Seminar in Oncology*, 2003.

[E.K00] C.P. Calderon E.K.Afenya. Diverse ideas on the growth kinetics of disseminated cancer cells. *Bull. Math. Biol.*, 62:527–542, 2000.

[E.K04] C.P. Calderon E.K.Afenya. Growth kinetics of cancer cells prior to detection and treatment: an alternative view. *Discrete Cont.Dynam.Syst.B*, 5:25–28, 2004.

[Eva] Lawrence C. Evans. An introduction to stochastic differential equations version 1.2.

[Eve10] Jessica Evert. Overview: Introduction to cancer. June 2010.

[F.N00] H.I.Freedman F.Nani. A mathematical model of cancer treatment by immunotheraphy. *Math.Biosci*, 163:159–199, 2000.

[Fue07] R. Deza H. S. Wio M. A. Fuentes. Noise-induced phase transitions: Effects of the noises statistics and spectrum. April 2007.

[GAI03] A.Bru S.Albertos J.L.Subiza G.L.Garcia-Asenjo and I.Bru. The universal dynamics of tumor growth. *Biophys J.*, 85:2948–2961, 2003.

[GJ00] PA Netti DA Berk MA Swartz AJ Grodzinsky and RK Jain. *Cancer Research*, 60:2497–2503, 2000.

[G.P04] R.D.Schreiber G.P.Dunn, L.J.Old. The three es of cancer immunoediting. *Ann.Rew Immunol.*, 2:322–360, 2004.

[G.Q04] C.Wu G.Q.Cai. Modeling of bounded stochastic processes. *Probabilistic engineering mechanics*, 19:197–203, 2004.

[G.Q05] Y.Suzuki G.Q.Cai. Response of systems under non-gaussian random excitations. 2005.

[GR02] H.Ikeda L.J.Old G.P.Dunn, A.T.Bruce and R.D.Schreiber. Cancer immunoediting: from immunosurveillance to tumor escape. *Nature Immunol.*, 3:991–997, 2002.

[GR10] P.Milazzo G.Caravagna, A.d'Onofrio and R.Barbuti. Tumour suppression by immune system through stochastic oscillations. *Journal of Theoretical Biology*, 265:336–345, May 2010.

[H.E86] Skipper H.E. *Bull. Math. Biol.*, 48:253–278, 1986.

[H.T97] A.J.Sober H.Tsao, A.B.Cosimi. Ultra late recurrence (15 years or longer) of cutaneous melanoma. *Cancer*, 79:2361–2370, 1997.

[I.D94] I.D.Bassukas. Gompertizian re-evaluation of the growth patterns of transplantable mammary tumors in sialoadenectomized mice. *Cell Prolif.*, 27:201–211, 1994.

[I.I74] A.V.Skorohod I.I.Gihman. *The theory of Stochastic processes*, volume 1. 1974.

[IL01] C.Zonneveld I.M.van Leeuwen. From exposure to effect: a comparison of modeling approaches to chemical carcinogenesis. *Mutat.Res.*, 489:17–45, 2001.

[IM03] M.A.A.Castro F.Klamt V.A.Grieneisen I.Grivicich and J.C.F Moreira. Gompertzian growth pattern correlated with phenotypic organization of colon carcinoma,malignant glioma and non-small cell lung carcinoma cell lines. *Cell Prolif*, 36:65–73, 2003.

[Jai01] RJ Jain. *Annual Review of Biomedical Engineering*, 1:241–263, 2001.

[J.H91] H.Kocak J.Hale. *Dynamics and Bifurcations*, volume 1. Springer-Verlag, New York, 15 Fifth Avenue, 1991.

[j.H01] Desmond j.Higham. An algorithmic introduction to numerical simulation of stochastic differential equations. 43:7–15, 2001.

[J.S01] O.J. Finn J.Schmielau. Activated granulocytes and granulocyte-derived hydrogen peroxide are the underlying mechanism of suppression of t-cell function in advanced cancer patients. *Cancer Res.*, 61:4756–4760, 2001.

[JSP94] M.Marusic Z.Bajzer J.P.Freyer and S.Vuk-Pavlovic. Analysis of growth of multicellular tumor spheroids by mathematical models. *Cell Prolif.*, 27:73–94, 1994.

[JtA94] N.Olea M.Villalobos M.I.Nunez J.Elvira and J.M.Ruiz the Almodovar. Evaluation of the growh rate of mcf-7 breast cancer multicellular spheroids using three mathematical models. *Cell Prolif*, 27:213–227, 1994.

[JTT99] H Shaikh JK Tunggal, DSM Cowan and IF Tannock. *Clin. Cancer Research*, 5:1583–1586, 1999.

[Lai64] A.Kane Laird. Dynamics of tumor growth. *Br.J. Cancer*, 18:278–290, 1964.

[Lai65] A.Kane Laird. Dynamics of tumor growth: comparison of growth rates and extrapolation of growth curve to one cell. *Br.J. Cancer*, 19:278–290, 1965.

[L.Na] R.Simon L.Norton. *Cancer Treat. Rep.*, 61:1303–1317.

[L.Nb] R.Simon L.Norton. *Cancer Treat. Rep.*, 70:163–169.

[M.G89] G.Webb M.Gillenberg. Quiescence as an explanation of gompertzian tumor growth. *Growth.Dev.Aging*, 53:25–33, 1989.

[M.M03] J.Konarski M.Molski. Coherent states of gompertzian growth. *Phys.Rev E*, 68(Ar.No.021916 Part 1), 2003.

[MR97] Catherine E.Serraf Malcom R.Alison. *Understanding Cancer: from basic science to clinical practice.* The press syndicate of the University of Cambridge, United Kingdom, The Pitt Building, Trumpington Street, Cambridge CB2 1RP, 1997.

[OCCR03] D.Rodriguez-Perez J.C Antonranz O.Sotolongo-Costa, L.Morales-Molina and M. Chacon-Reyes. Behavior of tumors under non stationary therapy. *Physica D*, 178:242–253, 2003.

[P.C04a] D.Zappala' P.Castorina. Energetic model of tumor growth. *arXiv:q-bio.TO/0412040*, 22, December 2004.

[P.C04b] D.Zappala' P.Castorina. Tumor gompertzian growth by cellular energetic balance. *ar-Xiv:q-bio.CB/0407018*, 2, December 2004.

[P.W03] J.Konarski P.Waliszewski. The gompertzian curve reveals fractal properties of tumor growth. *Chaos Solitons Fractals*, 16:665–674, 2003.

[R.L79] H.Horsthemke R.Lefever. *Bull Math Biol*, 41:469–490, 1979.

[RV05] Andrzej Chrezeszczyk Roman V.Bobryk. Transitions induced by bounded noise. *Physica A*, 358, 2005.

[S.P85] S.Piantadosi. A model of growth with first-order birth and death rates. *Comput.Biomed.Res*, 18:220–232, 1985.

[TW01] M. A. Fuentes R. Toral and HS Wio. *Physica A*, 295:114–122, 2001.

[V.A01] G.D.Knott V.A.Kuznetsov. Math.comput.modell. 33, 2001.

[VVJ97] S.A.Rosenberg V.T.De Vito Jr., J.Hellmann. Cancer: Principle and practice on oncology. *J.P.Lippncott,Philadelphia*, 1997.

[W.H77] R.Lefever W.Horstemke. *Phys. Lett*, 64A:19–21, 1977.

[W.H84] R.Lefever W.Horsthemke. *Noise-Induced-Transitions: Theory and Applications in Physics, Chemistry, and Biology*, volume 15. Springer-Verlag, 1984.

[Whe98] T.E Wheldon. *Mathematical models in cancer research.* Taylor and Francis, first edition January 1, 1998.

[Wil11] Robert Williams. Cancer. *Better Medicine*, January 2011.